UNIVERSITÉ DU QUÉBEC À MONTRÉAL

RECONSTITUTION DENDROCHRONOLOGIQUE DES ANNÉES DE FORTE ACTIVITÉ AVALANCHEUSE DANS LA CHAÎNE PRÉSIDENTIELLE (NEW HAMPSHIRE, ÉTATS-UNIS) : SCÉNARIOS MÉTÉOROLOGIQUES ET CLIMATIQUES

THÈSE

PRÉSENTÉE

COMME EXIGENCE PARTIELLE

DU DOCTORAT EN SCIENCES DE L'ENVIRONNEMENT

PAR

JEAN-PHILIPPE MARTIN

JUIN 2016

You have brains in your head.
You have feet in your shoes.
You can steer yourself
any direction you choose.
You're on your own. And you know what you know.
And YOU are the guy who'll decide where to go.

It's opener there
in the wide open air.

Out there things can happen
and frequently do
to people as brainy
and footsy as you.
And when things start to happen,
don't worry. Don't stew.
Just go right along.
You'll start happening too.

OH!
THE PLACES YOU'LL GO!
You'll be on your way up!
You'll be seeing great sights!
You'll join the high fliers
who soar to high heights.

So...
you're off to Great Places!
Today is your day!
Your mountain is waiting.
So... get on your way!

- Dr. Seuss, *Oh, The Places You'll Go!*

REMERCIEMENTS

En premier lieu, je tiens à remercier mon directeur Daniel Germain pour m'avoir donné l'occasion de travailler sur un sujet si passionnant, ainsi que pour sa disponibilité, ses encouragements, sa rigueur et ses nombreuses lectures critiques. Par ses connaissances sur la dynamique des versants, les risques naturels et la géomorphologie, il restera un mentor pour moi tout au long de ma carrière. Je garderai toujours un souvenir mémorable de nos longues discussions, plus ou moins profondes et sérieuses, sur la science et sur la vie, autour d'une bière, sur le terrain, lors des longs trajets en voiture ou dans son bureau lorsque je venais lui poser une question rapide et qu'il me répondait : « Assieds-toi deux minutes. » Merci Daniel pour ta générosité, ton support et ton amitié.

Ma gratitude va également à tous ceux qui en acceptant de partager leur vaste savoir ont contribué à la réalisation de ce projet, particulièrement Étienne Boucher, Guillaume Fortin, Eric Kelsey, Michelle Garneau et Patrick Lajeunesse. Je tiens à souligner la collaboration et la générosité des Snow Rangers du Mont Washington, Jeff Lane, Frank Carus et Brad Ray. Aucun doctorat ne permettra de connaître cette montagne comme ils la connaissent.

Merci à mes assistants de terrain, Mathieu Gratton, Jean-François l'Ours Milot, Jean-François Jasmin, Louis Bouchard, Pénélope Leclerc, Nicolas Sbarrato et Vincent Beaudette. Merci d'avoir rendu les randonnées si agréables et d'avoir travaillé avec autant d'ardeur à mon projet. Sans vous, je serais encore en train de scier des arbres (de moins de 6 pouces).

Cette thèse prend racine dans mon amour pour la montagne. À cet égard, je tiens à remercier tous ceux avec qui j'ai partagé ma corde sur des parois grisantes, j'ai laissé la trace de mes skis dans la neige folle ou j'ai arpenté les sentiers menant vers des sommets enchanteurs. Merci également à mes amis et collègues, pour les heures à discuter ou à apporter réponse à mes interrogations, pour les soupers, les cafés, les bières, les courses sur le Mont-Royal, pour tous ces précieux moments, sérieux ou déjantés. Je dois également souligner l'apport de tous les baristas montréalais qui ont su stimuler mes neurones (et mes papilles) par leurs cafés savoureux.

Je ne remercierai jamais assez ma famille et belle-famille, source intarissable d'inspiration. Chacun, à votre façon, avez su m'accompagner au travers de cette aventure. À mes parents qui ont cru en moi, dans mes entreprises les plus simples ou les plus folles, depuis que je suis haut comme trois pommes. À mes frères et ma sœur, mes neveux et nièces, pour votre appui et votre amour. Vincent, je ne saurai jamais exprimer, avec des mots suffisamment forts et éloquents, toute l'importance de ta présence à mes côtés. Merci pour nos discussions hebdomadaires ponctuant le labeur de la thèse d'un moment profond de réflexion sur sa place dans nos vies, et surtout pour ta manière inspirante d'incarner l'esprit scientifique, la générosité et l'abnégation.

Finalement, à l'instar d'une cordée en montagne, une thèse se vit avec ceux que l'on côtoie au quotidien. Je n'aurais jamais pu réaliser ce projet sans le soutien indéfectible de Bertille qui, par ses encouragements, son écoute, son dévouement et ses caresses, m'a permis de naviguer sereinement à travers les ressacs de la thèse. Éloi et Madeleine, mes p'tits bonheurs à moi, vous m'avez continuellement ramené à l'essentiel et enjolivé mon quotidien avec vos rires et vos câlins. À vous trois qui avez été à la fois mes phares et mon port, sous le soleil comme dans la tempête, un merci océanique.

TABLE DES MATIÈRES

LISTE DES FIGURES

LISTE DES TABLEAUX

RÉSUMÉ

Les avalanches de neige constituent un risque naturel important dans les chaînes de montagnes à l'échelle globale, mais également dans le Nord-Est nord-américain. La Chaîne Présidentielle (New Hampshire, États-Unis) constitue l'une des plus vastes superficies alpines au sud du Labrador. À cet effet, elle représente un lieu important pour la pratique des sports de montagne sur les versants raides. Bien qu'un programme de prévision des avalanches est instauré depuis 1959, aucune archive historique n'existe. La dendrochronologie est reconnue comme une technique valide pour reconstituer l'occurrence passée de processus géomorphologiques divers. Cette thèse vise à documenter par dendrochronologie l'historique des avalanches de forte intensité dans la Chaîne Présidentielle et à mieux comprendre comment les facteurs météorologiques et climatiques influencent cette dynamique.

Dans un premier temps, il importe de se questionner sur la singularité des milieux alpins du Nord-Est nord-américain. Une méta-analyse de la littérature scientifique a démontré que l'occurrence de cet environnement à si basse altitude dans la région d'étude résulte des interactions complexes entre la géosphère, l'atmosphère et la biosphère. Bien que la colonisation végétale ait suivi le même gradient sud-nord que le retrait de l'inlandsis Laurentien, trois facteurs contribuent à la mise en place, au maintient et à la diversité de ces environnements : l'élasticité du temps paraglaciaire, les effets de synergie entre les facteurs locaux tels que les dynamiques écologiques et les forçages climatiques, ainsi que la sensibilité et la résilience des milieux alpins.

Dans un deuxième temps, afin de contribuer à l'avancement des méthodes en dendrogéomorphologie, la possibilité de discriminer le signal attribué aux avalanches de neige d'autres perturbations climatiques, écologiques ou géomorphologiques a été étudiée. Ces cas d'études ont permis de démontrer que la surcharge nivale peut entraîner des séquences de bois de réaction suffisamment importantes pour être considérées comme des perturbations majeures à l'instar des avalanches de neige. D'autre part, la réponse dendrochronologique des châblis et de l'activité torrentielle présente des patrons spatiaux distincts des avalanches de neige, ce qui permet de les distinguer même si leur occurrence peut être synchrone à l'échelle annuelle.

Ensuite, une reconstitution dendrochronologique de l'activité avalancheuse de sept couloirs a permis d'identifier des variables météorologiques reliées à l'occurrence d'avalanches de neige de forte intensité grâce aux arbres de classification. Cet

algorithme s'est avéré supérieur aux régressions logistiques par sa capacité à prédire correctement les années avalancheuses. Leur architecture a permis de dégager des scénarios expliquant l'activité avalancheuse, soit : 1) une fréquence importance de tempêtes de neige; 2) un enneigement supérieur à la moyenne; 3) des températures favorisant la formation de couches fragiles et 4) la présence de vents violents.

Finalement, à partir de ces reconstitutions dendrochronologiques a été créé un indice d'activité avalancheuse de forte intensité à l'échelle régionale. Pour la période 1936-2012, 18 années de forte activité avalancheuse à l'échelle régionale ont été identifiées. Ces années se répartissent dans les quatre modes climatiques température/précipitation (froid et humide (FH), froid et sec (FS), chaud et humide (CH), chaud et sec (CS)). Cependant, la proportion d'années avalancheuses est significativement supérieures pour les années FH comparativement aux trois autres modes ou pour les années humides comparativement aux années sèches. Il existe d'autre part une relation significative entre l'activité avalancheuse à l'échelle régionale et l'Oscillation de l'Atlantique Nord (NAO). En effet, cette téléconnection, à l'instar de l'Oscillation du Pacifique Sud (ENSO) influence le climat de la région d'étude. La première est négativement corrélée avec les quantités de neige. La seconde permet de prédire la proportion de neige provenant des dépressions côtières, reconnues comme apportant d'importantes chutes de neige.

Outre sa contribution sur les aspects méthodologiques en dendrochronologie et sur la reconstitution de l'activité avalancheuse dans un massif où il n'y avait aucune archive, cette thèse constitue un apport original sur les relations entre les avalanches et le climat à une pluralité d'échelles spatiotemporelles. Le potentiel des arbres de classification pour déterminer les scénarios climatiques expliquant les hivers de forte activité avalancheuse y est démontré. Cette étude a permis d'identifier les mécanismes à l'échelle synoptique expliquant la relation entre les téléconnexions atmosphériques et l'activité avalancheuse dans la Chaîne Présidentielle.

En conclusion, dans une perspective de diminution du risque, nous souhaitons que cette thèse outillera les prévisionnistes responsables de la production d'un bulletin de risque pour notre site d'étude. En tant qu'une des premières études exhaustives sur les avalanches de neige dans le Nord-Est nord-américain, cette thèse ouvre la voie à un vaste champ de recherche où la compréhension du phénomène à une multitude d'échelles spatiotemporelles nécessite la prise en compte des particularités topographiques, écologiques, climatiques et humaines propres à cette région.

Mots clés :

Avalanches de neige; Environnement alpin; Chaîne Présidentielle; Dendrochronologie; Arbre de classification; Climat

INTRODUCTION GÉNÉRALE

Mise en contexte

Les avalanches de neige représentent un risque naturel recensé dans la plupart des grandes chaînes de montagnes. Bien qu'elles soient considérées comme relativement peu meurtrières, avec environ 250 victimes annuellement à l'échelle du globe (Meister, 2002), leur omniprésence sur les versants raides et enneigés en fait cependant un des aléas les plus destructeurs pour les personnes, les infrastructures et les activités récréotouristiques en montagne (Jamieson et Stethem, 2002; Stethem *et al.*, 2003; Nadim *et al.*, 2006).

À cet égard, il n'est donc pas surprenant que dans plusieurs régions montagneuses on note l'implantation de systèmes de prévision des avalanches de neige à différentes échelles spatiotemporelles à des fins de prévention. Or, la prévision constitue un processus complexe qui s'appuie à la fois sur un raisonnement inductif et sur l'interprétation de données complexes relatives à la structure du manteau neigeux, la météorologie et les éléments à risque (Thumlert, 2014). Selon McClung et Schaerer (2006), la prévision doit reposer sur trois types de données, à savoir : 1) les facteurs d'instabilité du couvert de neige; 2) les caractéristiques intrinsèques du manteau neigeux et; 3) les conditions météorologiques.

Les facteurs d'instabilité du couvert de neige font référence à l'observation de l'activité avalancheuse récente, à l'affaissement du manteau neigeux et aux résultats issus de tests de stabilité sur le terrain. Ces données sont considérées comme celles

apportant l'information la plus directe sur la probabilité d'occurrence des avalanches. Les caractéristiques intrinsèques du manteau neigeux consistent à l'épaisseur de la couverture de neige au sol mais aussi à sa structure et à son organisation interne (type et taille des cristaux, compacité, densité, humidité et température). Les variables météorologiques (vent, neige, pluie, température, insolation) sont des évidences indirectes de la stabilité actuelle et future du manteau neigeux. Ces trois facteurs dynamiques co-évoluent dans le temps et l'espace au cours de la saison froide afin de s'amalgamer en un système complexe où l'interrelation entre les trois types de variables crée des effets d'inertie et de seuil. À titre d'exemple, un évènement de précipitations sous forme liquide peut stabiliser considérablement le manteau neigeux en homogénéisant ses différentes couches. Le même évènement, dans d'autres conditions, peut potentiellement déclencher une avalanche, directement en surchargeant le manteau neigeux d'une couche de neige humide très dense, ou indirectement en favorisant la formation de cristaux à facettes (Germain *et al.*, 2009). De plus, ce système complexe est caractérisé par une réponse non-linéaire de l'activité avalancheuse en fonction de l'évolution des trois types de variables. En effet, des petites avalanches de surface peuvent être causées par une instabilité superficielle lors du dernier épisode de précipitations liquides et ne sont pas nécessairement le signe d'une forte probabilité d'avalanches à haut potentiel destructeur. Finalement, à ces trois types de variables s'ajoutent les caractéristiques topométriques du terrain (Birkeland 1997), lesquelles sont considérées comme les données de type 0, car représentant les facteurs prédisposant à l'occurrence des avalanches. Or, on note l'absence de consensus scientifique sur l'importance relative de chaque type de données dans la prévision avalancheuse. À titre d'exemple, un système de prévision basé sur un travail de terrain extensif privilégiera, certes, les données de type 1 alors qu'un système basé sur l'analyse de données à distance privilégiera les données de type 3 (LaChapelle, 1980).

Bien que les avalanches de neige soient un des mouvements gravitaires les plus largement étudiés (Germain, 2005), plusieurs tragédies survenues au 21^{e} siècle, notamment les avalanches extrêmes déclenchées par les tremblements de terre au Népal en 2015, témoignent de notre capacité limitée à prévoir les évènements de forte intensité, leur récurrence et à anticiper leur capacité de destruction. À cet effet, et considérant l'influence relative des différents types de données, mentionnés et décrits précédemment, dans le processus de prévision des avalanches, il n'est donc pas surprenant qu'une vaste littérature scientifique récente s'attarde à cette notion de prévision. On note, entre autres, plusieurs tentatives de prévision à travers une meilleure compréhension des caractéristiques des données de type 1 et 2, soit les propriétés physiques de la neige (p.ex. Colbeck, 1991; Schmid *et al.*, 2015), le processus de formation des avalanches (p.ex. Schweizer *et al.*, 1999; Gaume *et al.*, 2013), la propagation des instabilités dans le manteau neigeux (p.ex. Gauthier et Jamieson, 2006; McClung, 2015) ainsi que la modélisation déterministe ou empirique de la distance d'arrêt des avalanches (p. ex. Lied et Bakkehøi, 1980; McClung, 2001; Ancey *et al.*, 2004; Schläppy *et al.*, 2014).

Comme la prévision avalancheuse à l'échelle d'un massif ou d'une région se fait généralement à distance, l'importance accordée aux données météorologiques est donc accrue. Bien que la relation entre les avalanches et les facteurs météorologiques et climatiques soit indirecte, cette question a été fortement débattue dans la littérature scientifique, et ce, autant d'un point de vue opérationnel que phénoménologique. En effet, dans la perspective d'améliorer les prévisions de l'activité avalancheuse à grande échelle (i.e. à basse résolution sur une vaste superficie), les auteurs ont eu recours à différentes méthodes statistiques telles que les régressions logistiques (Jomelli *et al.*, 2007; Casterbrunet *et al.*, 2012), les arbres de classification (Hendrikx *et al.*, 2005, 2014), les analyses par plus proche voisin (Singh *et al.*, 2015) ou les prévisions d'ensemble (Vernay *et al.*, 2015), afin de concevoir des modèles prédictifs à partir des données météorologiques et nivologiques. D'un point de vue

phénoménologique, dans le contexte du changement climatique actuel et anticipé, certaines études se sont attardées sur l'évolution temporelle de la fréquence et l'intensité de l'activité avalancheuse dans les dernières décennies (Eckert *et al.*, 2013). Compte tenu de l'importante fluctuation interannuelle dans l'occurrence des avalanches de neige, il n'est pas surprenant que la plupart de ces études aient mis en lumière l'absence de tendance à moyen ou long termes (Schneebeli *et al.*, 1997; Laternser et Schneebeli, 2002; Bellaire *et al.*, 2016). Finalement, l'influence des patrons de circulation atmosphérique à l'échelle globale (oscillation de l'Atlantique Nord ou oscillation australe) sur l'activité avalancheuse a aussi été investiguée en Europe (Keylock, 2003; Jomelli *et al.*, 2007; Garcia *et al.*, 2009) et dans l'Ouest nord-américain (Dixon *et al.*, 1999; Mock et Birkeland, 2000; McClung, 2013; Thumlert *et al.*, 2014). Puisque ces patrons ont des incidences sur les conditions météorologiques à l'échelle locale, une meilleure connaissance de ces relations permettrait de comprendre comment les fluctuations climatiques influencent la période de retour des avalanches, et par conséquent le zonage et l'analyse du risque (Keylock, 2003). Or, bien que l'influence des variables météorologiques et climatiques sur les avalanches ait fait l'objet de nombreuses études, la plupart de celles énumérées précédemment ont en commun le recours à des archives complètes de l'activité avalancheuse comprenant des centaines, voire des milliers d'évènements répartis sur une période temporelle allant de la décennie au siècle.

En contexte de moyennes montagnes, les avalanches de neige dont la zone de départ ou d'arrêt se situe en milieu forestier subalpin ou montagnard ont fait l'objet de plusieurs études à des fins d'ingénierie écologique pour diminuer le risque (Motta et Haudemand, 2000; Stokes, 2008; Vacchiano *et al.*, 2015). Elles ont également été étudiées d'un point de vue phénoménologique pour mieux comprendre le déclenchement en milieu forestier (Bebi *et al.*, 2009; Teich, 2013) ou encore dans le but de reconstituer par dendrochronologie l'historique des évènements passés dans un couloir, un massif ou une région donnée (Boucher *et al.*, 2003; Voiculescu et Onaca,

2013). Dans les régions où les archives historiques n'existent pas, la dendrochronologie est considérée comme une approche fiable et reconnue pour appréhender les avalanches avec une démarche rétrospective (Luckman, 2010). En effet, depuis les premières investigations dendrogéomorphologiques appliquées aux avalanches de neige (Potter, 1969; Mears, 1975; Burrows et Burrows, 1976; Shroder, 1978, 1980; Butler *et al.*, 1979; Carrara, 1979), la validité de cette technique a été reconnue pour mieux comprendre et caractériser cet aléa dans une perspective de cartographie et de gestion du risque (Salm, 1997; Lerner-Lam, 2007).

Récemment, un nombre croissant d'investigations dendrogéomorphologiques portant sur les avalanches de neige ont été menées afin d'identifier les années avalancheuses et améliorer les techniques de reconstitution (Muntan *et al.*, 2004; Casteller *et al.*, 2007; Laxton et Smith, 2009; Garavaglia et Pelfini, 2011; Corona *et al.*, 2012; Schläpply *et al.*, 2013; Chiroiu *et al.*, 2015), d'évaluer le régime de fréquence-intensité des avalanches (Reardon *et al.*, 2008; Corona *et al.*, 2010; Germain *et al.*, 2010; Decaulne *et al.*, 2012, 2014), de calibrer les modèles de distance d'arrêt des avalanches (Casteller *et al.*, 2008; Schläppy *et al.*, 2014), de discriminer le signal dendrochronologique des avalanches versus celui des coulées de débris (Stoffel *et al.*, 2006; Szymczak *et al.*, 2010; Kogelnig-Mayer *et al.*, 2011; Voiculescu et Onaca, 2014), d'analyser l'impact écologique ou anthropique des avalanches (Germain *et al.*, 2005) ou d'identifier les scénarios météorologiques et climatiques responsables du déclenchement des avalanches à l'échelle locale et régionale (Dubé *et al.*, 2004; Germain *et al.*, 2009). Or, quoique ce dernier sujet ait été abordé par le passé, une seule étude a réussi à créer des modèles de prévision statistiques robustes en utilisant les régressions logistiques (Schläppy *et al.*, 2015). De plus, bien que la relation entre l'activité avalancheuse reconstituée par dendrochronologie et les années El Niño ait été identifiée en Patagonie par Casteller *et al.* (2011), cette étude comporte plusieurs faiblesses dont les deux principales sont : 1) un échantillonnage très limité (moins de vingt arbres par couloir) et 2) une relation avec El Niño inférée à partir de trois

années définies comme étant fortement avalancheuse alors que seulement un couloir sur neuf avait enregistré un évènement pour chacune de ces années. Ainsi, même si les avalanches répondent à des facteurs locaux, expliquant la difficulté à identifier des tendances à l'échelle des patrons de circulation atmosphérique globale (McClung et Schaerer, 2006), cette question mérite néanmoins d'être approfondie puisque ces patrons sont généralement prévisibles. En ce sens, même si leur relation avec les avalanches de neige est indirecte, ils peuvent toutefois permettre une meilleure planification à l'échelle saisonnière, surtout lorsque l'on considère les risques et les impacts économiques associés avec l'activité avalancheuse (McClung, 2013).

Les avalanches de neige ont causé 1018 décès aux États-Unis de 1951 à 2015 (Colorado Avalanche Information Center, 2015). À cet égard, elles sont plus létales que les tremblements de terre ou encore tous les autres mouvements de masse combinés (Committee on Ground Failure Hazards Mitigation Research, 1990). Depuis 1990, on enregistre une hausse significative des décès liés aux avalanches de neige et ce, malgré une forte variabilité interannuelle (Logan et Witmer, 2012). Entraînant annuellement de nombreuses fermetures de routes et des dommages au cadre bâti et aux forêts, on chiffre l'impact économique des avalanches de neige aux États-Unis à plusieurs millions de dollars (CGFHMR, 1990).

Les avalanches de neige sont surtout concentrées dans l'ouest du continent, mais elles sont également présentes et considérables dans le Nord-Est nord-américain malgré la dénivelée modeste des massifs montagneux. Les avalanches demeurent encore méconnues et sous-estimées (Germain, 2005). Pourtant, au Québec, où il s'agit du deuxième risque naturel le plus important en termes de décès (Hétu *el al.*, 2011, 2015), des évènements tragiques comme ceux de Blanc-Sablon (1995) et Kangiqsualujjuaq (1999) démontrent que les avalanches peuvent avoir une forte capacité de destruction sur de courtes pentes raides (Germain, 2016). D'ailleurs, des accidents mortels sont aussi survenus dans la plupart des régions administratives du

Québec (Hétu *et al.*, 2011). C'est toutefois au Labrador que la plus vieille catastrophe imputable à ce phénomène en Amérique du Nord est mentionnée, alors que 22 personnes sont décédées à Nain lors d'un seul évènement en 1781 (Liverman *et al.*, 2001). Au 20^{e} siècle, ce sont 28 accidents associés à des mouvements de neige qui ont été répertoriés dans cette province (Liverman *et al.*, 2001). En Nouvelle-Angleterre, des accidents mortels impliquant des skieurs ou des alpinistes ont été recensés dans les états de New York (4 décès), du Vermont (1 décès), du Maine (2 décès) et du New Hampshire (15 décès) (CAIC, 2015).

Il n'est pas surprenant que la plupart des décès et des accidents imputables aux avalanches de neige en Nouvelle-Angleterre soient concentrés dans le New Hampshire. En effet, la Chaîne Présidentielle dans cet état abrite la plus vaste superficie alpine – c'est-à-dire située au-dessus de la limite altitudinale des arbres – et le plus haut sommet (mont Washington, 1917 m) de la région. Fortement accessible, cette chaîne montagneuse est située à moins d'une journée de route pour plus de 80 millions de personne (Allen, 2000), ce qui en fait le berceau et un haut lieu de la pratique du ski hors-piste et de l'alpinisme du Nord-Est nord-américain.

Sites d'études

Cette étude a été menée dans différents couloirs d'avalanche de la Chaîne Présidentielle (New Hampshire, États-Unis, 44°16' N 71°18' W). Ce massif est constitué principalement de roches métamorphiques datant du Dévonien, hormis les plus hauts sommets composés de gneiss, de mica et de quartzite d'âge Jurassique (Billings *et al.*, 1979; Bennett *et al.*, 2006). La Chaîne Présidentielle est aujourd'hui constituée d'un plateau de 27,5 km^{2} situé au-dessus de la limite des arbres. Les glaciations alpines des périodes glaciaires de l'Illonien et du Wisconsinien y ont

laissé comme vestiges une douzaine de cirques glaciaires (Goldthwait *et al.*, 1987), dont les pentes raides sont propices au déclenchement des avalanches de neige. Deux de ces cirques sont fréquemment visités : le Tuckerman Ravine pour la pratique du ski hors-piste et le Huntington Ravine pour la pratique de l'alpinisme. Considérant une forte affluence, le United States Forest Service (USFS) a implanté un système de prévention du risque avalancheux dès 1959. En effet, selon les *Snow Rangers* responsables de la prévision des avalanches sur place, lors des fins de semaine printanières, il n'est pas rare que plus de 1000 personnes viennent skier dans le Tuckerman Ravine. Le mandat des *Snow Rangers* a évolué depuis l'implantation du programme. Aujourd'hui, ils émettent quotidiennement un bulletin de prévision à une échelle micro-locale dans lequel y est décrit le risque avalancheux pour chaque couloir du Tuckerman et du Huntington Ravines. Malgré l'ancienneté du programme de prévention, une base de données de l'activité avalancheuse au mont Washington n'a été instaurée qu'en 2007. Or, ces archives couvrent uniquement les avalanches du Tuckerman et du Huntington Ravines. De plus, on recense encore annuellement plusieurs accidents causés par les mouvements de neige dans la Chaîne Présidentielle. Le choix de procéder à une prévision micro-locale repose sur la forte fréquentation dans les deux sites susmentionnés. Dans le contexte actuel où on note une augmentation importante de la popularité des activités récréatives dans l'arrière-pays, l'achalandage augmente aussi dans les autres cirques non couverts par le bulletin de risque. Ainsi, une meilleure compréhension de la relation entre les avalanches et les conditions météorologiques à l'échelle de la Chaîne Présidentielle pourrait contribuer à opérationnaliser un bulletin de prévision à plus grande échelle.

La Chaîne Présidentielle est reconnue pour son climat hivernal rigoureux. Le slogan du Mount Washington Observatory, la station météorologique située au sommet de la montagne éponyme, est « The Worst Weather on Earth ». Au sommet du mont Washington, la température hivernale moyenne (de décembre à avril) est de -11,8 °C et les précipitations solides durant cette période atteignent en moyenne 714 cm. La

région d'étude est caractérisée par ses forts vents. En effet, la rafale record pour chaque mois de l'année dépasse 200 km/h et, durant l'hiver, on y enregistre des vents d'ouragan (> 119 km/h) deux jours sur trois (Gordon, 1989). Paradoxalement à ce climat arctique, le manteau neigeux est de type maritime (Allen, 2000). On y note un régime d'avalanche prédominant à action directe (Allen, 2000 ; Joosen, 2008), c'est-à-dire que la majorité des avalanches se produit directement à la suite d'un évènement météorologique, en opposition à un régime à action indirecte où l'évolution du manteau neigeux sur de longues périodes a une incidence majeure sur l'occurrence des avalanches.

À cet égard, la Chaîne Présidentielle est un site de choix pour l'étude de l'influence météorologique et climatique sur la dynamique des avalanches. De plus, puisque le bulletin émis quotidiennement à 8 heures s'appuie sur une évaluation visuelle rapide du terrain effectuée à distance, les données nivologiques collectées la veille et les données météorologiques obtenues le matin même, les données de type 3 (i.e. conditions météorologiques) revêtent donc un caractère important dans la détermination du niveau de risque. Finalement, comme le décrit McClung (2002, p.135) : « *Normally as the spatial scale decreases, the difficulty of the forecasting problem increases and the need for accuracy increases.* » Ainsi, l'acquisition et le couplage d'informations entre les variables atmosphériques et les avalanches dans la Chaîne Présidentielle devient davantage pertinente, puisqu'en dehors de l'industrie du héli-ski et des guides de montagne (Haegeli et McClung, 1999), l'émission d'un bulletin de risque avalancheux à si petite échelle par des prévisionnistes demeure un cas unique.

Objectifs et approche méthodologique

Cette thèse vise d'une part, à documenter l'historique des avalanches de forte intensité dans la Chaîne Présidentielle et, d'autre part, à mieux comprendre comment les facteurs météorologiques et climatiques influencent cette dynamique avalancheuse. De façon plus spécifique, les objectifs poursuivis sont : 1) de reconstituer par dendrochronologie l'occurrence des avalanches de neige de forte intensité dans plusieurs couloirs de la Chaîne Présidentielle ; 2) de discriminer le signal dendrochronologique des avalanches de neige des autres perturbations enregistrées, telles que la surcharge nivale, l'érosion torrentielle et les châblis ; 3) d'identifier et de modéliser les variables météorologiques expliquant l'occurrence des avalanches de neige, et 4) de vérifier et valider l'existence d'une relation entre les grands systèmes climatiques, plus particulièrement l'oscillation australe (ENSO) et l'oscillation nord-atlantique (NAO), les trajectoires de tempêtes et l'occurrence des avalanches de neige.

Notre analyse s'appuiera sur l'intégration d'une part, de données dendrochronologiques permettant une démarche rétrospective faisant appel à la dimension historique du phénomène dans la Chaîne Présidentielle au New Hampshire (États-Unis) et, d'autre part, de variables météorologiques et climatiques à différentes échelles spatiotemporelles. Bien que la quantité de données et de couloirs étudiés soit insuffisante pour élaborer des projections quant à l'évolution future du régime avalancheux dans la Chaîne Présidentielle, les conclusions permettent néanmoins d'envisager l'utilisation des méthodes développées dans cette thèse afin d'étudier le phénomène dans une démarche prospective.

Organisation de la thèse

Cette thèse est organisée en quatre chapitres distincts mais complémentaires constituant des articles scientifiques publiés ou soumis au sein de revues avec comité de lecture, cosignés par mon directeur de recherche et moi-même. Ma contribution comprend l'ensemble du travail de production scientifique : définition des objectifs de recherche, développement du protocole méthodologique, collecte et traitement des échantillons en laboratoire, analyse des données, interprétation des résultats et rédaction des articles. Ces activités ont été accomplies sous la supervision et les conseils de mon directeur de thèse, Daniel Germain, qui a contribué activement à la réalisation de chacune d'elles.

Le premier chapitre, publié en anglais dans la *Revue Canadienne des Sciences de la Terre* (2016, volume 53, pages 494-505), expose les résultats de la synthèse environnementale effectuée dans le cadre de ma scolarité doctorale. Il présente une mise en contexte générale dont l'objectif est d'identifier les processus de mise en place et de préservation des milieux alpins à si basse altitude dans le Nord-Est nord-américain. Diverses études de cas recensées dans la littérature scientifique illustrent trois concepts à la base de cette observation : 1) l'élasticité de la période paraglaciaire, 2) les effets de synergie entre les changements climatiques à l'échelle Holocène et la dynamique écologique et 3) la sensibilité et la résilience des milieux alpins. Un catalogue bibliographique supplémentaire contenant 140 références sur les environnements alpins du Nord-Est nord-américain, soumis comme matériel supplémentaire, a été placé en appendice afin d'alléger le texte. Le jury en charge d'évaluer cette thèse a suggéré des corrections mineures à ce chapitre. Ainsi, la version présentée ci-dessous inclut ces correctifs, notamment en ce qui a trait à certaines précisions offertes dans la figure 1.5.

Le second chapitre est publié en anglais dans la revue *Dendrochronologia* (mars 2016, volume 37, numéro 2, pages 17-32). Il porte sur le potentiel de la dendrochronologie pour discriminer les avalanches de neige des autres perturbations affectant un même couloir. Cette étude souligne que les patrons spatiaux des impacts causés aux arbres par la surcharge nivale (perturbation climatique), l'activité torrentielle (perturbation géomorphologique) et les châblis (perturbation écologique) diffèrent de celui des avalanches de neige. Il apporte ainsi une contribution méthodologique importante à la dendrochronologie appliquée aux avalanches de neige.

Le troisième chapitre est sous presse dans la revue *Progress in Physical Geography* (http://dx.doi.org10.1177/0309133315625863). Son objectif principal est d'identifier les conditions météorologiques propices à l'occurrence des avalanches de forte intensité dans sept couloirs de la Chaîne Présidentielle. Pour ce faire, la performance de deux modèles statistiques applicables aux phénomènes discrets – les régressions logistiques et les arbres de classification – est comparée. Ces derniers produisent des modèles plus robustes qui permettent une interprétation phénoménologique plus approfondie de la relation avalanche-météorologie.

Finalement, le quatrième chapitre, soumis en anglais à la revue *International Journal of Climatology*, porte sur la relation entre l'activité avalancheuse de forte intensité à l'échelle régionale, les patrons synoptiques dominants lors des évènements de tempêtes au cours des années avalancheuses, la NAO et l'ENSO. Les années avalancheuses ont été classées selon leur mode climatique dominant – chaud ou froid; humide ou sec – et les tempêtes de neige lors de ces années ont été classées selon l'origine du système dépressionnaire. Les résultats démontrent qu'il existe une relation statistique entre les années avalancheuses et l'indice de la NAO à l'échelle de l'hiver. Cette relation était attendue puisque les précipitations solides enregistrées lors des années de NAO négative sont généralement supérieures, particulièrement lorsque

l'anomalie maximale septentrionale est située à l'ouest du Groenland, ce qui favorise l'occurrence de tempêtes côtières de forte envergure. De plus, bien que la quantité de neige totale reçue au cours de l'hiver dans la Chaîne Présidentielle semble indépendante de l'ENSO, la provenance de celle-ci est influencée par cette téléconnexion, puisque les années d'ENSO positive favorisent les tempêtes côtières. Finalement, un phasage entre la NAO (négative) et l'ENSO (positive) a été identifié lors des années où l'indice d'activité avalancheuse à l'échelle régionale était le plus important, ce qui laisse présager que ce phasage peut engendrer des conditions d'avalanches extrême.

Afin de faciliter la lecture de chacun des chapitres, les articles ci-dessus apparaissent dans leur intégralité. Ceci entraîne certaines répétitions, principalement au niveau de la description des sites d'études, de la méthodologie et, dans une moindre mesure, dans l'introduction et la mise en contexte. De plus, la bibliographie contient les références de tous les chapitres, afin d'en assurer un enchaînement fluide. La numérotation des tableaux et figures a également été modifiée par rapport à la soumission afin d'inclure le numéro du chapitre correspondant.

CHAPITRE I

LATE-GLACIAL AND HOLOCENE EVOLUTION AS A DRIVER OF DIVERSITY AND COMPLEXITY OF THE NORTHEASTERN NORTH AMERICAN ALPINE LANDSCAPES: A SYNTHESIS

Jean-Philippe Martin[1] and Daniel Germain[2]

[1]Environmental sciences Institute, Université du Québec à Montréal, C.P. 8888 Succursale Centre-Ville, Montréal, Québec, Canada.

[2]Geography Department, Université du Québec à Montréal, C.P. 8888 Succursale Centre-Ville, Montréal, Québec, Canada.

Article publié dans la *Revue Canadienne des Sciences de la Terre* (2016, volume 53, pages 494-505)

Résumé

La moyenne montagne des latitudes tempérées représente un environnement complexe de par son héritage glaciaire datant du Pléistocène, l'importante géodynamique des versants raides et les conditions climatiques situées souvent à la limite du périglaciaire. Ces facteurs, combinés à la fragmentation des habitats alpins dans un tel milieu, favorise la diversité floristique et topographique de ces environnements dans le Nord-Est nord-américain. À travers différentes études de cas, la présente synthèse met en relief les interactions entre la géosphère (processus glaciaires, paraglaciaires et périglaciaires), l'atmosphère (les fluctuations climatiques) et la biosphère (colonisation végétale et évolution des écosystèmes jusqu'à aujourd'hui) à la base de la complexité systémique qui explique l'occurrence d'un milieu alpin à si basse altitude dans le Nord-Est de l'Amérique du Nord. La colonisation végétale a d'abord eu lieu dans les massifs méridionaux, suivant le même gradient sud-nord que le retrait de l'inlandsis Laurentidien. Cependant, l'effet de synergie entre plusieurs facteurs locaux, tels que le retrait glaciaire, les forçages climatiques ou les processus paraglaciaires, a augmenté la résilience et a influencé la mise en place des milieux alpins. La localisation et l'étendue des milieux alpins peuvent donc être considérées azonales. Finalement, cette méta-analyse souligne l'absence de cadre conceptuel, d'études systémiques et de reconstructions multi-proxys des environnements alpins du Nord-Est nord-américain situés à la limite bioclimatique entre les zones à dominance biostasique et rhexistasique.

Mots clés :

Holocène; Paysage alpin; Environnement alpin; Paraglaciaire; Résilience; Synergie

Abstract

Mid-altitude, mid-latitude mountains are complex environments due to their Pleistocene glacial heritage, the importance of geomorphic processes on the steep slopes, and the climatic conditions which are often close to periglacial. These factors, along with the fragmentation of the alpine habitats, enhance the topographic and floristic diversity of these environments in northeastern North America. Through case studies, this synthesis underlines the interactions between the geosphere (glacial, paraglacial, and periglacial processes), the atmosphere (climatic fluctuations) and the biosphere (vegetation establishment and evolution to the present-day) that explain the low elevation of the northeastern North American alpine environment and that testify to its complexity. Vegetation established earlier in the southern ranges, following the same general trend as the Laurentian Ice Sheet recession. However, local factors such as ice retreat, response to global scale climate changes and paraglacial processes acted in synergy to increase the resilience and to influence the occurrence of alpine landscapes. The establishment of the latter environment can therefore be considered to be azonal. Finally, our findings highlight the lack of a conceptual framework, systemic studies and multi-proxy reconstructions of alpine environments located at the limit of bioclimatic zones controlled by the equilibrium between biostatic and rhexistatic regimes.

Keywords

Holocene; Alpine landscape; Alpine environment; Paraglacial; Resilience; Synergy

1.1 Introduction

The diverse and combined influences of many orogenies – some in the recent past on a geological timescale – with the many subsequent erosion agents, which depend on climatic variations at local and regional scales, increase the complexity of the mountain environments and their spatiotemporal evolution. If alpine glaciers and permafrost recession are at the heart of recent scientific interest because of ongoing climatic change (e.g., Harris *et al.*, 2009; Jomelli *et al.*, 2011), the ecological evolution of alpine and subalpine environments at lower altitudes is equally concerning (Grabherr *et al.*, 2010; Engler *et al.*, 2011; Dullinger *et al.*, 2012). Indeed, mid-altitude mountains are also foreseen to undergo profound modifications in the next decades and century, hence the interest to better understand the past and ongoing evolution of these unique environments which support a rich biodiversity, generate many natural georisks, and sustain numerous anthropogenic activities and needs such as agriculture, water resources, tourism and outdoor activities (Messerli and Ives 1997; Sagoff, 2002; Price *et al.*, 2004).

While mid-altitude mountains often lack distinct glacial and periglacial levels, the presence of a topographic gradient influences the development of a variety of environments with distinct biophysical characteristics. In light of these observations, mid-altitude mountains should be thought of as the outcome of a long and complex evolutionary process, the latter being driven by non-linear feedbacks in space and time between many components of the geosphere (tectonics, pre-Quaternary and glacial heritages, geological structure, sediment transfer processes), the atmosphere (climatic variations at different spatial and temporal scales) and the biosphere (vegetation cover, disturbance regime, ecosystem resilience). While recent recognition of potential global-scale interactions between tectonics, climate, surface processes and vegetation dynamics is well documented (e.g., Winkworth *et al.*, 2005;

Bishop, 2007; Whipple, 2009), very few examples are available in the scientific literature concerning mid-altitude mountains. Moreover, the general lack of fine-scale temporal and spatial resolution in existing studies impedes the provision of detailed information regarding the patterns and processes of these systems' interactions.

In northeastern North America (i.e., latitude 43 to 50° N), where the elevation of the treeline is well below the worldwide pattern established by Körner (1998) (Figure 1.1), the low level of human disturbance of the alpine and subalpine belts provides a unique opportunity to study and document the synergistic influence of causal factors responsible for the current mountain landscapes. At a regional scale, Cogbill and White (1991) reported the mean July temperature of 13 °C isotherm as a climatic control of the treeline in these mountain ranges. However, fine-scale observations show significant discrepancies related to, among other factors, the proximity of the ocean and climate variability, the toxicity of the serpentine bedrock, the importance of geomorphic processes on steep slopes, and the ecological disturbance regime. It is the aim of this paper to use case studies to illustrate the diversity of northeastern North American subalpine-alpine environments as a complex evolution based on the timing of deglaciation, the pattern of vegetation establishment, the frequency-magnitude of geomorphic processes and the ecological disturbance regime, and their responses to climate variability throughout the Holocene epoch. Future challenges and opportunities in the context of the ongoing global change will also be discussed.

1.2 Study area

1.2.1 Geographic setting

Mountain ranges with considerable alpine environments are spread throughout the northeastern United States and eastern Canada (Figure 1.2). The ranges included in this synthesis are the Catskills (New York), the Adirondacks (New York), the Green Mountains (Vermont), the White Mountains (New Hampshire) and the Mount Katahdin range (Maine) from New England (USA). The ranges from the province of Quebec in Canada are the Charlevoix Highlands, as well as the Chic-Chocs of the Gaspé Peninsula, the latter also including the McGerrigle Mountains if not specified otherwise. The ranges from the Atlantic provinces of eastern Canada include the Cape Breton Highlands (Nova Scotia) and the Long Range Mountains (western Newfoundland).

1.2.2 Physical characteristics

Most of northeastern North America's current alpine environments were uplifted during the Taconic or the Alleghenian phases of the Appalachian orogeny – 450 M yrs ago and 325 to 260 M yrs ago respectively (Titus, 2004). The difference in lithology between certain Appalachian ranges has a profound ecological impact. For example, the Chic-Chocs Mountains are composed of Ordovician limestone, shale, argilite, greywacke, as well as siltstone with occasional layers of sandstone (Enos, 1969). The Mont Albert plateau, one of the highest peaks of the range, can be considered a distinct unit because of its high serpentine content which supports a

unique flora within the studied region (Sirois, 1984). Intruded Devonian magmatic material forms the highest summits of the range adjacent to the Chic-Chocs, the McGerrigle Mountains, which are composed mainly of granite and granitoid material (Gray and Brown, 1979). The proximity of these three distinct units (i.e., limestone, serpentine and granite) in an otherwise similar environment in terms of topography and climate led early scientists to conclude that the geology controlled the alpine floral diversity (Fernald, 1907). The High Peaks of the Adirondack Mountains and the Charlevoix Highlands are the only ranges from the Grenville Province, composed mainly of Precambrian gneiss, granite and anorthosite (Hargraves and Roy, 1974). Table 1.1 presents the maximal elevation of the aforementioned ranges. The highest summit of the study region is Mount Washington (1 971 m) in the White Mountains.

1.2.3 Alpine environment

The high mountains of northeastern North America follow a classical altitudinal zonation. Montane mixed-coniferous forest covers the lower elevations, followed by a subalpine spruce-fir or boreal forest, which spreads upward to the treeline. The alpine environment is defined as the treeless, cold and windy high-altitude area above treeline on mountains (Löve, 1970). In northeastern North America, the alpine environment presents a mosaic of patches on the highest summits, and not a continuous territory (Table 1.1). At the regional scale, there are gaps of many hundreds of kilometers between the alpine ranges. At the range scale, alpine environments are also distributed in patches, separated by forested valleys. The elevation of the treeline follows the same decreasing trend along a latitudinal gradient that is observed worldwide (Figure 1.1). The Chic-Chocs and the Long Range have the largest areas of land above the treeline. This is consistent with the flat summit

topography of these ranges, which are post-orogenic planation surfaces (Jutras and Schroeder, 1999), along with their higher latitude.

1.3 Methods

The last decade has seen an increasing scientific interest in these altitude environments for various reasons such as the increase of extreme hydrometeorological events (Germain and Hétu, in press), the decrease of the woodland caribou populations in Quebec (Johnson *et al.*, 2015) or the response of the arctic-alpine flora to the ongoing climate changes (Bailey *et al.*, 2015). The onset of different initiatives demonstrate this renewed interest: a yearly occurrence of the workshop entitled Northeast Alpine Stewardship Gathering, the publication of the Eastern Alpine Guide (Jones and Willey, 2012) — a book about wildness and conservation with the contribution of twenty authors, most of them scientists — and a scientific paper highlighting research priorities and the need for a network of long-term alpine monitoring sites where a standardized protocol would be used to collect data on biotic and abiotic parameters (Capers *et al.*, 2013). In that regards, two sites located in the Chic-Chocs Mountains (Quebec) and the White Mountains (New Hampshire) were implemented following the international protocol of GLORIA (GLobal Observation Research Initiative in Alpine environments) in the last few years. However, as recently reported by Capers *et al.* (2013, p.559), *research in alpine areas of northeastern North America has been poorly coordinated, with minimal communication among researchers, and it has rarely been multidisciplinary.*

As a first attempt to address the aforementioned gap, the following results lean on a meta-analysis of the existing literature about the glacial, palaeoecological and geomorphological evolution of the mountain ranges of Northeastern North America. Indeed, there is a wide corpus of papers in regional and international scientific journals that provide chronologies with regard to the glacial retreat, the vegetation settlement, the evolution of geomorphic processes and systems. A bibliographic database containing 109 references was created (Supplementary material 1), but to increase the readability, only the most relevant are integrated to this paper. We are aware that the present analysis does not include every aspects of the alpine environment that is covered by the scientific literature, such as the insects, the lichens, the mammals (especially the woodland caribou), local climatology or the geology (lithology and past orogenies). Rather than an exhaustive catalogue of every previous study done in the alpine environment of northeastern North America, this work represents the first step of a transdisciplinary, large-scale analysis of alpine environments since the Late-Glacial. It is the hope of the authors that this synthesis serves as a starting point for more detailed analysis and scientific work about the long-term biophysical conditions that characterise these mid-altitude mountains.

Tables 1.2 and 1.3 detail the sites and types of records that were used in the following glacial and paleoecological reconstructions. Most of the chronological data are therefore derived from ^{14}C dates of pollen assemblages and macrofossils. Unless specified otherwise, all dates are given in calendar years. CALIB 6.0 software (Reimer *et al.*, 2009) was used to calibrate radiocarbon dates with a standard deviation of 100 years when calendar dates were unavailable. Calibrated dates were rounded to the nearest 100 years and are labeled Before Present (BP).

1.4 Results and discussion

The meta-analysis of the literature allowed the reconstruction of the chronology of the general deglaciation and vegetation establishment throughout the study region. These general patterns provide an overlook of the inception of alpine environments on the higher summits of Northeastern North America. Different case studies are then presented in order to propose concepts that encompass the complex relationships explaining the local discrepancies in the altitudinal and latitudinal localisation of the treeline. First, from a geomorphological standpoint, the elasticity of the paraglacial period, explicated by local topographical, geographical and geological factors, will influence nowaday's equilibrium between rhexistatic and biostatic processes on the steep slopes. Next, the late-Holocene fluctuations in climate acted in synergy with punctual ecological disturbances to create localized alpine environments on previously forested summits. Finally, the inception and preservation of permafrost in the study regions, along with the fact that the alpine treeline is controlled by disturbances rather than temperature, explain the delicate balance between the sensitivity and the resilience of the alpine landscape.

1.4.1 Deglaciation pattern, vegetation establishment and regional climatic changes

1.4.1.1 Deglaciation

Although the patterns of deglaciation of the Appalachian Highlands and the supposed presence of nunataks have been debated for nearly a century across the study area (Fernald, 1925; Bradley, 1981; Gosse *et al.*, 2006; Olejczyk and Gray, 2007), it is

now well-established that the Laurentian Ice Sheet (LIS) flowed across the mountain ranges and highlands of New England and Quebec, and connected with regional ice caps in the Atlantic Provinces and in the Chic-Chocs Mountains during the Last Glacial Maximum (LGM).The recession of the LIS in New England followed a general South to North trend. The onset of the glacial recession is poorly dated; the best estimate of its beginning is the onset of varved sedimentation at the south end of Glacial Lake Hitchcock in southern Connecticut, at 15,600 ^{14}C yr BP (Dyke *et al.*, 2002). The southwestern ice masses, such as the White Mountains ice cap, remained connected with the LIS, while the Gaspé Peninsula and Newfoundland ice caps were isolated.

The approximate date of ice recession in the different alpine ranges covered in this paper is presented in Figure 1.3. These data show the general trends, but any comparison between them remains uncertain, since the recessional dates were determined by various proxies (Table 1.2) that represent a range of spatial scale dynamics from regional (e.g. pollen) to local (e.g. gyttja). Moreover, there is much variation in the elevation at which the data were derived. At the global scale, New England was deglaciated before the Younger Dryas (12,900-11,400 BP). There is then a long time gap before deglaciation begins in the northernmost ranges, which suggests that the Younger Dryas delayed the melting of alpine ice caps located further north. In most ranges, the timing of ice recession is consistent with the deglaciation isochrones map of Southern Quebec and adjacent territories (Richard, 2009), with the exception of the White Mountains, for which the local data are older. This implies that the regional scale pattern might not reflect the local specificities of ice recession in the alpine ranges.

In the Gaspé Peninsula, variations in basal dates from different records are important to consider. Some are much younger than others, which led Richard *et al.* (1997) to propose the presence of late small glaciers in some of the cirques of the Chic-Chocs.

While some hypotheses have been proposed to explain the discrepancy (e.g., presence of an alpine desert or late ice), the absence of direct evidence dictates that caution must be taken when interpreting regional trends from a single or few basal dates.

1.4.1.2 Vegetation establishment

The postglacial vegetation establishment in northeastern North America followed three stages: tundra, afforestation and closed-forest stages. The general chronology for the vegetation dynamics of different mountain ranges is presented in Figure 1.3, which must, however, be treated with caution for several reasons:

1) *Contamination from organic carbon and radiocarbon accuracy.* The dates from the Chic-Chocs Highlands are from Richard *et al.* (1997), who demonstrated that the basal date of a core sampled in 1979 was too old, due to the contamination of the dissolved CO_2 by inactive carbon from the bedrock. Based on this evidence, other dates are potentially too old at other sites as well;
2) *Altitude*. The altitude at which the studies were conducted varies greatly, from the mixed-coniferous montane forest to the upper limit of the spruce-fir subalpine belt;
3) *Availability of accelerator mass spectrometry (AMS) dating.* As for old carbon contamination, AMS dating of macrofossils instead of total organic matter has allowed more accurate chronologies. However, northeastern North American alpine paleoecology was mainly published before 1995, when these dating techniques still were not widespread. However, above the treeline in the alpine environment, the pollen influx is low. The pollen from distant sites is over-represented and therefore allows only the

reconstruction of the vegetation at the regional level and makes the interpretation of treeline evolution particularly difficult; hence the need for macrofossil analysis in treeless environments (Birks and Birks, 2000).

At the regional scale, the vegetation establishment pattern in alpine environments followed the ice recession during the Late-Wisconsinan (Figure 1.3), the southernmost ranges being colonized first. At Mount Katahdin, the tundra stage was synchronous with the Adirondacks and the White Mountains, but the afforestation stage was longer and potentially delayed by the onset of the Younger Dryas. Moreover, there is a wide temporal gap in the vegetation establishment between the alpine ranges of New England and of Quebec (Figure 1.3). The proximity of the Quebec ranges with the Gulf of St. Lawrence and the Atlantic Ocean would have increased the cooling effect of the Younger Dryas compared with the southern, more continental ranges (Cwynar and Spear, 2001), therefore making it impossible for vegetation establishment to begin during this climatic period. Afterward, the recurrence of cold episodes following the Younger Dryas (Atlantic Preboreal Oscillation and the 8,200 BP cooling period), enhanced by the proximity with the LIS, the late recession of local ice caps in the Gaspé Peninsula (Richard *et al.,* 1997), and a high volume of freshwater runoff in the St. Lawrence River, would have delayed it further (Anderson *et al.*, 2007).

There are however some discrepancies between the deglacial and paleoecological records. For example, in the Charlevoix region, deglaciation is thought to have occurred around 12,500 BP at low altitudes from the presence of the St. Narcisse moraine. However, the oldest record from organic material in the Highlands dates from 10,500 BP. Two hypotheses could explain the gap of 2,200 years between ice recession and vegetation establishment; i) like in the Gaspé Peninsula, the Younger Dryas period might have been favourable to the build-up of alpine glaciers on the highest summits of Charlevoix; ii) it is likely that an alpine desert occurred between

the ice recession and the tundra stage, such as reported for the Chic-Chocs Mountains.

This regional picture allows depicting the general trend of ice retreat and alpine environment establishment along a SW – NE gradient. At the local scale, the following case studies illustrate that complex interactions between geomorphological, ecological and climatic systems create a set of conditions for the establishment, the diversity and the preservation of the alpine environments throughout the Holocene.

1.4.2 Complexity as the basis of the inception and conservation of alpine landscapes

1.4.2.1 Paraglacial time magnitude and elasticity impact on the alpine landscape

The alpine landscapes of northeastern North America have been geomorphologically active since the Late-Glacial period, but the frequency, magnitude and efficiency of the processes involved have varied following deglaciation and the Holocene climatic fluctuations. The recession of the LIS or the Appalachian ice caps exposed the landscape to paraglacial processes corresponding to isostatic instability and high sediment availability, providing a context of high geomorphic activity on the steep slopes. However, the scientific literature on Holocene hillslope geomorphology in the alpine ranges of northeasterm North America comes almost exclusively from the Gaspé Peninsula (regional synthesis are provided by Hétu and Gray, 2000; Germain *et al.*, 2010), with few studies focusing on the present-day processes in the Adirondack Mountains (e.g. Bogucki, 1977), the White Mountains (e.g. Kull and

Magilligan, 1994), the Cape Breton Highlands (e.g. Wahl *et al.*, 2007) and the Newfoundland Long Range (e.g. Hiscott and James, 1985).

The paraglacial processes were central in shaping the alpine landscape in this region through their dynamic interactions with ecological processes. Hillslope processes in the White Mountains during the Early-Holocene rendered the vegetation establishment more complex. The beginning of pollen accumulation was approximately synchronous at low (200 and 650 m) and high (1,325 and 1,542 m) altitudes (Spear *et al.*, 1994). Before 13,500 BP, all these sites recorded tundra vegetation. During this period, there is an absence of vegetation in the pollen records at mid-elevation sites (1,140 and 1,275 m), the earliest ones corresponding to 11,500 BP. Spear *et al.* (1994) suggested that the mid-altitude active steep slopes prohibited vegetation establishment until their stabilization, which points to the role of paraglacial geomorphic agents in the ecological evolution of the White Mountains.

The duration of the paraglacial period is directly related to the glacially conditioned sediment availability and varies from 10 to > 10,000 years. It is assumed that for an isolated landsystem, the paraglacial period ends at the exhaustion of this sediment stock, the latter being characterized by an exponential decline. However, secondary processes such as debris flows occurring in primary paraglacial stock in scree slopes, can rework glacigenic sediments stored in primary paraglacial stocks, further extending the duration of this period (Ballantyne, 2002). Hétu and Gray (2000) define the end of the paraglacial period in the northern Gaspé Peninsula as the complete burial of the rock walls by rockfalls, and later reworking of the debris by dry grain flows, frost-coated clasts flow, debris flows, snow avalanches and niveo-aeolian transport. At present, the coastal valleys of the northern Gaspé Peninsula have a diachronous pattern of paraglacial influences. For example, in the Mont Saint-Pierre valley, forest vegetation covers the east-facing slopes where rockwalls have been almost completely eliminated, while on the west-facing slopes, where summit

rockwall segments are still active, the upper part of the scree slope is still devoid of vegetation. As many studies highlight (cf. Hétu and Gray, 2000), the upper limit of the forest on these slopes has been changing constantly throughout the Holocene, in response to hydroclimatic conditions. A warmer and drier climate generally tends to favour an upward movement of the treeline via a decrease in the frequency and magnitude of mass wasting processes; this tendency reverses in colder and wetter periods. However, the treeline on the scree slopes of Mont Saint-Pierre has been extending upward from the end of the Little Ice Age until 1950. Since then, geomorphic processes have increasingly fragmented the treeline despite a positive trend in the temperature (Lafortune *et al.*, 1997). Therefore, in a lithologic context favourable to high rates of weathering through frost-related processes – and subsequently to a constant reloading of sediment stocks –, vegetation dynamics and paraglacial processes reach a dynamic equilibrium conditioned by complex geomorphic responses to the changes in hydroclimatic conditions.

The differences in the duration of the paraglacial period are even more striking on a larger scale. The Long Range and the Chic-Chocs contain similar drift-mantled landsystem based on similar processes and with similar lithologies, and have been deglaciated for approximately the same length of time. However, there seems to be an important difference in the efficiency and the magnitude of the present-day geomorphic processes. For example, on the Tablelands in Newfoundland, debris fans of a few hundred meters wide are common and still active, since they are not colonized by vegetation at an altitude close to sea level. On Mont Albert in the Chic-Chocs, debris fans of this magnitude are relict nowadays, but are superimposed by active debris cones with a surface and debris size smaller by close to an order of magnitude (Germain, 2005). This hydrosedimentological transition appears related to hydroclimatic conditions, which were favourable to the definitive closure of the regional forest cover as established by pollen analysis (Hétu and Bail, 1996). This example underlines the importance of local ecological and hydroclimatic conditions

in controlling the duration of exhaustion of glacially conditioned sedimentary stocks and consequently the delay of paraglacial responses of geomorphologic landsystems. Moreover, the overlapping of landforms, such as the debris cones of different scales on Mont Albert, is evidence of a more mature, postglacial landscape, with similar processes driving the sediment cascade, but to a different magnitude.

This section highlights the importance of the paraglacial concept to understanding the formation of the northeastern North American montane landscape, as well as the ecological evolution of the steep slopes by the rhexistatic forcing that influenced the vegetation establishment and vice versa. Considering that the essence of the paraglacial concept is to define recently deglaciated areas that are in an unstable geomorphological state, vulnerable to erosion processes, some slopes of the mountain regions of northeastern North America are still influenced by paraglacial processes more than 10,000 years after the onset of the Holocene period. This dichotomy between active and relict paraglacial periods is visible at the local and regional scales. Therefore, not only is there an overlapping of temporal scales amongst paraglacial periods from different landsystems (Mercier, 2008), but also an overlapping of spatial scales controlled by external variables such as vegetation and hydroclimatic conditions.

1.4.2.2 Synergistic effects of climate change and ecological disturbances

The data in Figure 1.1 shows the expected negative relationship between the altitude of the treeline and the latitude of the mountain range for northeastern North America. However, the altitude of the treeline in some ranges, such as the White Mountains and the Charlevoix Highlands, is lower than would be expected from this figure, as well as from a comparison with other mountain ranges at similar latitudes around the

world. While regional climatic latitudinal gradient as well as deglaciation and vegetation establishment processes explain the general trend, local dynamics are responsible for such discrepancies. As the following case studies demonstrate, it is not one system that is directly responsible for the lower elevation of the treeline in certain ranges but rather the synergistic effects of different systems.

The subalpine spruce-fir forest composition of the Appalachians differs from that of the boreal forest in disturbances controlling their dynamics, among other factors (Cogbill and White, 1991). The subalpine spruce-fir forest is controlled by wind and individual tree mortality (Sprugel, 1976), whereas the boreal forest dynamics are mainly controlled by ecological disturbances such as fire and insect outbreaks (Cogbill, 1985).

The Charlevoix Highlands are located within the boreal forest belt. Charcoal found on a summit was dated to 3,150 BP, which shows that it was previously forested and then decimated by fire (Bussières *et al.*, 1996). Today, open bogs occupy depressions in the upper slopes of these summits. The low regeneration rate following these fires is probably due to the deterioration of climatic conditions, since evidences of synchronous climatic cooling responsible for the increase in fire activity have been recorded in Charlevoix and in the Gaspé Peninsula. The paludification of the alpine zone is also indicative of a generally positive moisture surface balance during the Neoglacial. This case highlights the azonal nature of alpine and subalpine altitudinal belts of the Charlevoix Highlands, since they do not result from a climatic gradient associated with topography, but rather from a modification in the ecological dynamics caused by the large-scale Late-Holocene climatic deterioration.

In the White Mountains, the treeline of the subalpine spruce-fir forest moved upslope during the Younger Dryas (between 12,900 and 11,500 BP), reaching altitudes higher than in the present-day. This caused scientists to state that the Younger Dryas had not influenced the high-elevation vegetation of the White Mountains (Spear *et al.*, 1994).

However, later studies based on loss-on-ignition and chironomids suggest that even if there was an attenuation of the effects of this cooling episode westward from the Maritime provinces, the temperature of mid-altitude lakes in the White Mountains dropped by approximately 5 °C during the Younger Dryas (Cwynar and Spear, 2001). Therefore, the treeline was highest in the White Mountains during one of the coldest periods since ice recession. The beginning of Younger Dryas saw the occurrence of a shift from northwesterly winds during the Bolling-Allerod period to northeasterly katabatic prevailing winds in New England (Thorson and Schile, 1995) and Quebec (Filion, 1987). Present-day winds at the top of Mount Washington are extremely strong (Gordon, 1989), which is the result, among other causes, of the orientation of the mountain range perpendicular to the prevailing winds. The upward progression of the treeline at Mount Washington, controlled primarily by these extreme winds and rime episodes, could be caused by this shift in prevailing winds to an axis more parallel to the range, and thus decreasing their velocity. This anomaly in treeline position was preserved during the warmer, Mid-Holocene climatic optimum to finally regress to its present elevation during the Neoglacial, showing that the lower altitudinal limit of the alpine environment in this area does not respond to cold episodes or strong winds individually, but rather to a synergistic relationship between these two variables.

1.4.2.3 Sensitivity and resilience of the alpine landscape

Permafrost. Permafrost patches are still present in the Charlevoix Highlands, Mont Jacques-Cartier in the McGerrigles, Mount Washington in the White Mountains and in western Newfoundland (Figure 1.4; Clark and Schmidlin, 1992). Except for the latter, these ranges are well beyond the latitudinal limit of discontinuous permafrost distribution in Canada. Based on temperature extrapolation, Walegur and Nelson

(2003) estimated that the presence of permafrost would be possible on the highest summits of the High Peaks of the Adirondacks (Mount Marcy and Whiteface) and of northern Maine (Sugarloaf Mountain, Snow Mountain, Crocker Mountain and Mount Katahdin).

Permafrost is considered to be a system that is sensitive to ongoing and anticipated climate change (Camill and Clark, 2000). In the Chic-Chocs, however, 30 years of monitoring a permafrost patch led to the conclusion that the latter is stable (Gray *et al.*, 2009). The permafrost of Mont du Lac des Cygnes in the Charlevoix Highlands is well below the elevation trend of the other summits where permafrost bodies were observed. The approximate mean annual temperature of around 0°C for adjacent summits would not be sufficiently cold for the inception of permafrost. This suggests that it was formed during a colder period. In Charlevoix, the climatic conditions during the Neoglacial were not cold enough to trigger the formation of perennially frozen ground (Zimmerman and Lavoie, 2001). Therefore, the permafrost islands in Charlevoix are estimated to have formed during the Little Ice Age, in the last 500 years, in response to a unique set of climatic and ecological conditions. Fires were very frequent in the Charlevoix Highlands in the last 3,000 years (Bussières *et al.*, 1996). The opening of the vegetation, combined with the strong winds characteristics of this region and the cooling of the climate, led to little snow accumulation on the summits and to deeper ground penetration of the frost wave during the winter. The cool climate reduced evaporation and was favourable to the accumulation of moss, which isolated the ground ice. These cases show that permafrost patches in this study area are not climate driven, but their inception rather occurred in a precise eco-climatic context. Since present-day ecological conditions are responsible for their resilience, they evolved into an ecosystem-protected permafrost, which means that they are unlikely to recover after a significant disturbance with the ongoing change in climate (Shur and Jorgenson, 2007).

The resilience of mountain top permafrost in marginal environmental conditions at latitudes lower than the regional pattern of permafrost distribution is surprising and must be caused by the interaction of the different systems. While the mean annual air temperature following the Little Ice Age got warmer, the absence of trees on the summit allowed the strong winds to cause enough snow drifting to clear the snow or compact it sufficiently to increase its thermal conductivity. Both cases would result in a negative mean annual ground temperature.

Rock glaciers. Rock glaciers are widespread in the study region (Hétu *et al.,* 2003). Many were identified at low (20 m) and high (>600 m) elevations in the Chic-Chocs and almost all of these rock glaciers were located on a scree slope at the base of a rock wall (Hétu *et al.*, 2003; Germain, 2005). These objects form by the combination of paraglacial processes and periglacial conditions (Humlum, 1998) that influenced the landscape during the Late-Holocene. The distribution of the altitudinal limit of rock glaciers followed the same latitudinal trend as present-day summit permafrost (Figure 1.4). Nowadays, most of these features are relict, but there are some exceptions at surprisingly low altitudes in the Gaspé Peninsula or in the Laurentian Highlands. Putnam and Putnam (2009) identified two inactive rock glaciers with an ice core in Maine, at an altitude of less than 500 m. However, these authors only recorded the underground temperature for one year; therefore one cannot conclude that the ice core lasted for a sufficient duration to be considered to be permafrost.

While there is no evidence of the sustainability of these ice cores beyond one year under present-day conditions, their resilience to summer melting is still surprising at such low altitudes. Cold talus scree slopes exhibiting a cold ventilation mechanism have been found at elevations close to or even lower than the Early-Holocene permafrost altitudinal limits (Figure 1.4). Therefore, even if it is impossible to conclude the interannual sustainability of these ice cores, the existence of sufficient winter frost ground penetration for the onset of a ventilation mechanism in some rock

glaciers and scree slopes at low elevations can be concluded, contributing to the thermal inertia of the cores and delaying the melting, at least, to the end of the thawing season. Because of the sporadic distribution of these ventilation systems in northeastern North America, we can conclude that they are located at the boundary of the climatic conditions necessary for their development. Hence, their onset must be controlled by the local topographic, geomorphologic, and climatic conditions.

Given the latitude of the study region, it is unlikely that discontinuous permafrost is frequent at such moderate elevations. However, these cold scree slopes create favourable conditions for the annual conservation of ice, as reported elsewhere in mountainous environments under the discontinuous permafrost limit (e.g., Morard *et al.*, 2010; Gądek, 2012). This dynamic testifies to the increased complexity associated with local processes such as the ground thermal regime among the paraglacial coarse-grained sediment stocks. More long-term data could permit insight into whether there is an actual (discontinuous) permafrost regime at mid- to low altitudes in the mountains of northeastern North America.

Treeline position. Altitudinal and latitudinal treelines and ecotones are often considered to be sensitive to temperature, and hence to ongoing climate warming (Harsch *et al.*, 2009). However, the increase in the elevation of the treeline in response to climate change is heterogeneous at the global scale. Harsch *et al.* (2009) reported an increase in elevation for 52% of the treelines at the global scale and failed to associate the probability of treeline advance with either mean annual or summer temperature increase, the latter being considered to be the main control over treeline position (e.g., Cogbill and White, 1991). At the Holocene temporal scale, since the establishment of alpine tundra at high elevations (ca. 9,000 BP), climatic fluctuations had significant impacts on lower elevation vegetation assemblages, but they had little influence on alpine plant communities (Spear, 1989). At a smaller temporal scale, diachronic comparisons of treeline position all yield the same results: the treeline is

generally stable but the shrub species cover in the lower alpine tundra increases (Robinson *et al.*, 2010; Capers and Stone, 2011; Dumais *et al.*, 2014). However, the few studies undertaken on the climate of mountain ranges in our study region did not find significant trend in temperature or precipitation for high elevation sites (Seidel *et al.*, 2009; Fortin and Hétu, 2014). At the regional scale, over the last four decades there has been a notable warming trend in the mean annual temperature in Gaspé (0.11 °C per decade; Yagouti *et al.*, 2006) and in the mean winter temperature in the northeastern United States (0.1 °C per decade; Burakowski *et al.*, 2008). However, one has to exercise extreme caution in the extrapolation of general temperature trends to local alpine environments, especially with the quasi-absence of high altitude weather stations with reliable long-term data in the current study region.

Other environmental conditions must control the treeline elevation resilience to climate warming. Carlson *et al.* (2011) report that the alpine environment of the Adirondacks exhibits a spatial pattern that corresponds with the prevailing wind direction, providing further evidence that the alpine treeline of northeastern North America is primarily controlled by winds and winter icing events. The treeline of our study region does exhibit the presence of a wind dominated disturbance regime, since almost every tree community located in the subalpine-alpine ecotone grows in krummholz. At the global scale it can be observed that, contrary to the diffuse treelines, the krummholz treelines fail to exhibit a significant relationship between their upward progression (or lack thereof) and temperature warming (Harsch *et al.*, 2009). The krummholz growth form of trees at the treeline forbidding the production of viable seeds, the lack of suitable germination sites on the mountaintop bedrock and felsenmeers, or the absence of a soil layer have also been mentioned as factors restricting the upward progression of the treeline (Dumais *et al.*, 2014). The presence of permafrost bodies on the concerned summits may also prevent the progression of the treeline to higher elevations. The permafrost system and the treeline system therefore mutually increase the resilience of one another. A permafrost body

underneath a shallow active layer could limit the altitudinal progression of the treeline as reported for latitudinal treelines in Alaska (Lloyd *et al.*, 2002). The absence of trees above the treeline allows for higher wind speeds and greater snow drifting from the summit, which, as was stated earlier, is a key factor in allowing sufficient frost ground penetration for the conservation of the permafrost. The permafrost lying on the summit of these mid-altitude mountains is thus particularly vulnerable and depends on complex interactions between snow cover, vegetation and local climate (Johansson *et al.*, 2013).

Hence, as long as there are rime or ice storms episodes during the winter, the wood abrasion by wind transported ice crystals and the mechanical breakage will prevent the upward progression of the treeline (Rochefort *et al.*, 1994). However, the Northern Hardwood Boreal Ecotone is controlled by temperature, as reported by Beckage *et al.* (2008) who estimate an upslope shift of 2.1 to 2.8 m yr^{-1} in the Green Mountains. It is therefore the subalpine spruce-fir belt that is the most vulnerable. The ongoing warming is expected to contribute to the narrowing of the altitude range of the subalpine spruce-fir belt with an upward displacement of the underlying ecotone (Carlson *et al.*, 2011).

1.4.3 Holocene climate reconstruction in northeastern North American alpine landscapes – discrepancies and the need for a multi-proxy approach

Figure 1.5 compares different indicators of Late-Glacial and Holocene climatic changes in the alpine ranges of northeastern North America. From this synthesis, several statements can be made:

1) Among different ranges across the studied region, there seem to be important differences in the response to global scale Holocene climate fluctuations. There seem to be regional differences between some of the climatic periods across the studied regions. For example, from the vegetation records, there is a lag of approximately 2,000 years for the occurrence of a Mid-Holocene climatic warming between New England and the Gaspé Peninsula.;

2) At local scale, there has been no clear evidence of the Younger Dryas episode from the pollen records of the White Mountains (Spear *et al.*, 1994). Indeed, these records suggest an opposite trend, with the upward progress of the treeline due to shifting prevailing winds mentioned above. Other indicators (i.e., % organic matter, chironomids) showed clearer evidence of the Younger Dryas in the White Mountains synchronously with the Atlantic Provinces, but to a lesser extent (Cwynar and Spear, 2001). The steep topography in the mountain ranges of northeastern North America could reinforce these climatic variations, supported by the orographic effect. There is, however, a lack of data to distinguish how the impacts of the different climatic fluctuations are related to zonal (e.g., latitude) and azonal (e.g., distance to the ocean, topography) variables;

3) On a regional scale, there is also an important difference in the quantity of data available, with some ranges having been studied more thoroughly than others. Alpine environments of northeastern North America are characterized by non-linear responses due to interactions and feedbacks between geological, geomorphological, ecological and climatic factors. This complexity results in singular environments exhibiting a resilient permafrost state despite being at boundary conditions, a unique arctic-alpine flora on the summits, original geomorphic processes such as the frost-coated clast flows (Hétu *et al.*, 1994), climatic particularities like the extreme winds on Mount Washington and puzzling ecological dynamics

like the lowering of the treeline in the Gaspé Peninsula despite the warming trend of the climate. Therefore, a global and thorough understanding of the alpine environment of northeastern North America remains a scientific challenge. In the context of the ongoing climate change, which could result in profound alterations of these systems, it is the opinion of the authors that an integrated and multi-proxy approach (Lotter, 2003) would be necessary to get a valuable prospective view of the evolution of these altitudinal bio-geo-ecosystems.

1.5 Conclusions

Through different case studies, this synthesis underlined the imbricated interactions of Pre-Holocene history with the Late-Glacial and Holocene evolution of climate, biosystems and geosystems leading to the modern alpine landscapes. Regional ice recession and postglacial vegetation establishment followed a south to north temporal trend, with each mountain range displaying a distinct evolution. However, there is a need for further studies on mountain environments to better understand, among others, the origin and evolution of the felsenmeers on the summits of many ranges discussed in this paper, the impacts and duration of cold-based vs warm-based glaciers on the shaping of the alpine landscapes, and the complexity of this environment at the regional scale. Further studies using innovative datation techniques in this study region, such as cosmogenic nuclide dating (e.g. Gosse *et al.*, 2006), Schmidt hammer (e.g. Matthews and Wilson, 2015) or optically stimulated luminescence (e.g. Rémillard *et al.*, 2015) could refine the resolution and enhance our understanding of the evolution of the alpine environment of the Northeast. The case studies presented above show how the complex interactions between the different systems underlie the presence of alpine environments at such low elevations, their

different responses in terms of landscape evolution and of their resilience to climate change. In that matter, a better understanding of past and present-day processes in the alpine environments is central in developing prospective models of mountain landscape evolution in the study region. For example, given the expected rise in the North Atlantic Oscillation (NAO) (IPCC, 2013), one can expect a decrease in avalanche activity in the White Mountains (cf chapter 4), hence a decrease in the fragmentation of the subalpine forest due to subaerial slope processes. However, the expected increase in the intensity of cyclonic activity (IPCC, 2013), coupled with the fact that the authors observed intense debris slide and debris flow activity in the Adirondacks and the White Mountains during the passage of hurricane Irene, leads us to postulate that the ongoing climate changes should increase the fragmentation of the subalpine forest in New England.

The synergistic interactions between the different systems demonstrate the need for an interdisciplinary approach in order to better understand how this unique environment will evolve in the coming decades. Capers *et al.* (2013) recognized this need by doing a survey of scientists from diverse disciplinary fields to establish alpine research priorities in the Northeast, but the bias towards ecology is still apparent in the proposed research projects. The paraglacial concept seems to be a promising framework within which to achieve this interdisciplinary need, since it considers the landscape as a complex system that integrates many feedbacks at different temporal scales (Mercier, 2008). There is a need to broaden its definition further by considering ecological dynamics not only as variables influencing the sedimentary budget, but as an inherent subsystem of the paraglacial environment, and by recognizing the overlapping spatial scales with regards to the temporal duration of the paraglacial period and to its dominant processes. Finally, the synthesis of the climate proxies presented in Figure 1.5 shows that alpine ranges responded differently to major climatic changes and highlights the relevance of a multi-proxy approach in reconstructing past alpine environments. Some hypotheses were

proposed to explain the discrepancies between the different records. The fact that the studies were only conducted locally and many decades apart might be the primary cause of these inconsistencies. The complex systems of alpine environment of the Northeast are characterized by their nonlinear responses. As an example, in some fine-grained scree slopes of the Gaspé Peninsula, due to an increased sediment flux related to frost-coated clast flows over the last decades, the altitude of the treeline is decreasing since the middle of the twentieth century even considering the ongoing climate warming favourable to the growth of the tree cover. In this regard, there is a need for broader-scale multi-proxy research since the uniqueness of the alpine landscapes of northeastern North America holds keys to better understanding past and upcoming environmental changes (Germain and Hétu, *in press*).

Acknowledgements

This research was financially supported by the Fonds québécois de Recherche sur la Nature et les Technologies through a scholarship granted to J.P. Martin. The authors would like to thank Gabriel Magnan, Pierre Richard, Patrick Lajeunesse and especially Michelle Garneau for their thoughtful insights that contributed to this review, as well as André Parent who assisted in the design of the figures.

Tableau 1.1 Physiographic characteristics of different alpine ranges of northeastern North America across a SW (Adirondacks) to NE (Long Range) gradient. Data with an (e) represent rough estimates made by the author using satellite imagery (Google Earth).

Range Name	Surface area (km^2)	Maximal elevation (m)	Area of alpine environment (km^2)	Proportion of alpine environment (%)	Minimal elevation of alpine environment (m)
Adirondacks (High Peaks)	1200	1629	0,7	0,06	1350
White Mountains	3500 (e)	1917	11,3	0,32	1330 (e)
Mount Katahdin	809	1606	7,3	0,90	1200 (e)
Charlevoix Highlands	1000 (e)	1180	2,25 (e)	0,23	700 (e)
Chic-Chocs	950 (e)	1261	45 (e)	4,97	900 (e)
Long Range	4100 (e)	812	>500 (e)	12,19	200 (e)

Tableau 1.2 Sites used in the deglaciation reconstruction.

Range	Location	Latitude (°)	Dated material	Sources
Catskills	Balsam Lake (762 m a.s.l.)	42.1	Inferred from age-depth curve	Ibe, 1985
Adirondacks	Upper Wallface Pond (948 m a.s.l.)	44.1	Pond sediment	Jackson and Whitehead, 1991
White Mountains	Deer Lake Bog (1,325 m a.s.l.)	44.3	Pond sediment	Spear ,1989
Mount Katahdin	Lower Tongue Pond (183 m a.s.l.)	45.9	Lake sediment	Davis and Davis, 1980
Charlevoix Highlands	Lac Malbaie (800 m a.s.l.)	47.8	Peat	Lavoie and Richard, 2000
Chic-Chocs high plateaux	Lac du Diable (494 m a.s.l.)	48.9	Gyttja	Richard et al, 1997
	Lac Côté (915 m a.s.l.)		Organic matter above sand and silt	Lebuis and David, 1977
	Lac Bouliane (992 m a.s.l.)		Gyttja	Richard et al., 1997
Chic-Chocs low plateaux	Lac du Triangle (465 m a.s.l.)	49.2	*Dryas integrifolia* and *Salix herbaceae*	Asnong and Richard, 2003
	Lac Turcotte (457 m a.s.l.)		Marl interbedded with gyttja	Labelle and Richard, 1984
Chic-Chocs coastal valleys	60 m a.s.l.	49.2	*Hiatella arctica*	Hétu and Gray, 2000
Long Range	NA	49.6	NA	Dyke, 2004

Tableau 1.3 Sites used in the paleoecological reconstructions.

Range	Location	Altitude (m a.s.l.)	Latitude (°)	Sources
Catskills	Balsam Lake	762	42.1	Ibe, 1985
Adirondacks	Heart Lake	661	44.1	Jackson and Whitehead, 1991
	Livingstone Pond	850		
	Upper Wallface Pond	948		
	Elk Pass Bog	1,024		
	Lake Arnold	1,150		
	Lake Tear of the Clouds	1,320		
White Mountains	Mirror Lake	213	44.3	Spear et al. 1994
	Lost Pond	625		
	Little East Pond	793		
	Lonesome Lake	831		
	Carter Notch Pond	1,004		
	Kinsman Pond	1,140		
	Eagle Lake Bog	1,275		
	Deer Lake Bog	1,325		
	Lake of the Clouds	1,542		
Mount Katahdin	Upper South Branch Pond	300	45.9	Anderson et al. 1986
Charlevoix Highlands	Lac Malbaie	800	47.8	Lavoie and Richard, 2000
	Lac à l'Empêche	950		Bussières et al. 1996
	Lac des Cygnes Mountain	960		Zimmerman and Lavoie, 2000
Chic-Chocs high plateaux	Lac du Diable	494	48.9	Richard et al, 1997
Chic-Chocs low plateaux	Lac Turcotte	457	49.2	Labelle and Richard, 1984
Chic-Chocs coastal valleys	Lac à Léonard	17	49.2	Labelle and Richard, 1984

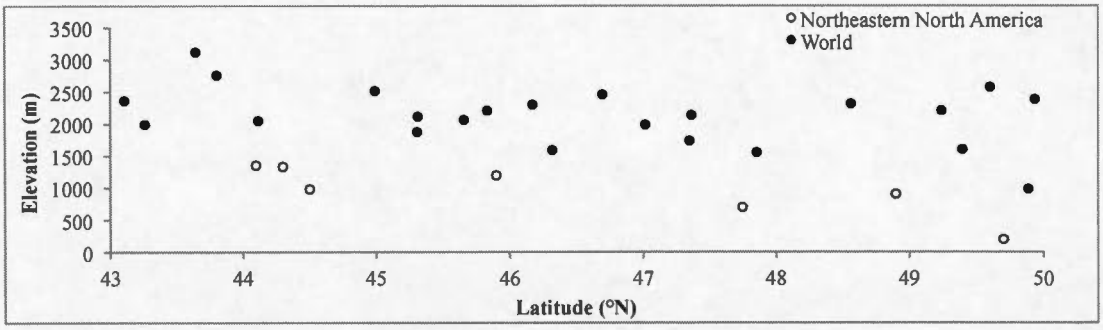

Figure 1.1 Worldwide altitudinal treeline elevation, showing the unique character of northeastern North America. Worldwide data from Körner (1998).

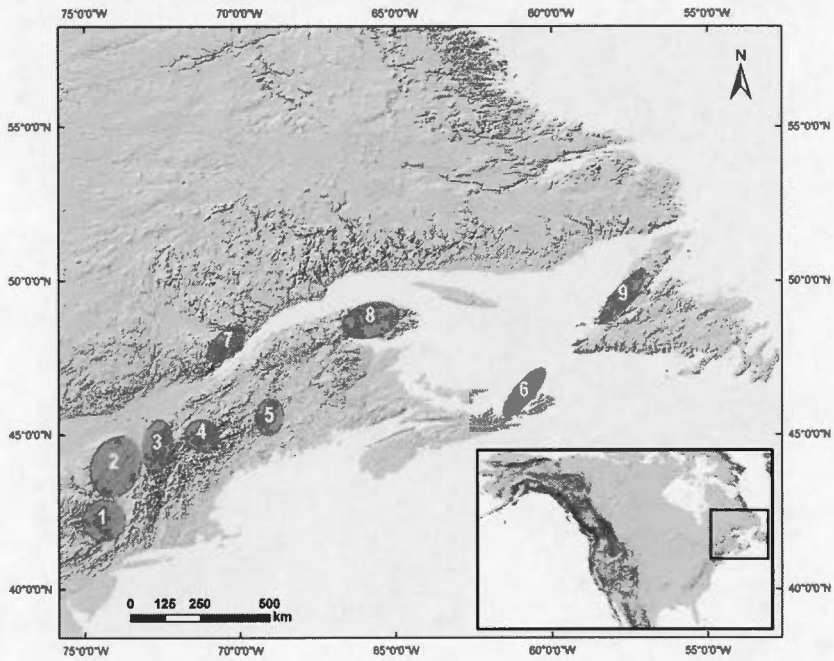

Figure 1.2 Major alpine environments of northeastern North America. 1) Catskills; 2) Adirondack Mountains; 3) Green Mountains; 4) White Mountains; 5) Mount Katahdin; 6) Cape Breton Highlands; 7) Charlevoix Highlands; 8) Chic-Chocs and McGerrigle Mountains; and 9) Long Range.

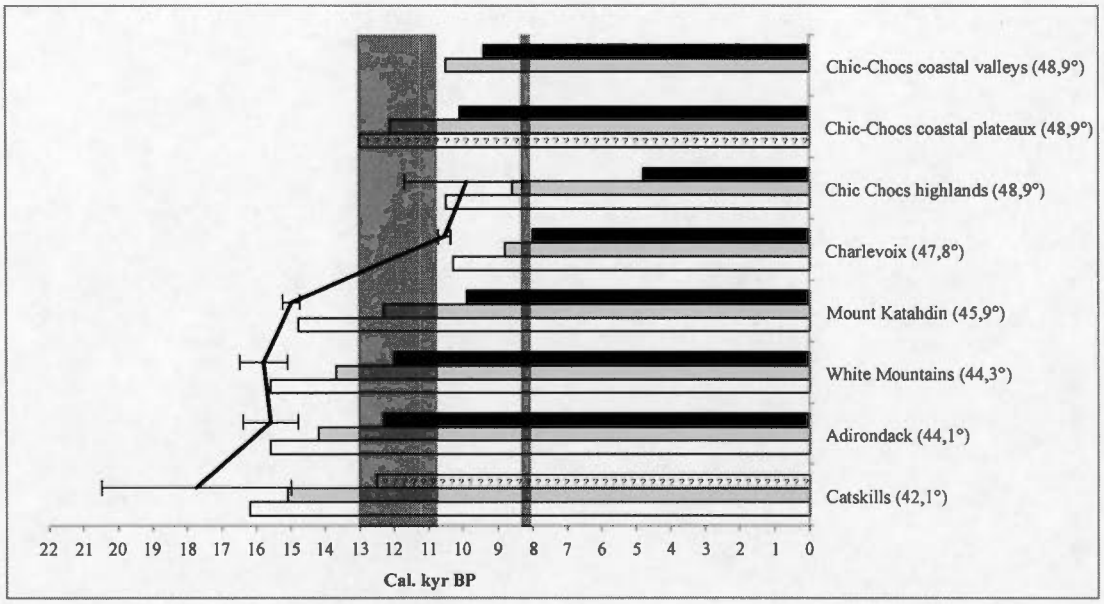

Figure 1.3 Time of establishment of the vegetation stages on different ranges of the northeastern North America. The white line represents the tundra stage (unavailable for the Chic-Chocs coastal plateaux), the gray line represents the afforestation stage and the black line represents the closed-forest stage (unavailable for the Catskills). The top two are from Gaspé Peninsula lowland. The gray boxes represent Early Holocene cold episodes. The black trendline represents minimum glacial recession age, with error bars related to either different data sources or from radiocarbon calibration.

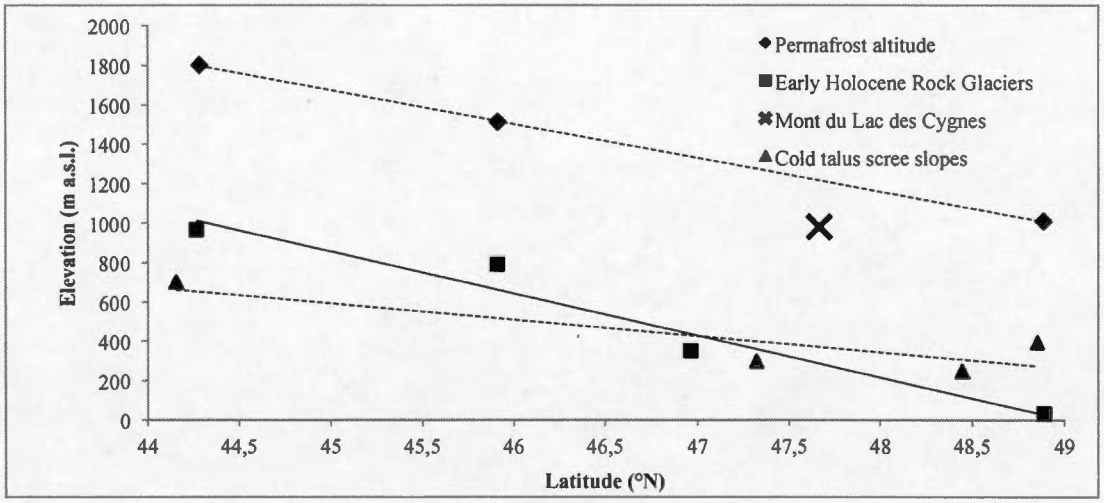

Figure 1.4 Modern and paleo-permafrost elevation following a latitude gradient. The dashed lines represent the modern elevation of permafrost and of cold talus scree slopes. The solid line represents the Early-Holocene elevation of permafrost, as inferred from rock glacier elevations. Even today, the ventilation system of the cold scree slopes provides them with sufficient thermic resilience to exist at similar altitudes as the Early-Holocene rock glaciers. (Data from Putnam and Putnam, 2009)

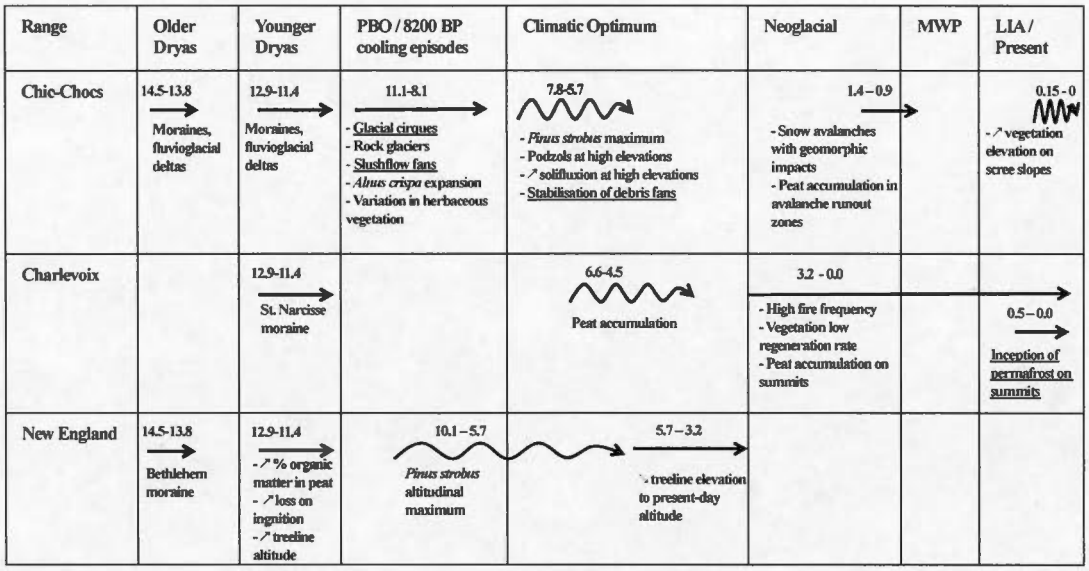

Figure 1.5 Climatic indicators of the different alpine regions of northeastern North America Straight arrows represent indicators of colder episodes. Underlined events represent hypothesis. Waved arrows represent indicators of warmer episodes. PBO: Pre-Boreal Oscillation; MWP: Medieval Warm Period; LIA: Little Ice Age. Sources: Chic Chocs (Labelle and Richard, 1984; Richard and Labelle, 1989; Hétu and Bail, 1996; Lafortune et al., 1997; Richard et al., 1997; Hétu and Gray, 2000; Germain, 2005), Charlevoix (Bussières et al., 1996; Lavoie and Richard, 2000; Zimmermann and Lavoie, 2001; Occhietti, 2007), mountain ranges of New England (Spear, 1989; Jackson and Whitehead, 1991; Spear et al., 1994; Miller and Spear, 1999; Thompson et al., 1999; Cwynar and Spear, 2001)

CHAPITRE II

CAN WE DISCRIMINATE SNOW AVALANCHES FROM OTHER DISTURBANCES USING THE SPATIAL PATTERNS OF TREE-RING RESPONSE? CASE STUDIES FROM THE PRESIDENTIAL RANGE, WHITE MOUNTAINS, NEW HAMPSHIRE, UNITED STATES.

Jean-Philippe Martin[1] and Daniel Germain[2]

[1]Environmental sciences Institute, Université du Québec à Montréal, C.P. 8888 Succursale Centre-Ville, Montréal, Québec, Canada.

[2]Geography Department, Université du Québec à Montréal, C.P. 8888 Succursale Centre-Ville, Montréal, Québec, Canada.

Article publié dans *Dendrochronologia* (mars 2016, volume 37, numéro 2, pages 17-32, http://dx.doi.org/10.1016/j.dendro.2015.12.004)

Résumé

La dendrogéomorphologie est reconnue comme une technique permettant de reconstituer l'activité avalancheuse passée, particulièrement dans les régions où il y a absence d'archives historiques. Ceci a provoqué une multiplication des études sur les avalanches de neige reposant sur l'analyse des cernes de croissance des arbres. Or, à l'intérieur de la communauté scientifique, on note encore aujourd'hui une absence de consensus quant aux procédures dendrogéomorphologiques appliquées à la reconstitution des mouvements de neige. Cette étude illustre quatre études de cas reliées à cette méthode rencontrées sur des données issues de 293 arbres échantillonnés dans 4 sites différents dans les White Mountains (New Hampshire, États-Unis). 1) La séparation de notre échantillon en sous-groupes représentant l'amont et l'aval de la zone d'arrêt des avalanches a permis une reconstitution plus exhaustive de l'activité avalancheuse. 2) Par ailleurs, un signal dendrochronologique très fort enregistré à l'abris des avalanches a été attribué à la surcharge nivale lors d'un hiver où l'enneigement exceptionnel avait une période de récurrence supérieure à 100 ans. 3) En plus des perturbations climatiques, les perturbations écologiques comme les châblis peuvent causer des réponses anatomiques similaires aux avalanches de neige, surtout qu'un couloir d'avalanche agissant comme un tunnel de vent favorise l'occurrence de ce processus dans la zone d'arrêt des avalanches. L'échantillonnage en transects peut permettre de déterminer la limite entre la réponse dendrochronologique issue des mouvements de neige de celle causée par les châblis. 4) À un site où se produisent à la fois des avalanches de neige et de l'activité torrentielle au début du printemps, le patron spatial du signal dendrogéomorphologique inhérent à ces deux processus sera suffisamment distinct afin de permettre de les discriminer dans la reconstitution des chronologies. Ces études de cas démontrent l'importance des patrons spatiaux dans la réponse dendrochronologique et pourraient permettre de mieux comprendre les interractions entre les différents processus sus-mentionnés sur les versants raides situées à l'interface entre le milieu alpin et la forêt subalpine.

Mots clés :

Avalanches; Dendrogéomorphologie; Cernes de croissance; White Mountains; Multi-processus; Perturbations écologiques

Abstract

Dendrogeomorphology has been recognized as a useful tool to reconstruct past snow avalanche chronologies, especially in remote areas where archives are non-existent. In recent years, there have been a multiplicity of snow avalanche studies based on tree-ring analysis. Yet, the dendrogeomorphic procedure applied to snow avalanches still lacks consensus within the scientific community. This paper illustrates four issues regarding this method encountered on a dataset encompassing 293 trees sampled from 4 sites in the White Mountains (New Hampshire, United States). 1) Separating a sample in an upslope and downslope subgroup allowed to reconstruct a more thorough avalanche chronology. 2) On the other hand, a strong response at a site sheltered from any avalanche track was attributed to extreme snow loadings with a return period well above 100 years. 3) In addition to climatic disturbances, ecological disturbances such as windthrows can cause an anatomical response in the trees similar to snow avalanches. An avalanche track might act as a wind tunnel, making the underlying runout zone a suitable site to windfalls. Sampling in transects can assist in determining the limit between avalanche-related and wind-related disturbances. 4) Early-spring torrential floods and avalanche activities at a multi-process site exhibit distinct spatial patterns in the dendrogeomorphological response that allow discrimination between the two processes in the reconstruction of past chronologies. While the dendrogeomorphologist should be cautious of these issues, their acknowledgement is an opportunity to understand the interactions between the different ecological, climatic and geomorphological processes operating on the forested slopes in the alpine-subalpine environment.

Keywords

Snow avalanche; Dendrogeomorphology; Tree-ring; White Mountains; Multi-processes; Ecological disturbances

2.1 Introduction

The term dendrogeomorphology was defined by Alestalo (1971) as "*the analysis of growth reactions of trees affected by geomorphological processes by dendrochronological methods*". Since then, tree-ring analysis has become an accepted technique applied to several geomorphic and geological phenomena (cf Solomina, 2002; Speer, 2010; Stoffel *et al.*, 2010). The approach is based on datable disruptions in the ring pattern that occur: (i) when the environment surrounding a tree changes or, (ii) when the tree is damaged, i.e., scarring, broken branches, foliage loss, or tilting. In recent years, there has been an increasing number of studies on snow avalanches using tree-ring analysis to reconstruct years of avalanche activity (e.g., Boucher *et al.*, 2003; Muntan *et al.*, 2004; Casteller *et al.*, 2007; Laxton and Smith, 2009; Garavaglia and Pelfini, 2011), to identify the weather scenarios responsible for the triggering of regional snow avalanche activity (e.g., Dubé *et al.*, 2004; Germain *et al.*, 2009; Muntan *et al.*, 2009, Casteller *et al.*, 2011), to calibrate avalanche models (e.g., Casteller *et al.*, 2008; Eckert *et al.*, 2013; Schläppy *et al.*, 2014) or to analyze the impact of ecological and anthropogenic disturbances on snow avalanche regimes (e.g., Germain *et al.*, 2005). Since the pioneer works in dendrogeomorphology (Potter, 1969; Mears, 1975; Burrows and Burrows, 1976; Shroder, 1978, 1980; Butler, 1979; Carrara, 1979), it has been recognized as a useful tool to provide a better understanding of snow avalanches, particularly in regions where historical documentation is lacking, and to characterize the relative hazard degree in mountainous environments for risk determination and mapping (Salm, 1997; Lerner-Lam, 2007).

There have been many recent studies (e.g., Heinrich *et al.*, 2007; Butler and Sawyer, 2008; Germain *et al.*, 2010; Corona *et al.*, 2012; Stoffel *et al.*, 2013, Chiroiu *et al.*, 2015) concerning tree-ring analysis methodology applied to snow avalanches, but

consensus is still lacking. Indeed, the accuracy of this methodology has yet to be examined (Luckman, 2010), particularly in regard to other forces, such as soil creep, snow creep, and wind, which may contribute to observable impacts on tree rings. With this in mind, and considering the methodological and statistical developments in dendroclimatology as well as our understanding of spatiotemporal sensitivity and the non-stationary responses of trees to climate (i.e., Briffa *et al.*, 1998; Loehle, 2009, Leonelli *et al.*, 2011, Housset *et al.*, 2015), it is surprising that many of these issues with dendrogeomorphology are still poorly documented. The fact that dendrogeomorphology is now a sub-discipline of tree-ring analysis, but with its own original methods of investigation (Stoffel *et al.*, 2013), may partially explain this methodological weakness, considering that the only studies which compared tree-ring inferred avalanche activity with historical archives only succeeded in reconstructing $\leq 40\%$ of avalanche years (Butler and Malanson, 1985; Reardon *et al.*, 2008; Kogelning-Mayer *et al.*, 2011; Corona *et al.*, 2012; Schläpply *et al.*, 2013). Indeed, small avalanches might not have a sufficiently long runout or the destructive capacity to be recorded by trees. As for higher magnitude events, they can destroy earlier evidences of avalanche activity (Germain *et al.*, 2009).

Some authors warn us about the validity of avalanche chronologies in sites affected by other geomorphic (e.g., torrential floods, debris flows, etc.), ecological (e.g., windthrows, epidemics, fires, etc.) or climatic (e.g., ice storms, snow loading, etc.) disturbances (e.g., Stoffel *et al.*, 2013). There is however a lack of data-based evidence to support the fact that the dendrochronological responses of these different disturbances can be discriminated from the snow avalanche signal in the tree rings. Dendrochronology has been recognized as a useful tool for avalanche risk assessment in areas where no historical archives exist on the occurrence and extension of past snow avalanches. Moreover, many of these avalanche paths are also affected by other disturbances. In that regard, there is a need to explore the possibilities of discriminating different disturbances from snow avalanches in tree-ring series. A

method to differentiate tree-ring signals induced by avalanches from those by debris flow was developed using the position of the reaction within a tree-ring (Stoffel *et al.*, 2006). The authors inferred that if the reaction is located in the dormant wood or the early-earlywood, the response was caused by a snow avalanche, whereas responses located in later during the growth season were attributed to debris flow. However, this time and resource-consuming method is limited in the discrimination of disturbances co-occurring during the dormant season. For example, a late-spring snow avalanche or torrential floods related to the melting of snow could both occur before or at the very beginning of the growth season.

The aim of this paper is to test whether it is possible to isolate the dendrochronological signal caused by snow avalanches from other disturbances in different avalanche paths of the White Mountains (New Hampshire, United States). First, in a forested environment where the runout zone is not clearly defined and where it can be located on slopes > 10°, collecting samples to the extreme limit of the runout zone can give precious information about the spatial extension of major avalanches. However, most methods in the literature on tree-ring data applied to snow avalanches use a threshold of impacted trees above which one can infer avalanche activity for a given year. Collecting samples until the extreme limit of the runout zone can dilute results from smaller avalanches in the noise of the growth disturbance (GD) time-series. Therefore, even a sampling network covering the entire runout may not allow to develop a representative chronology of avalanche events. We thus test whether we could build a more complete chronology by treating different subsamples in a same path affected by an extreme avalanche. Second, the 1969 winter, where the extreme snowfalls correspond to a 325-year return period, provides an opportunity to compare the signal from extreme snow loading to the disturbance in snow avalanche couloirs. Third, a windthrow next to a closed forest that was disturbed by a snow avalanche in 1969 allows the evaluation of the difference in the tree-ring response. This is especially relevant in a mountain environment such as Mount Washington,

where the strong winds have an important ecological impact on the forested slopes. Finally, we question whether spatial patterns of tree-ring response can lead to the discrimination of avalanche-related dendrochronological signal from torrential floods occurring in early spring. Indeed, major floods occurred statewide in 1987 and 2007 springs; these events were likely to have caused torrential erosion in mountain environments. At a larger scale, since 1951, in New England, the months of March, April and May exhibit the highest annual flood relative frequency following either rainstorms, rain-on-snow or a combination of rainstorms and snowmelt (Collins *et al.*, 2014).

2.2 Regional setting

This study was carried out on different avalanche paths in the Presidential Range of the White Mountains (New Hampshire, United States, 44°16' N 71°18' W, Figure 2.1). The highest summit, Mount Washington (1,917 m a.s.l.), is located in the Presidential Range, a North to South oriented ridge of 2748 ha above treeline. Most avalanche paths in the range are located in Pleistocene glacial cirques all around this alpine ridge and extend into the subalpine red spruce-balsam fir forest. As a result of the intense winter activity by backcountry skiers and alpine climbers, and of the spatial variability of avalanche regimes (Joosen, 2008), a micro-scale forecasting by the United States Forest Service (USFS) Snow Rangers has provided daily avalanche conditions for the different avalanche paths in the two most visited cirques since the winter of 1959. However, the avalanche database only begins in 2006 and there is no record of activity prior to that date. A retired USFS Snow Ranger recalls the unique avalanche activity of the 1969 winter, during which important snowfalls (1,394 cm on Mount Washington summit) caused extreme runouts in many avalanche paths of the Presidential Range.

The average winter temperature (December–April) on the summit of Mount Washington is -11.8 °C. The precipitation from November to April falls primarily as snow, with an annual amount of 714.2 cm. Mount Washington is known for its extreme winds, with monthly recorded peak gusts above 200 km/h for every month. In winter, the summit station records hurricane strength gusts (119 km/h) on average for two days out of three (Gordon, 1989). Due to snow drifting, there is frequently high avalanche danger associated with a 5-7 cm snowfall and high winds (Joosen, 2008). In 1987 and 2007, heavy rain in April associated with snowmelts caused statewide floods in New Hampshire (Fontaine, 1987; Flynn, 2008). During both of these events, peak discharges equalled or exceeded the 100-year recurrence interval at stream gages close to Mount Washington. This study presents tree-ring chronologies from four sites on the eastern side of Mount Washington (Figure 2.1). The physiographic characteristics of each site are presented in Table 2.1.

2.2.1 Hillman's Highway (HH)

Hillman's Highway (HH) is a confined avalanche track comprising two different starting zones. Because they are located downhill from a large alpine plateau, they are prone to accumulate snow drifting. Avalanches of low magnitude occur yearly. Indeed, the USFS Snow Rangers witnessed 42 avalanches between 2006 and 2012. Early-winter avalanches generally stop higher in the track and as the winter progresses, the snow avalanches run farther downhill. Retired Snow Rangers confirmed the occurrence of an extreme avalanche in 1969. During the 2008 winter, Snow Rangers reported a class 4 avalanche on the Canadian avalanche danger scale (Schaerer and McClung, 2006) that destroyed 16 000 m^2 of forest in the runout zone. The different spatial extents of the runout of these two events are visible on aerial photographs (Figure 2.2). Moreover, the absence of gullies or channels confirmed the

information given by the Snow Rangers that there were no other slope processes disturbing the forest in the runout zone. The vegetation in the upper runout zone is composed of heavily impacted dwarf *Abies balsamea* (L.) Mill. The middle part, which was opened by the 2008 snow avalanche, is an open land colonized by herbaceous species with sparse fallen dead trees. An open forest composed almost exclusively of *Abies balsamea* covers the lower part.

2.2.2 Reference Chronology (CR)

A reference chronology was sampled at site CR (1160 m), which is sheltered from the wind and snow drifting but is located at a similar altitude than the other runout zones. This location was chosen to test whether the signal from snow loading interferes with avalanche activity. Both active and former USFS Snow Rangers confirmed that they never witness an avalanche at this location, which is located next to a trail that they use on a daily basis during winter.

2.2.3 Raymond's Cataract (RC-RC2)

Raymond's Cataract (RC–RC2) has a wide, shallow starting zone. Avalanches seldom occur in the part of the drainage above treeline. Between 2006 and 2012, the USFS Snow Rangers recorded four events; none were of sufficient magnitude to reach the treeline. A former Snow Ranger reports that during the winter 1969, an avalanche ran down through the forest and crossed the trail (Figure 2.1). RC is located upslope from the trail in an open forest mostly composed of *Abies balsamea* on a humic soil where decayed trees oriented parallel to the slope are still partially

visible. RC2 is located downslope from the trail next to a windthrow that was identified on recent aerial photographs (Figure 2.1). The forest is denser than at RC and is mostly composed of *Abies balsamea*.

2.2.4 Gulf of Slides (SM)

The third avalanche path (SM) is located in a glacial cirque South of the other sites. Its location is below a ridge, which makes it less prone to accumulate westerly snowdrifts than HH. Torrential activity resulting from the action of fast-flowing stream eroded the center of the runout zone in a v-shaped, 2 m deep channel, hence the question whether torrential activity occurred during the major floods of 1987 and 2007. Vegetation on the right bank of the stream is composed of an open forest of mature *Abies balsamea*. A denser forest of younger balsam fir covers the left bank. This site is positioned outside of the avalanche-forecasting zone of the USFS Snow Rangers who nonetheless confirm that there is indeed avalanche activity at this location.

2.3 Methods

The methods presented below follow a similar protocol to many recent dendrogeomorphic investigations (e.g., Dubé *et al.*, 2004; Stoffel and Bollschweiler, 2008; Germain *et al.*, 2009; Stoffel *et al.*, 2013) with regards to the sampling strategy, the preparation of the samples, and their laboratory analysis.

2.3.1 Collection and preparation of samples

The major avalanche paths around Mount Washington were identified following a discussion with the USFS Snow Rangers who are responsible for the avalanche forecasting as well as the search and rescue. Site HH was selected for the clear identification of the extent of the runout zones of 1969 and 2008 on aerial photographs. Sites SM and RC were selected based on the presence of a second disturbance, torrential flooding and windthrow, respectively. The absence of disturbance by snow avalanches or any other slope process was the criterion to choose site CR. Snow avalanches of small magnitude flow annually in some of the studied avalanche paths. The sampling effort was thus concentrated further in the runout zones to gather information on the low-frequency high-magnitude events.

At sites SM and HH, trees that showed external damage (e.g., scars, broken branches, loss of apical dominance, toppling or tilting) were sampled. For trees of smaller diameter (approximately 15-20 cm), especially in the presence of a scar, a stem disc was collected at the height of every visible impact. Trees of larger diameter were cored at the height of the external damage, or at breast height if the latter was too high. A minimum of two cores were collected per tree – one uphill and one downhill. When a scar was visible, a lateral core was collected through the callus growth adjacent to the scar and another one was collected on the downhill side. For each tree, sampling height, diameter at breast height and a description of damages with pictures were collected. The position of the tree was recorded using a GPS. At site HH, we sampled 62 trees; half of this sample was collected around the clearing caused by the 2008 avalanche and the other half was collected further downslope in the zone identified as being impacted by the avalanche of 1969 (Figure 2.2). At site SM, we sampled 63 trees from the forest on the edge of the avalanche track until no visual clues of avalanche impact were visible on the adjacent forest. Since visual clues of

avalanche activity were almost absent at these sites, RC and RC2 were 20 m x 3 m (RC) or 30 m x 3 m (RC2) transects perpendicular to the avalanche flow where every tree was sampled. In order to test whether the dendrochronological signal from the windthrow decreases to reveal the signal from another disturbance (snow avalanches in the present case), the location of transect RC2 was selected next to the windthrow in a forest that looked homogenous. At site CR, trees that were not impacted by any slope processes in appearance were randomly selected and cored. The presence of healthy piths, which is quite rare on >100 years old balsam fir (*Abies balsamea* (L.) Mill) in this region, determined if a sample was kept or rejected. In the entire study, 474 samples (240 cores and 234 discs) were collected on 293 different trees (Table 2.5).

Samples were dried and sanded, then analyzed visually under a binocular microscope to identify and date GDs. The GDs were defined as the presence of scar tissue, the onset of compression wood, significant growth reductions and the presence of traumatic resin ducts (TRD). Each GD was assigned a score which takes into consideration the quality of the indicator following the approaches found in many recent dendrogeomorphic studies (e.g., Germain *et al.*, 2005; Reardon *et al.*, 2008, Corona *et al.*, 2010; Schläppy *et al.*, 2013). The selection criteria for the different score classes are described in Table 2.2, following guidelines by Corona *et al.* (2010) and subsequently used by different authors (e.g., Schläppy *et al.*, 2013; Chiroiu *et al.*, 2015).

2.3.2 Age structure

The age of every tree sampled was estimated by counting the number of tree rings on the sample taken at the lowest height on this tree. Therefore, the age of trees refers to

the minimum age at sampling height. The age of the stand – as well as the annual probability presented below – were then estimated by using an inverse distance weighted interpolation using ArcGIS 10.1. Since trees were not sampled at their stem base, the age structure is biased and represents a rough estimate of the germination dates. Nonetheless this method was shown to provide insights into the spatial distribution of major disturbance events with reasonable precision (Lopez Saez *et al.*, 2012).

2.3.3 Reconstruction of snow avalanche chronology

Since avalanches leave high-intensity impacts compared to other processes (e.g., snow creeping; Stoffel and Corona, 2014), low impact indicators of Classes 1, 2 and 3 were discarded for further analysis. For every year t at each site, an index I_t was calculated based on the percentage of trees that show GD over the number of trees alive at year t (Shroder, 1978):

$$I_t = \left(\frac{\sum_{i=1}^{n}(R_t)}{\sum_{i=1}^{n}(A_t)}\right) \times 100 \quad (1)$$

where R_t represents the binary response of a tree showing a high-impact GD at year t and A_t represents the number of trees alive at year t. The data were then summarized in event-response diagrams (Shroder, 1980). Although different thresholds are used in the literature to discriminate years with snow avalanche activity (e.g., Chiroiu *et al.*, 2015), the objective of this article is not to make an absolute inference about the presence or absence of an avalanche at year t, but to observe the variation in the dendrogeomorphological response to different factors. We thus chose to use the $I_t \geq 10\%$ threshold and a minimum of 10 trees given its extensive use in the literature

(e.g., Dubé *et al.*, 2004; Butler and Sawyer, 2008; Reardon *et al.*, 2008; Germain *et al.*, 2009; Butler *et al.*, 2010; Decaulne *et al.*, 2014).

For the sampling sites HH and SM, the samples were separated in two subsamples of trees located upslope or downslope. The purpose was to test if there were events only recorded in a specific region of the sampling zone. While we acknowledge that two independent groups would have been better, sampling restrictions (impacted trees, permission by the USFS) limited the depth to 63 trees. Each group was formed with approximately 40 trees, following a natural break in the sampled tree altitude (i.e., we did not separate two trees at the same altitude). The trees located in the middle of the runout zone were in both groups, since a sample size above approximately 40 trees does not increase substantially the probability of detecting any avalanche (Germain *et al.*, 2010).

2.3.4 Calculation of return period and annual probability

The return period is defined as the average time interval at which the snow reaches a given point in an avalanche path (Schaerer and McClung, 2006). Using tree-rings it is designated as the mean time interval between two GD sequences in a given tree:

$$R_i = \frac{Y_i}{\sum_{i=1}^{n}(GD)} \quad (2)$$

where R is the return period and Y is the age of the i^{th} tree. While sensitive to the age of the tree, this approach has shown to provide useful information about the return period of avalanches at different points of the runout zone (Corona *et al.*, 2010; Lopez Saez *et al.*, 2012).

The probability of occurrence of an avalanche at a given point should theoretically be modeled using a Poisson distribution. Indeed, the frequency of avalanches of sufficient size to impact trees can be considered as a series of rare, discrete and independent events, and thus matches the assumptions of a Poisson distribution (Smith and McClung, 1997). The probability for an event with a given return period to occur in a given number of years (fixed to 10 years – close to the average return period of recorded avalanches) was calculated for site SM as follows:

$$p_i = 1 - \left(\frac{-N}{R}\right)^e \quad (3)$$

where p is the probability of occurrence, N is the number of years and R is the return period (Lopez Saez *et al.*, 2012). These annual probabilities were then spatially interpolated using an inverse distance weighted interpolation algorithm using ArcGIS 10.1.

2.3.5 Weather analysis

Total snow accumulation for each winter at Pinkham Notch, at the base of Mount Washington (619 m a.s.l.), was calculated from the monthly data acquired from a National Weather Service (NWS) cooperative station operated by the Appalachian Mountain Club (AMC; COOP #276818, NCDC station ID 20018701, NWS Location ID HGMN3). For a similar time period, total snow accumulation for each winter was also calculated for the Mount Washington summit from the daily data acquired by the weather station operated by the Mount Washington Observatory. However, until 2013, solid precipitation measurements were acquired using a snow gage. Since the summit of Mount Washington is known for its high winds, the accuracy of this data is doubtful. Longer-term series are not available from moderate to high elevation

weather stations in New Hampshire. Total annual snow accumulation for the period 1870–2011 was acquired from the NWS Forecast Office based on weather stations at Concord, New Hampshire (88 m a.s.l.). Finally, to verify the impact of the aforementioned early spring floods on the tree-ring record, the April maximum 72-hour liquid precipitation was calculated from the daily data of the Pinkham Notch weather station (Table 2.3). For each of these records, the return period of the most extreme events was calculated following the best fit between a normal and a Gumbel distribution.

2.4 Results

2.4.1 Age structures

Table 2.4 presents some characteristics of the age structures of the different sites. HH, SM and RC2 exhibit large intervals between the youngest and oldest tree as well as important standard deviation to mean ratios. Trees are generally older at site CR. RC presents the younger age structure with the smallest standard deviation. Figure 2.3 presents the interpolated age structures of the stands. At site HH (Figure 2.3a), trees upslope are younger and the average age increases downslope. The youngest trees at sampling height were located in the upper part of this site. At site CR (Figure 2.3b), there is no clear pattern following the topography in the age structure. Younger trees were generally located on the border of the clearing and on the side of the trail. Site RC exhibits an heterogamous pattern with younger and older trees spread uniformly along the transect. As for site RC2, there is a drastic change in the age structure in the middle of the transect, with the trees on the southern section (mean: 83.4 years; SD: 36.9 years, n=30 trees) being significantly older than the trees on the northern side

(mean: 40.6 years; SD: 17 years, n=30 trees). Both sites are located far into the runout zone (approximately 1,050 m (RC) and 1,300 m (RC2)) on relatively plane surfaces (9° (RC) and 7° (RC2)). However, the small sample sizes advocate for caution in the interpretation of the spatial interpolations.

2.4.2 Tree-ring analysis

From the sites CR, RC, RC2, HH and SM, 1,233 GDs were identified, 461 of which were considered strong avalanche indicators (Class 4 or 5) (Table 2.5). This makes an average of 4.21 (all GDs) and 1.57 (Class 4 or 5) GDs per tree. GDs of Class 3 were the most frequent (547 counts), followed by the GDs of Class 4 (377 counts) (Table 2.5). The former and GDs of classes 1 and 2 were excluded, because high-intensity GDs (classes 4 or 5) have been demonstrated to allow doubtless dating of avalanche events (Corona *et al.*, 2012). It is possible than GDs of lower classes are still valid avalanche indicators. However, given the possibility for other, weaker, disturbances of higher frequency on Mount Washington (e.g., rime ice, snow creeping, wind gusts, blizzards, etc.), a strict criterion was necessary to respect the objective of focusing on high-magnitude avalanches and co-occurring disturbances.

2.4.2.1 Hillman's Highway (HH)

From the whole sample (N=62), the 122 identified high-impact GDs allowed to reconstruct 3 avalanche years: 1952, 1969 and 1977 (Table 2.5 and Figure 2.4a). Since the sampling was made deep in the runout zone, the sample was then divided in an uphill and downhill subsample, with some of the trees located in the middle of the

sampling zone being included in both subsamples to meet the approximate sample size of 40 trees suggested by Germain *et al.* (2010). From the uphill subsample, the years 1939, 1952, 1958, 1969, 1993 and 2008 were considered avalanche years, being above the 10% I_t threshold (Figure 2.4b). In the downhill subsample only the years 1952, 1969 and 1993 were above the 10% I_t threshold to determine avalanche activity (Figure 2.4c).

2.4.2.2 Reference Chronology site (CR)

The reference chronology site exhibits a significantly lower quantity of high impact GDs (22) than the other sites (Table 2.5), even if its trees are generally older (Table 2.4). Also, only one scar was recorded, every other high impact GDs being sequences of reaction wood of ≥ 3 years. This is due to its sheltered location away from any avalanche paths, and thus the absence of a disturbance that can cause mechanical damages. However, the presence of many growth disturbances coupled with its topographic situation suggests that other processes still disturbed this site. Two significant years with an I_t value above 10% were identified: 1874 (2 GDs) and 1969 (7 GDs) (Figure 2.5). In 1874, the number GDs (two on widely separated trees) may be too low to be conclusive. However, in 1969, the results would be above common GD thresholds (Corona *et al.*, 2013).

2.4.2.3 Raymond's Cataract transects (RC-RC2)

In the RC transect, the 55 high-impact GDs allowed the reconstruction of the 1969 avalanche year (Table 2.5 and Figure 2.6a), which was confirmed by a retired USFS

Snow Ranger who was active back then. In the RC2 transect, the 71 high-impact GDs allowed the reconstruction of two avalanche years: 1969 and 1982 (Table 2.5 and Figure 2.6b). If the RC2 transect is separated in two subsamples: the northern and the southern part; they both exhibit different patterns. On the northern side, 1996 is the only year with an I_t above the 10% threshold (Figure 2.6c). On the southern side, 1948, 1969, 1971, 1973 and 1982 are above the threshold and therefore should be identified as avalanche years (Figure 2.6d).

2.4.2.4 Gulf of Slides (SM)

Of the 63 trees sampled at SM, 191 high-impact GDs were identified (Table 2.5), going back to 1889. The years 1903, 1924, 1937, 1952, 1958, 1969, 1982, 2001 and 2008 were above the threshold and thus considered avalanche years (Figure 2.7a). Using only the 39 trees uphill, all the aforementioned years were present in the avalanche years reconstruction, with the addition of 1931, 1943, 1977 and 2003 (Figure 2.7b). A more complete chronology in the uphill section is coherent with the dynamic of snow avalanches. Indeed, avalanches of higher magnitude will travel further down than more frequent events of smaller magnitude. As several authors pointed out (Reardon *et al.*, 2008; Corona *et al.* 2010), the area covered by the impacted trees for a given year can give an approximation of the spatial magnitude of the event. The uphill-only reconstructed events are therefore interpreted as smaller magnitude avalanches.

Doing the same analysis with the 40 trees located downhill, the years 1937, 2001 and 2008 from the whole site are missing, but the years 1910, 1943, 1987 and 2007 were above the 10% I_t threshold (Figure 2.7c). 1943 is considered an avalanche year in both subsamples, but was absent from the whole sample chronology, since most

impacted trees are located in the overlap zone between the uphill trees and the downhill trees; smaller sample depth increased the I_t value. However, the cases of 1987 and 2007, where an event was exclusively reconstructed in the downhill chronology, are more problematic. Based on their spatial distribution, the general flooding pattern of New England and the floods associated with those years and discussed below, we therefore suspect that spring torrential floods caused them.

2.4.3 Probability map

The probability of an avalanche event being recorded in a 10-year period by a high-impact GD in a tree shows the highest values in the upper section of the runout zone of site SM (Figure 2.8). The probability decreases downslope to the middle of the sampled zone, where it increases again (Figure 2.8a). The lowest annual probabilities were thus located in the middle and at the downhill end of the sampled runout zone. The interpolated age of the forest at site SM followed the same trend, with the oldest trees in the middle of the runout zone as a transition between an uphill and downhill younger forest (Figure 2.8b). To verify the possibility that younger, smaller trees are more likely to show the effects of the impacts than older and thicker, trunk, R^2 value was calculated between the age and the probability. The latter is very low ($R^2 = 0.08$ for the interpolated raster datasets, $R^2 = 0.19$ for the trees). Even if the correlation coefficient associated with the second R^2 value is significant at $\alpha = 0,1$ level, this regression analysis demonstrates that the age of the tree can only explain a small fraction of the variance in the probability of impact recorded by a tree in a 10-year period.

The distribution of the magnitude of the GDs between a suspected avalanche year (1982; Figure 2.8a) and a suspected torrential flood year (1987, Figure 2.8b) differs.

In the latter case, trees showing high-quality GDs are located downslope compared to the former case, where the distribution is more widespread. Contrary to what was expected, trees farther from the channel did record high-quality GDs in 1987.

2.4.4 Weather

Annual total snowfall in 1969 was 323 cm at Pinkham Notch and 1,394 cm on the summit of Mount Washington, which is the maximum value for the 1931–2014 period (Figure 2.9a). Based on this record, the return period for the snowfall of 1969 at Pinkham Notch was estimated at 325 years following a Gumbel distribution ($R^2 = 0.97$). At the low-elevation station of Concord, the winter 1873-1874 holds the record for the highest amount of snow with a total snowfall of 310 cm (Figure 2.9b). The data fitted a Gumbel distribution quite well ($R^2 = 0.95$), but this model overestimated the extreme values. Following a normal distribution ($R^2 = 0.985$), the return period for the snowfall of 1874 is approximately 200 years. The highest amount April 72-hour rain was measured in 1987 (191.7 mm) and 2007 (171.1 mm) (Figure 2.9c). Based on a Gumbel distribution ($R^2 = 0.96$), the return periods were of 275 and 175 years, respectively.

2.5 Discussion

2.5.1 Impact of the spatial extent of the sampling zone on the dendrogeomorphic signal (HH)

The primary objective of the field campaign was to identify the years with high-magnitude avalanche activity, hence the sampling further downhill in the runout zone. Hillman's Highway is a site where the USFS Snow Rangers identified 40 avalanches from 2007 to 2011. Avalanches of a category 3 or above according to the Canadian avalanche danger scale (Schaerer and McClung, 2006), which refers to an avalanche of sufficient power to break trees thus to record GDs, were recorded during this period every year except during winter 2011. Since tree-rings are a proxy with an annual resolution, sampling the upper part of the runout zone would be of little scientific interest considering the steeper slope and the annual frequency of avalanches with a sufficient destructive capacity to damage trees. It is acknowledged that standard dendrogeomorphic investigations include a primary assessment of the extent of the mass movement process using diachronic aerial photographs (Stoffel *et al.*, 2013). This procedure was followed (Figure 2.2), but it is evident that for a site that has been recently affected by an extreme avalanche such as the 1969 event in HH, the choice of sampling all the way over the maximal extent of the runout zone diluted the impacts of smaller avalanches. However, the 2008 event, which had a runout extent of 16 000 m^2, did not create sufficient ecological damage to be recorded in the tree-ring records using moderately severe thresholds.

Interestingly, the 1970 decade had the highest winter snowfall (Figure 2.9) since the beginning of the weather record on Mount Washington summit. However, no avalanche years were recorded between 1969 and 1977, even if snowfall must be the primary factor to explain high-magnitude avalanche activity in a range where most of

the avalanches are triggered by direct weather action (Joosen, 2008). One or both of the following reasons could explain this:

1) The extent of the 1969 clearing of trees was so important that further avalanches were too small to have an impact on the remaining trees localized too far in the runout zone. The 2008 avalanche, which was recorded as a class 4 event in the Canadian avalanche danger scale, created extensive damages to the forest, yet did not reach the limits of the 1969 event. If avalanches of similar magnitude (i.e., class 4) occurred in the decade following 1969, they were likely to not reach a sufficient distance to have an impact on the treeline that was farther downhill.
2) The trees that were not broken by the avalanche of 1969 were already recording a sequence of compression wood. Since the avalanches run following a downslope trajectory, their impacts are preferentially recorded downslope in the compression wood. Minor variations in the angle of compression wood were not taken into account since they can be caused by phototropism or geotropism of a readjusting tree following an avalanche impact. However, the ratio of mechanical damages (mostly scars) to anatomic reactions (mostly compression wood sequences) recorded was similar in 1977 to the other avalanche years. Another evidence that leads to this conclusion is the fact that 3 out of 6 trees that recorded GDs in 2008 also recorded the 1969 avalanche, which means that trees were still standing during this decade higher in the runout zone.

Using the complete dataset for HH, following 1969, on the basis of the $I_t \geq 10\%$ criterion, the only avalanche year that would have been identified would be 1977 for which the dendrogeomorphic signal was stronger downslope than upslope (Figure 2.4b and c). Indeed, out of the six trees that presented a class 4 or 5 GD in 1977, four are located close to the boundary of the 1969 avalanche, and two are located inside

the runout zone of the 2008 avalanche. We suppose that the trees in the upper part of the runout zone were either too young to record high-impact GDs or were still recording a wood reaction sequence from the 1969 avalanche. Moreover, the opening in the forest in 1969 would allow the subsequent avalanches to reach farther (Germain *et al.*, 2005), thus the higher quantity of responses in the downslope part of the sampling zone.

This example thus shows that while sampling in the upper runout zone seems to allow the identification of a higher number of avalanche years (Figure 2.4b), there is a possibility that some events following the occurrence of an avalanche of extreme magnitude will not be identified because of a lack of trees able to record a dendrogeomorphic signal (e.g., trees too young or already recording the signal from the previous avalanche). The division of the sample into an upslope and downslope group seems to be a promising approach to increase the quantity of avalanches that we can identify using tree-rings.

2.5.2 Climatic disturbances (CR)

The older age structure at site CR (Table 2.4), as well as the spatial distribution of tree ages (Figure 2.3b) indeed demonstrates that the forest at site CR is less disturbed than the other sites. This clear distinction in the age structure is not surprising, since it was not affected by the high-magnitude avalanche cycle of 1969. However, site CR exhibits important responses for the years 1874 (I_t = 14.28%; GD = 2) and 1969 (I_t = 14.28%; GD = 7) (Figure 2.5). The response in 1969 would be important enough to infer avalanche activity using a 10% threshold, a double threshold of $I_t \geq 5\%$ and GD $\geq$ 5 (Corona *et al.*, 2013; Stoffel *et al.*, 2013), a classification tree procedure (Schläppy *et al.*, 2013), or a $10 \cdot n^{-1}$ threshold with the *lev* criteria (Casteller *et al.*,

2011). Moreover, ordering the intensity of the GD in five different classes is supposed to prevent the identification of other disturbance of lower magnitude, such as snow creeping, in the tree-ring record (Butler and Sawyer, 2008; Corona *et al.*, 2012; Stoffel and Coronal, 2013). However, as Bégin and Boivin (2000) point out, a single-orientation sequence of reaction wood is a normal response of trees to heavy snow load episodes. Therefore, given the extreme snowfalls with > 100-year recurrence periods in 1874 and 1969, and the fact that with the exception of one out of 21 trees, every high-quality GD (class 4 or 5) identified at that site was compression wood, it seems plausible that the tree-ring data from 1874 and 1969 at site CR recorded snow loading disturbance. Indeed, since no morphologic evidence of any mass wasting events at this site, a different process is therefore required to account for these results. The spatial distribution of the impacted trees requires a process that is evenly distributed, contrary to snow avalanches where clustering in tree damage has been considered an indicator of activity (e.g., Corona *et al.*, 2010; Schläppy *et al.*, 2013; Chiroiu *et al.*, 2015). Moreover, the ratio of trees recording a mechanical impact of class 5 at site CR is 2%, which is significantly lower than at the other sites, where it ranges from 17% to 48%. Removing RC2, which is really far from the treeline, the minimum ratio of trees recording a class 5 GD at avalanche sites is 30%. Since major reaction wood can also be caused by avalanches, and that a high quantity of snow is the primary driver of avalanche activity, it remains probable that reaction wood events recorded within an avalanche track are likely due to the latter process. However, this example shows that compression wood sequences might not be sufficient to discriminate between possible snow loading and avalanches at avalanches affected sites. It thus seems necessary to exert extreme caution when inferring avalanche activity in the absence of mechanical damages.

The small sample size advocates for a cautious interpretation with regards to climatic signal. This is especially true with regards to inferences about the statistical significance of tree-ring reconstructed climatic trends. In the present case, since snow

loading can be considered a discrete disturbance leaving clear anatomical indication (i.e., reaction wood), a sample size of 49 trees is in line with other studies with regard to climatic disturbances such as ice storms (n=15; Lafon and Speer, 2002) or drought (n=31; Li *et al.*, 2006).

2.5.3 Ecological disturbances (RC-RC2)

While Stoffel *et al.* (2013) suggest that it is important to avoid sectors affected by other ecological disturbances, there was no data based evidence to answer whether it is possible to discriminate them from avalanche related disturbances in the tree-ring record. The distinctive North and South age structures (Figure 2.3d) and event-response diagrams (Figure 2.6c and 2.6d) shows that half of RC2 transect was impacted by a windthrow following strong westerlies. The occurrence of this event was dated to 1996 according to the northern part of RC2 event-response diagram. The peak gust from July recorded by the Mount Washington Observatory came from the west at a velocity of 248 km/h and occurred in 1996. Since avalanche paths in the Presidential Range are often found with an easterly aspect, the fragmentation caused by avalanches creates a wind corridor where the prevailing westerly winds can funnel and accelerate, thus making them preferential sites for windthrows.

The few tree-ring studies on windthrow chronologies are based on growth suppression and release as their primary indicators (Zielonka *et al.*, 2010; Hadley and Knapp, 2011). The present example shows that similar indicators that avalanche can be used to infer the occurrence of a windthrow. However, in the event of a windthrow of limited extent in an avalanche path, it is possible to discriminate between both processes by implementing a sampling strategy using long transects and by looking at the spatial distribution of the age structure of the stand.

The age structure and the event-response diagram at site RC2 coupled with the identification of the windthrow on aerial photographs and the wind data from 1996 all suggest that the transect method indeed allowed to discriminate a windthrow and an avalanche event at site RC2. However, the sampling size is small and therefore one should exert caution before making any definitive statement about ecological signals. Further studies are needed in order to corroborate these findings or refute them as conjectural.

2.5.4 Multi-processes path (SM)

Event-response diagrams at site SM illustrate a case where two events – 1987 and 2007 – were recorded only in the downslope part of the sampling zone (Figure 2.7c). Since these events did not occur during years of abundant snowfall but the impacted trees were nonetheless located in the extreme runout zone, the GD of these years were likely caused by another process. The pronounced v-shaped channel without lateral levees in the center of the runout zone attests of the presence of torrential erosion. 1987 and 2007 are the years of the highest 72-hour rain events in April. These precipitation episodes were responsible for statewide floods (Fontaine, 1987; Flynn, 2008). During spring, at the elevation of the study sites, either the snow surface is hardened by daily freeze-thaw cycles limiting the infiltration and favouring higher surface runoff or the snowmelt is accelerated by positive temperature. Both cases can eventually trigger torrential floods of significant magnitude in the occurrence of extreme rain.

Contrary to previous successful attempts to discriminate avalanches with other geomorphological processes such as debris flows (Stoffel *et al.*, 2006) or rock falls (Stoffel and Hitz, 2008), as the hypothesized floods occurred in the early-spring, the

seasonality of the tree-ring evidence cannot be used to differentiate avalanche and other geomorphological processes. However, the mapping of the data illustrates the difference in the spatial pattern of an avalanche and a torrential event. The former creates more impacts in the uphill part of the runout zone and the intensity of the GDs, in the case of an important event, is evenly distributed in the sampling area (Figure 2.8). The latter damages the trees preferentially in the lower part of the sampling area with a gradient in the intensity of the disturbance, the uphill trees recorded lower classes GD than the downhill trees. These results of increasing disturbance downslope follow the normal gradient of torrential flows (Ruiz-Villanueva *et al.*, 2010) where water needs to be sufficiently funnelled before having a discharge with a significant ecological impact and are in agreement with previous research (Stoffel *et al.*, 2012).

Trees recording GDs in 1987 were not all adjacent to the main channel (3 out of 5 were), but there was an absence of any geomorphic evidence of secondary streams. Water flowing on a spring hard snow or ice cover can have the competence to create ecological damages by funnelling in gullies within the snowpack without having any geomorphological impact on the underlying ground, which could likely explain this pattern.

Stoffel *et al.* (2013) does not encourage the use of multi-process sites for dendrogeomorphological purposes. While respecting this guideline allows the most scientifically sound avalanche reconstructions, in practical cases of risk management, where there is a need to map the frequency-magnitude of processes or model the extent of the runout zone, the latter can overlap with torrential activity. Yet, the data presented in this paper exhibits a spatial pattern that suggests that one could differentiate the zones controlled by both processes that were otherwise impossible to distinguish in the field using visual geomorphic or ecological indicators. The interpolation of the sampling age of the trees (the annual probability of recording a

GD) shows lower (higher) values uphill, then reaches a maximum (minimum) in the middle of the sampling area and then decreases (increase) uphill (Figure 2.8). This is coherent with an uphill avalanche zone where the frequent low magnitude events controls the age structure of the forest, followed by a transition zone only reached by high magnitude avalanches where the runoff during torrential episodes are not channelled enough to create damage on the trees, and a downhill, torrential-controlled zone where the volume of funnelled water and the steep slope create a sufficient discharge to have an important ecological impact. One might argue that the similar spatial relationship in the age structure and the 10-year probability data is the result of a biased sampling protocol, younger trees being able to record more event thus having a lower return period. However, the low R^2 values between these variables exclude this possibility. Therefore, while producing possible biases in the avalanche chronology, the use of dendrogeomorphology at a multi-processes site can shed a light on the spatial dynamic of the different processes involved. Creating a multi-processes chronology could eventually lead to better understand the interactions between the timing of high magnitude events for both processes. Moreover, this spatial pattern exhibited as a response to a torrential event shows new possibilities in the field of dendrogeomorphology where the location of different classes of GD could allow a better understanding of the magnitude of the process and its spatial dynamic.

2.6 Conclusions

Since tree-ring analysis is recognized as a useful tool in the evaluation of the avalanche risk where historical archives are lacking, and given the fact that many avalanche paths are located in alpine environments prone to different climatic, ecological and geomorphic disturbances, there is a need to develop methods that can

allow to discriminate the occurrence of different processes, especially when they co-occur in the dormant season.

This article discusses innovative procedures to analyze the spatial patterns of tree-ring data in avalanche path by investigating the age structure and the probability maps, by considering subsamples in independent event-response diagrams, or by implementing a transect sampling protocol to determine the extent of closely occurring disturbances. We acknowledge that four case-studies are not enough to conclude that these methods are consistently reliable. However, they illustrate that there are opportunities to discriminate snow avalanches from other disturbances that occur during the dormant season through a scrupulous spatial analysis. Moreover, acknowledging these issues is also an opportunity to better understand the synergistic interactions between the different ecological, climatic and geomorphic processes acting on steep slopes in the alpine-subalpine environment. It is our hope that further studies are conducted to refine these methods and to corroborate (or not) our findings, which would contribute to improve the utility of dendrochronology for risk management purposes.

Acknowledgements

This work was supported by a PhD grant to Jean-Philippe Martin from the Fonds Québécois de Recherche Nature et Technologies (FQRNT). The authors would like to thank Jean-François Milot, Jean-François Jasmin and Mathieu Gratton for their help in the field. The Mount Washington Observatory provided weather data from the summit. Finally, the Authors are particularly thankful for the many insights from the USFS Snow Rangers, particularly Jeffrey Lane and Brad Ray.

Tableau 2.1 Physiographic characteristics of the study sites. The elevation and slope angle of the runout zone were measured at the end of the track.

Site	Starting zone		Runout zone		Length (m)
	Maximum elevation (m.a.s.l.)	Slope angle (°)	Elevation (m.a.s.l.)	Slope angle (°)	
HH	1550	41.4	1200	11.3	1050
RC	1530	29.1	1070	15.6	1230
SM	1450	33.2	1100	22.0	1000

Tableau 2.2 Scores assigned for the different growth disturbances (GD).

Class	Criteria
5	Impact scar associated with compression wood **OR** Presence of TRD **OR** Significant major growth reduction
4	Impact scar without any other indicator **OR** Compression wood filling the entire tree ring width and lasts ≥ 3 years **OR** Significant growth reduction
3	Compression wood filling the entire width of the tree ring and that lasts < 3 years
2	Compression wood that does not fill the entire tree-ring width **OR** Complete sequence of compression wood on a tree younger than 10 years old
1	Compression wood that is poorly defined

Tableau 2.3 Weather data used in this study.

Data	Period	Source	Altitude (m a.s.l.)
Annual snow accumulation	1931-2012	Pinkham Notch weather station	619
Annual snow accumulation	1936-2012	Mount Washington Observatory	1917
Annual snow accumulation	1870-2011	Concord weather station	88
April maximum 72-hour liquid precipitation	1931-2012	Pinkham Notch weather station	619

Tableau 2.4 Descriptive statistics of the age structure of the different sites.

Site	Mean (yr)	Standard deviation (yr)	Minimum (yr)	Maximum (yr)
HH	78.9	28.6	15	149
CR	110.1	32.7	51	169
RC	51.1	12.5	18	95
RC2	61.6	35.6	25	190
SM	81.1	34.0	30	137

Tableau 2.5 Sample depth and intensity class for GDs assessed at the different study sites. The sampling strategy for each site is specified in parentheses. ED: trees showing external damages in the runout zone. TS: transect sampling strategy where every tree in the transect is sampled. RS: random sampling.

Site	Beginning of chronology	Trees sampled	Number of samples	Number of GDs					
				Class 1	Class 2	Class 3	Class 4	Class 5	Total
HH (ED)	1903	62	109	14	40	185	95	30	364
SM (ED)	1889	63	114	1	43	188	172	19	423
RC (TS)	1951	60	69	10	33	28	31	24	126
RC2 (TS)	1925	59	84	8	30	70	61	10	179
CR (RS)	1865	49	98	13	33	73	21	1	141
Total		**293**	**474**	**46**	**179**	**544**	**380**	**84**	**1233**

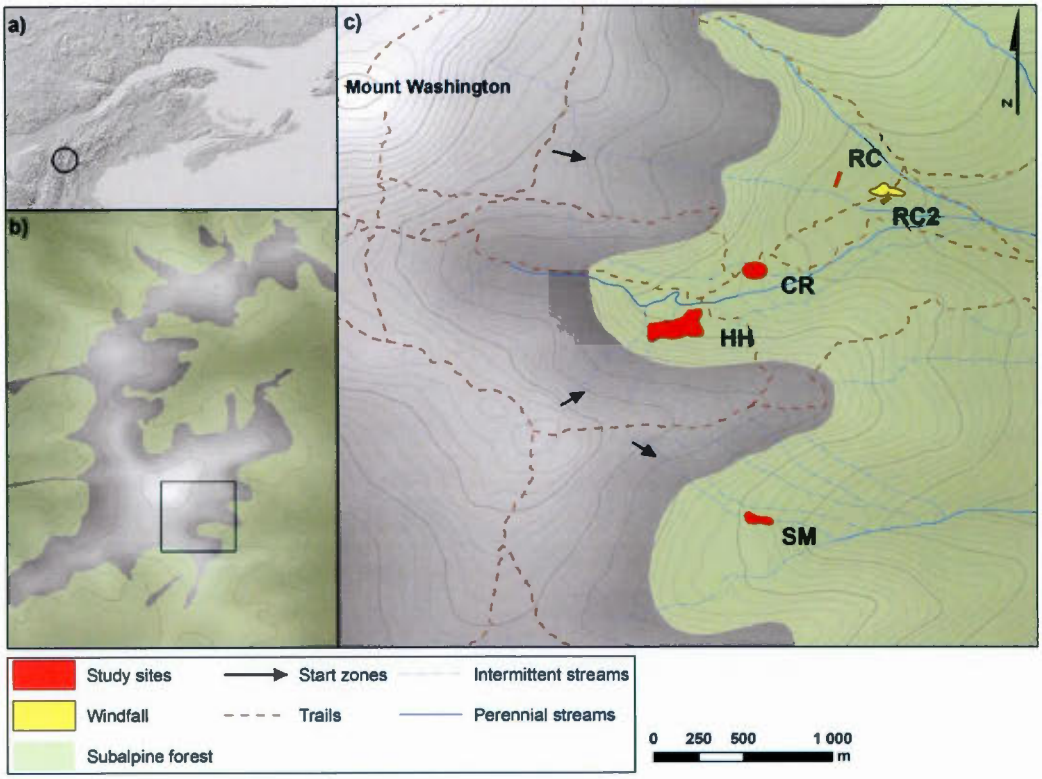

Figure 2.1 Map of the study area and the different study sites, showing a) the general location of the White Mountains in Northeastern North America, b) the Presidential Range alpine ridge, and c) detailed location of the study sites discussed in this paper. SM: site in the Gulf of Slides (Figure 2.8) HH: Hillman's Highway (Figure 2.2, Figure 2.3c), CR: reference chronology site (Figure 2.3d), RC and RC2: Raymond's Cataract transects (Figure 2.3b).

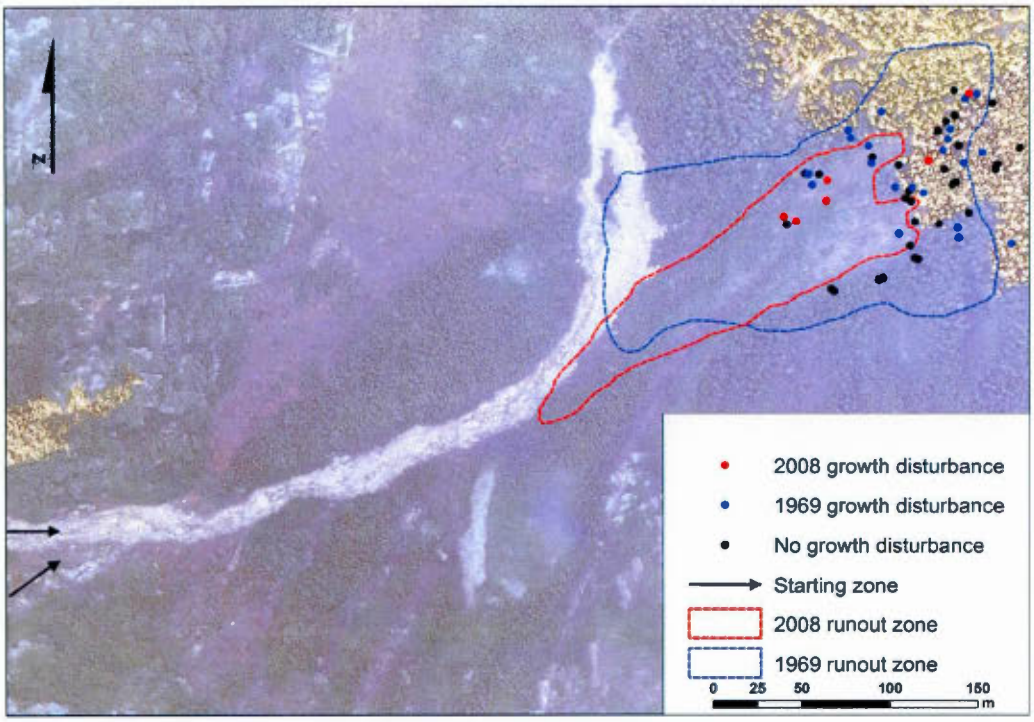

Figure 2.2 Spatial extent of the runout zones of the 1969 and 2008 avalanches at site HH delimited by aerial photographs. Areas in yellow are sunlit forest (upper right) or krummholz (left). The bare surface is the track of a debris flow that occurred in 2011. During this event, a levee of boulders with an a-axis > 10 m blocked the avalanche runout zone and the debris flowed to the left. Its occurrence in 2011 is posterior to every avalanche in the tree-ring chronology. What appears to be the down track of the avalanche path flowing to the north is the erosion of this debris flow event. Avalanches still flow in the direction of the runout zones shown on the map.

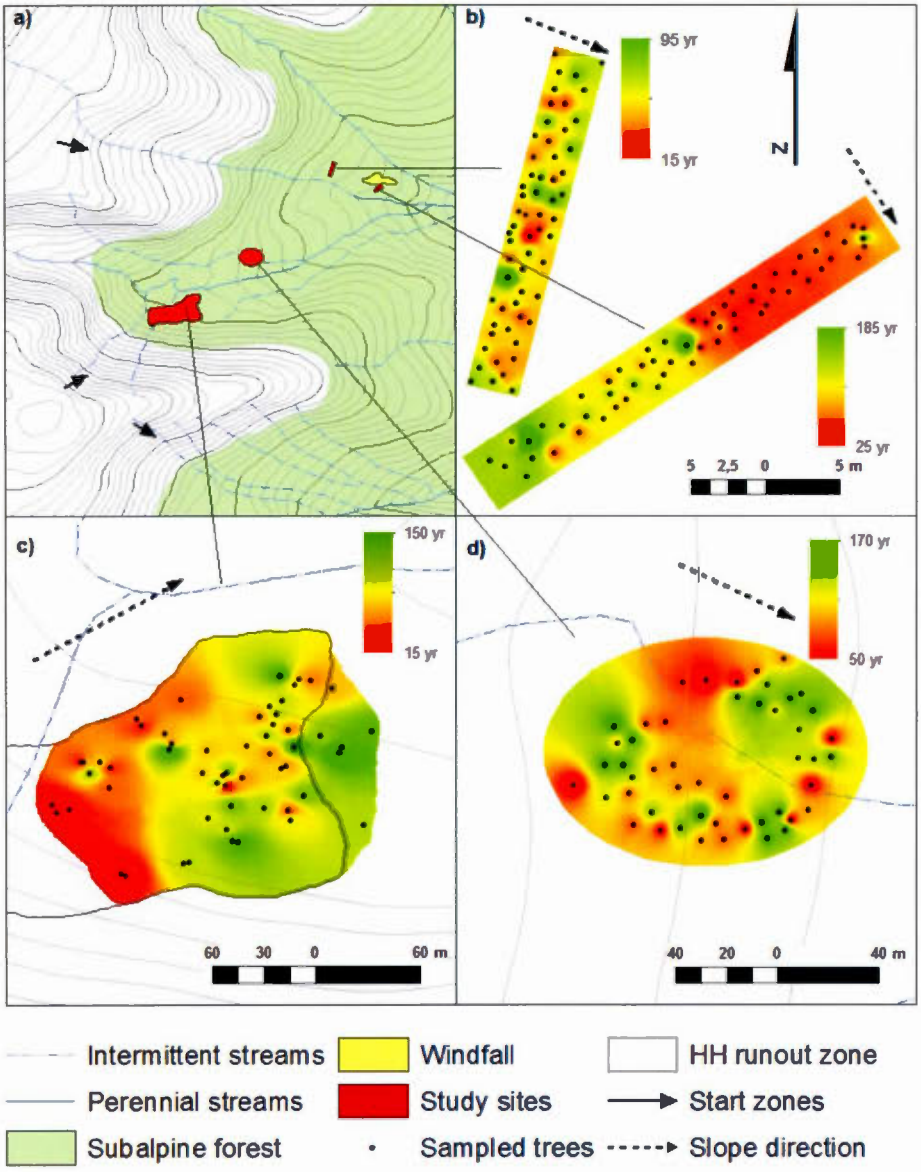

Figure 2.3 Comparison of the interpolated age structures at sites RC and RC2 (b), as well as HH (c) and CR (d). The contour of the 1969 avalanche at HH was added in (c).

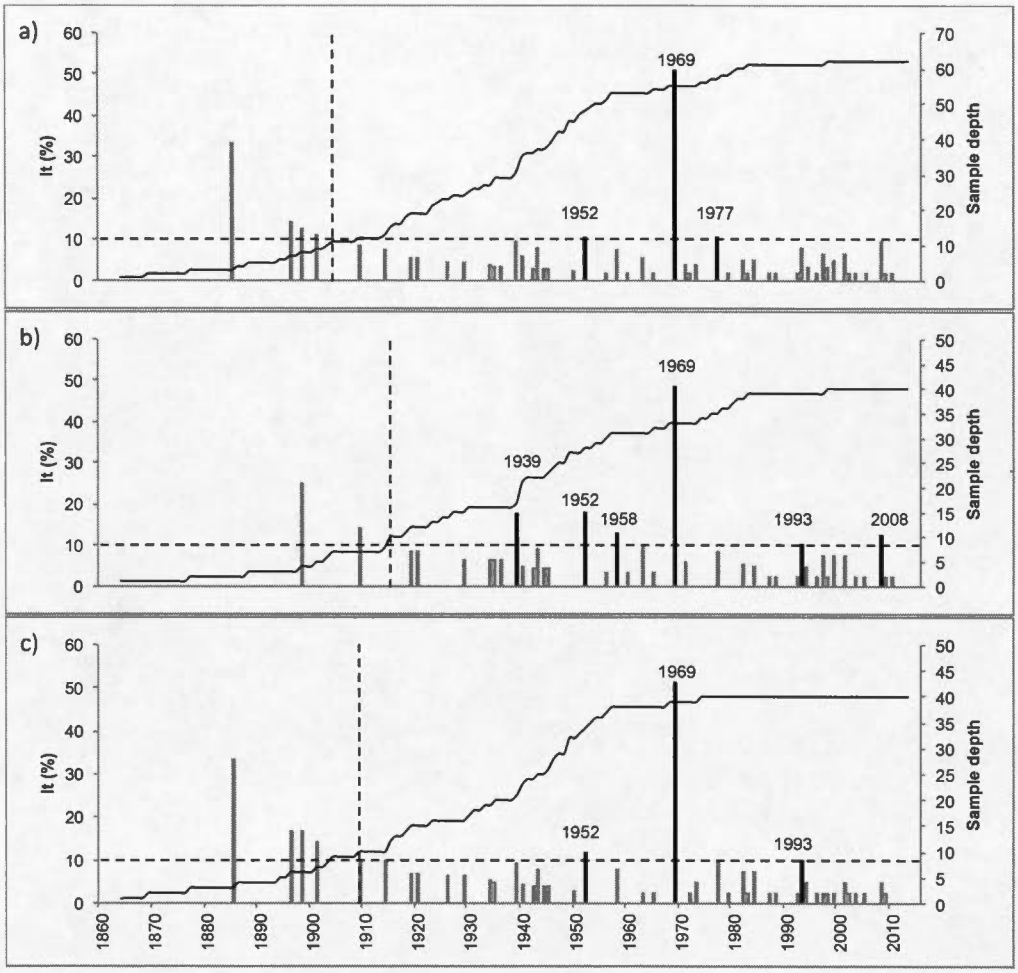

Figure 2.4 Event-response diagrams for HH site presenting all the samples (a), and the uphill (b) and the downhill (c) subsamples. The uphill and downhill subsamples overlap in the middle of the runout zone. The scale of the sample depth differs between the diagrams.

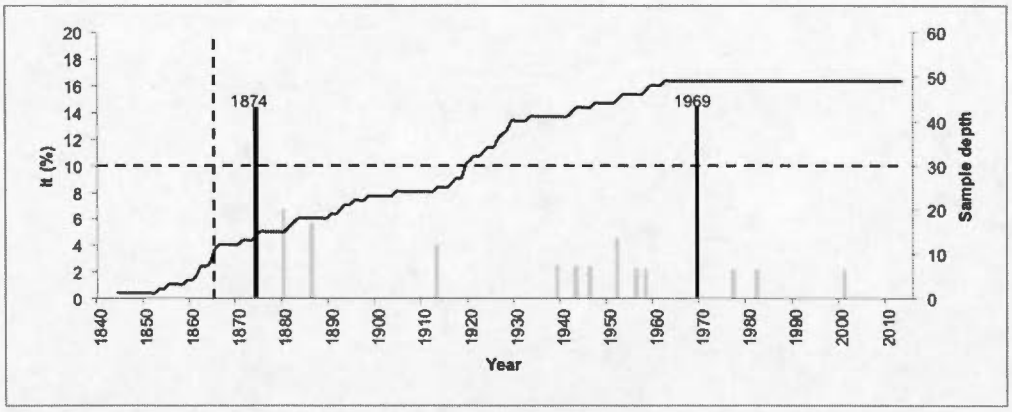

Figure 2.5 Event-response diagram for the site CR. The vertical dashed line indicates the first year with valid sample depth. The horizontal dashed line indicates the 10% threshold to consider an avalanche year. The black bars indicate years which meet the criteria for avalanche years.

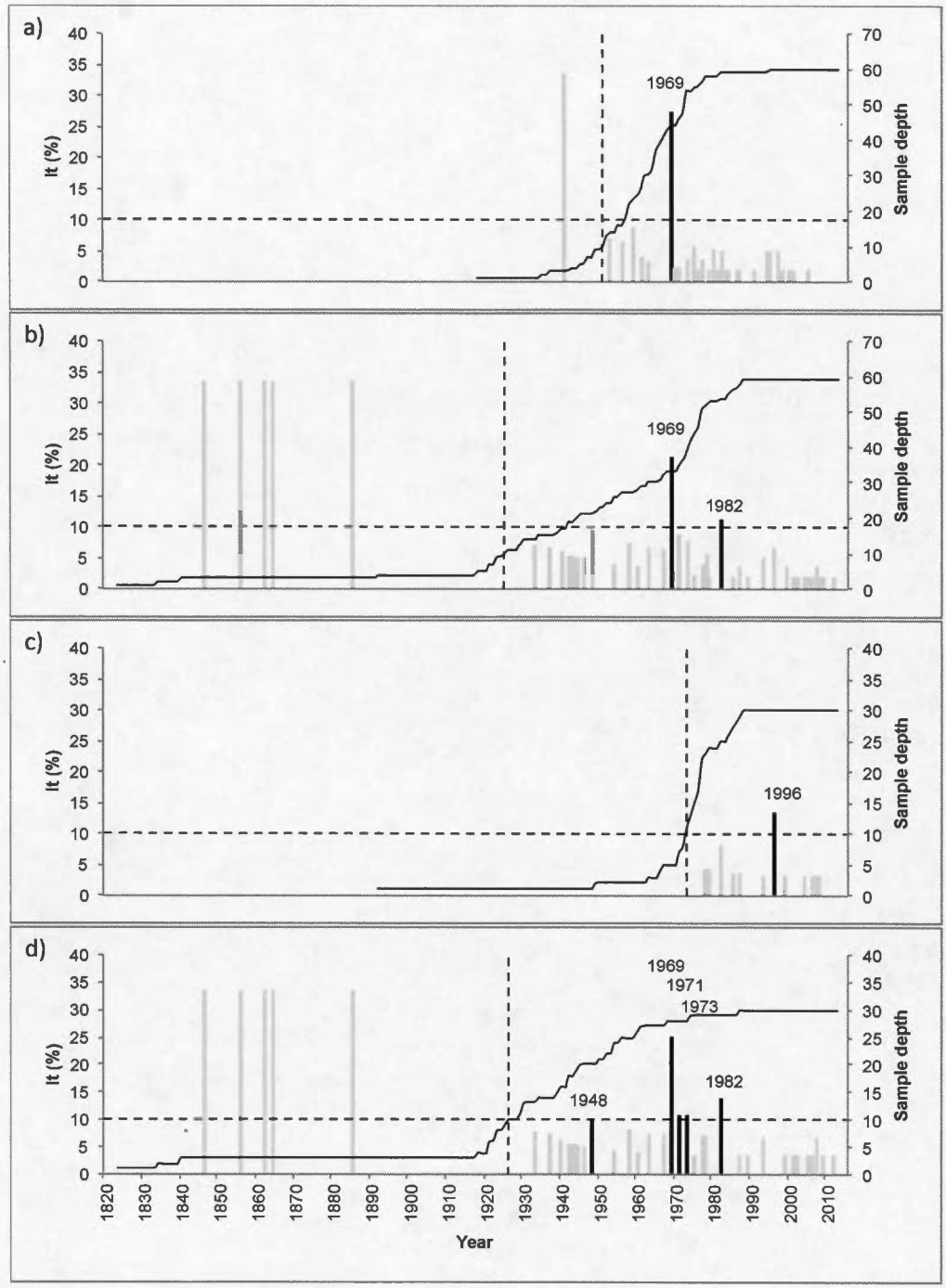

Figure 2.6 Event-response diagrams for Raymond's Cataract site presenting the RC (a) and RC2 (b) samples, as well as the northern, windthrow affected, (c) and southern (d) subsamples of RC2.

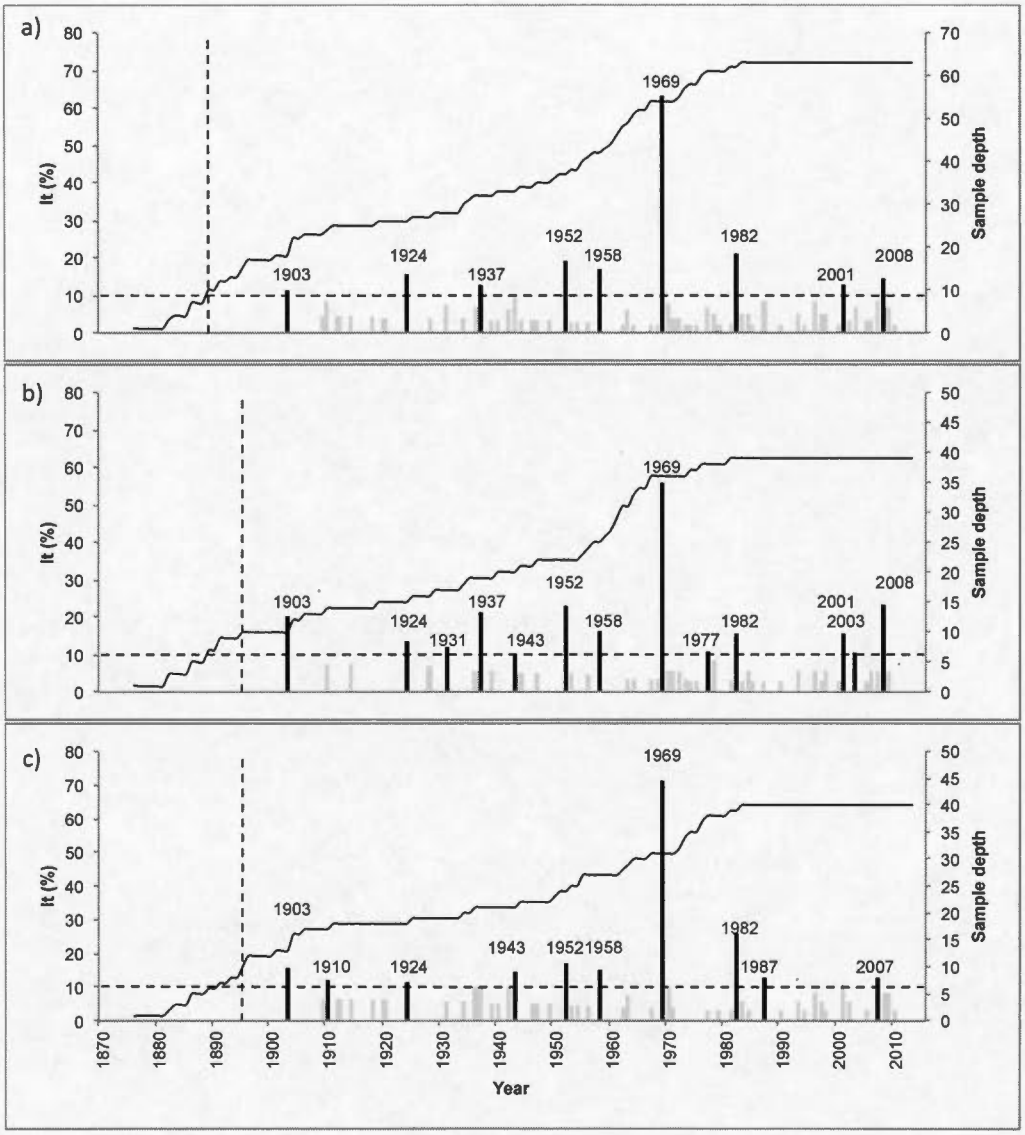

Figure 2.7 Event-response diagrams for SM site presenting all the samples (a), and the uphill (b) and the downhill (c) subsamples. The uphill and downhill subsamples overlap in the middle of the runout zone.

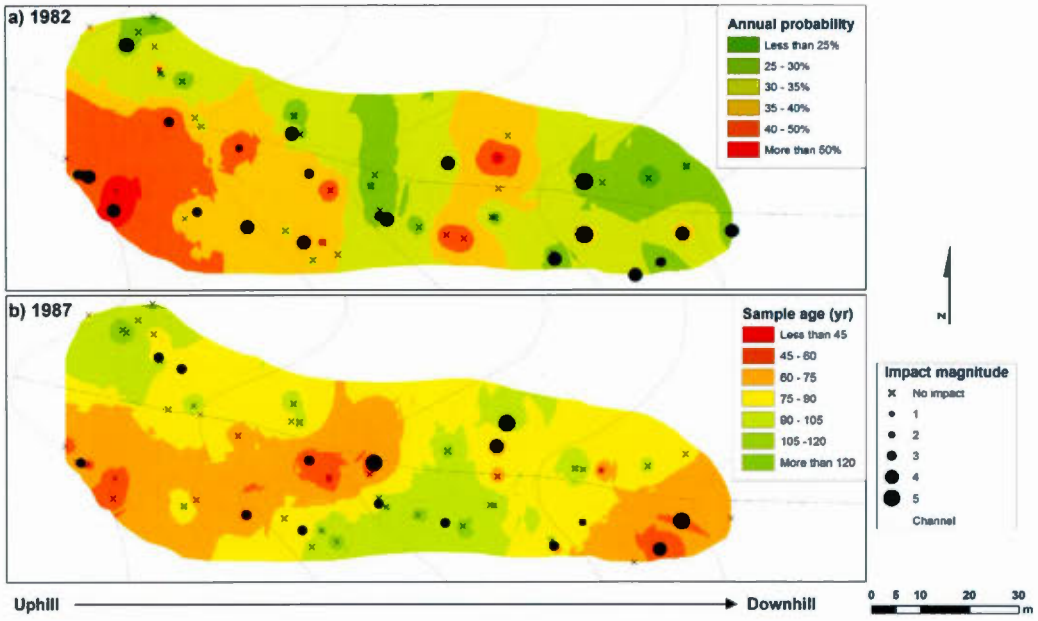

Figure 2.8 Maps of the 10-year probability of recording an impact and of the age structures at site SM. (a) Spatial interpolation of the annual probability of recording damage in the runout zone and impact magnitude of the different trees affected by the 1982 event. (b) Spatial interpolation of the sampling age of the forest and impact magnitude of the different trees affected by the 1987 event.

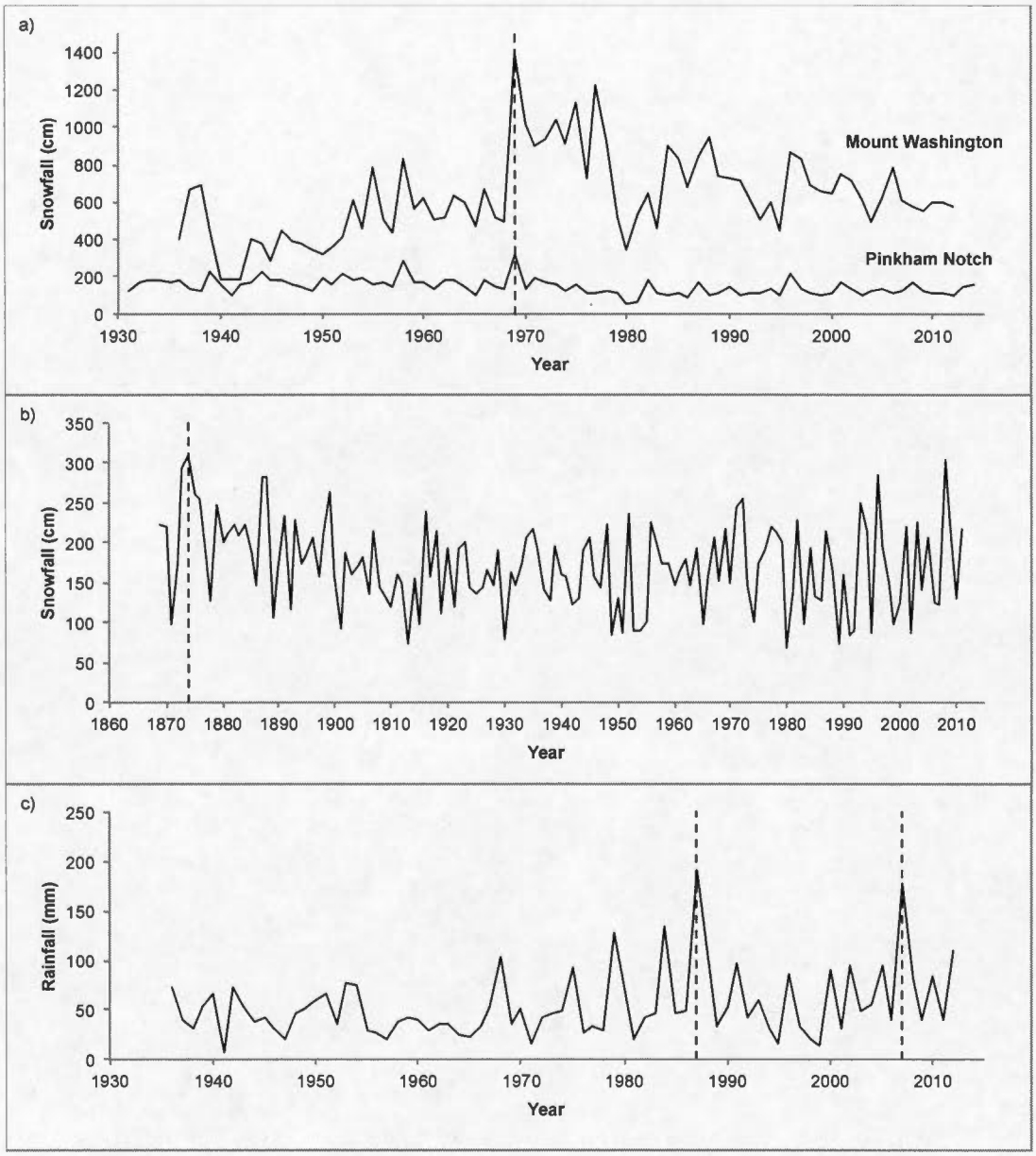

Figure 2.9 Precipitation data. (a) Annual snowfall on Mount Washington summit and at Pinkham Notch. The dashed line indicates the data for 1969. (b) Annual snowfall at Concord, New Hasmphire. The dashed line indicates the data for the record winter of 1873-1874. (c) 72 hour precipitation maximum in April at Pinkham Notch. The dashed line indicates the data for 1987 and 2007.

CHAPITRE III

DENDROGEOMORPHIC RECONSTRUCTION OF SNOW AVALANCHE REGIME AND TRIGGERING WEATHER CONDITIONS: A CLASSIFICATION TREE MODEL APPROACH

Jean-Philippe Martin[1] and Daniel Germain[2]

[1]Environmental sciences Institute, Université du Québec à Montréal, C.P. 8888 Succursale Centre-Ville, Montréal, Québec, Canada.

[2]Geography Department, Université du Québec à Montréal, C.P. 8888 Succursale Centre-Ville, Montréal, Québec, Canada.

Article sous presse dans *Progress in Physical Geography*
(http://dx.doi.org10.1177/0309133315625863)

Résumé

La dendrogéomorphologie est aujourd'hui reconnue comme une technique valide afin de reconstituer l'activité avalancheuse passée. Or, on note très peu d'études s'intéressant à la détermination des scénarios climatiques et météorologiques expliquant l'occurrence d'avalanches de neige reconstituées par dendrochronologie. La présente étude compare le potentiel des régressions logistiques et des arbres de classification pour souligner les scénarios météorologiques responsables de l'activité avalancheuse de forte intensité dans la Chaîne Présidentielle (New Hampshire, États-Unis). La méthode dendrochronologique utilisée améliore celle basée sur le seuil moderne grâce à l'implantation d'un second critère s'appuyant sur l'indice de Moran. 450 arbres échantillonnés dans sept différents couloirs ont permis de reconstituer 45 avalanches dont l'occurrence est réparti lors de 19 années différentes dans la période 1936-2012. Les résultats démontrent que les modèles issus des régressions logistiques sont moins précis que ceux créés par les arbres de classification afin d'inférer l'activité avalancheuse à partir de variables météorologiques à l'échelle mensuelle et annuelle. De plus, bien que les variables indépendantes de tous les noeuds racine sont en rapport avec les chutes de neige, l'addition de variables indépendantes représentant le vent et la température augmentent considérablement la robustesse des arbres de classification. Ainsi, l'occurrence des avalanches de neiges dans la Chaîne Présidentielle n'est pas seulement attribuable à la neige, mais également aux conditions atmosphériques responsables de la présence de couches fragiles à l'intérieur du manteau neigeux.

Mots clés :

Avalanche de neige; Dendrogéomorphologie; Cernes de croissance; Régression logistique; Arbres de classification; Chaîne Présidentielle

Abstract

While dendrogeomorphology has been recognized as a useful tool to identify past avalanche activity, there is only a handful of papers that focus on the assessment of weather or climatic triggers of tree-ring reconstructed avalanche events. This paper compares the potential of logistic regression and classification tree algorithms to highlight weather scenarios responsible for the occurrence of high-magnitude avalanche activity in the Presidential Range of the White Mountains, New Hampshire (USA). Our tree-ring procedure improves the modern GD-I_t threshold with the implementation of a second criteria based on the Moran index. 450 trees sampled in seven different avalanche paths allowed reconstructing 45 avalanches that occurred during 19 different years for the period 1936-2012. The results shows that while statistically significant, the logistic regression models are less accurate than classification trees to assess avalanche activity based on annual and monthly weather variables. Moreover, even if snow related covariates are located at the root node of every classification tree model, the addition of temperature and wind predictors increases their robustness. This suggests that high-magnitude avalanches in the Presidential Range not only respond to snow, but also to atmospheric conditions responsible for the creation of weak layers within the snowpack.

Keywords

Snow avalanche; Dendrogeomorphology; Tree-ring; Logistic regression; Classification tree; Presidential Range

3.1 Introduction

Snow avalanches are one of the main slope processes of high-mountains (Luckman, 1977). Because their occurrence is related to the characteristics of the snowpack, they are sensitive to climatic variation like other cryogenic physical systems (Eckert *et al.*, 2010; Haeberli *et al.*, 2010; Jomelli *et al.*, 2011). In recent years, an increasing number of studies on snow avalanches using tree-ring were published with the objective to provide a long-term record of avalanche activity (e.g., Corona *et al.*, 2013), to calibrate runout models (e.g., Casteller *et al.*, 2008; Schläppy *et al.*, 2014), to investigate and improve the accuracy of the dendrogeomorphological method (e.g., Corona *et al.*, 2012), to analyze the impact of anthropogenic or ecological disturbances on the avalanche regime (e.g., Germain *et al.*, 2005) or to evaluate the frequency-magnitude relationships of avalanches (e.g., Reardon *et al.*, 2008).

In mountain ranges where thorough archives of past avalanche activity exist, the relationship between climatic drivers of avalanche activity has been highly investigated at different spatiotemporal scales from a phenomenological and an operational perspective. Recent papers focus, among others, on the application of different statistical frameworks — such as logistic regressions (e.g., Castebrunet *et al.*, 2012; Jomelli *et al.*, 2007), classification trees (e.g., Hendrikx *et al.*, 2005, 2014), nearest neighbour (Singh *et al.*, 2015) and ensemble forecasting (Vernay *et al.*, 2015) — to better understand the relationship between avalanches with climate variables, on the temporal trends in avalanche activity (e.g., Eckert *et al.*, 2013) and on the relationship between avalanche activity and global circulation patterns (e.g., McClung, 2013; Keylock, 2003) or synoptic meteorology (e.g., Birkeland *et al.*, 2001).

Even if tree-ring analysis has been recognized as a useful tool in regions where no historical archives exist (Luckman, 2010), given the annual resolution of

dendrogeomorphology and the fact that avalanches respond to punctual meteorological triggers as well as winter climatic conditions responsible for the characteristics of the snowpack, only few tree-ring based studies have tried to establish relationships between weather and the triggering of snow avalanche activity (e.g., Casteller *et al.*, 2011; Corona *et al.*, 2010; Decaulne *et al.*, 2014; Dubé *et al.*, 2004; Germain *et al.*, 2009; Muntan *et al.*, 2009). Significant statistical relationships between different weather predictors at the month scale with tree-ring based avalanche chronologies were found using logistic regression models (Schläppy *et al.*, 2015). The logit framework provides a list of covariates influencing the triggering of avalanches, but this process can occur following different meteorological scenarios that are not taken into account in a regression model where all the predictors are on the same hierarchical level. Therefore, we suppose that in the case of avalanche activity with an annual resolution such as a tree-ring based chronology, the fact that different prevailing scenarios could explain the triggering of avalanches, the adequacy of using a logistic regression framework is limited by its incapacity to split the dataset in more homogeneous subsets that could represent different conditions leading to the triggering of an avalanche. Amongst the different classification algorithms, classification trees (CT) have the added benefit to provide insights in the cascade of events leading to a positive outcome.

The aim of this study is to outline the relationship between weather conditions responsible for avalanche activity and a tree-ring based record of high-magnitude events for the period 1936-2012 in the Presidential Range of the White Mountains. We define high-magnitude as events of sufficient size to reach the subalpine zone and to maintain the fragmentation of the treeline, which corresponds to avalanches of class 4 or above according to the Canadian avalanche danger scale (Schaerer and McClung, 2006). The objectives of this paper are the following: i) to create a tree-ring reconstruction of high-magnitude snow avalanche years in seven major paths of the Presidential Range; ii) to verify the existence of a statistical relationship between

weather predictors and avalanche activity using logit models; iii) to compare the performance of the latter with classification trees to identify avalanche activity based on weather predictors, and iv) to explore the potential of CT models to capture the physics of snow avalanches.

3.2 Study sites

The snow avalanche paths studied are located in the Presidential Range of the White Mountains (New Hampshire, United States, 44°16' N 71°18' W, Figure 3.1), which consists of many peaks along a North to South ridge of 2,748 ha above the balsam fir-red spruce treeline. Alpine glaciations during the Illinoian and Wisconsinan periods carved twelve cirques (Goldthwait *et al.*, 1987). The steep slopes of their headwalls located above the treeline comprise most of the starting zones of major avalanches paths (Table 3.1). Slopes varied between 10 to 30° in the runout zones indicating that even large snow avalanches had not penetrated the forest down into the geomorphic runout zone, which is usually <10° (Germain *et al.*, 2005). The Presidential Range of the White Mountains (New Hampshire, United States) is one of the premiere alpine destinations of the region to practice winter activities (hiking, climbing, backcountry skiing) on the avalanche-prone steep slopes. The United States Forest Service (USFS) Snow Rangers began to forecast the avalanche hazard on a daily basis in 1959 in the most visited cirques: Tuckerman and Huntington Ravines. The small spatial extent covered and the high spatial variability of the snowpack explains the decision to proceed to micro-scale forecasting for every avalanche paths in both cirques. However, no database of avalanche activity exists prior to 2006.

3.2.1 Sites GS and SM

Sites GS and SM are located in the Gulf of Slides, an eastern aspect glacial cirque south of Tuckerman Ravine located underneath a ridge which makes it less prone to accumulation from snow drifting than the other eastern aspect sites described below (Figure 3.1). These avalanche paths are popular ski destinations that are not monitored or forecasted by the USFS Snow Rangers. The upper part of the runout zone of GS is composed of heavily impacted dwarf *Abies balsamea* (L.) Mill. The middle part of the runout zone is colonized by herbaceous species with fallen dead trees and the lower part is covered by an open forest composed almost exclusively of *Abies balsamea*. The intermittent stream that flows in the central part of the runout zone of site SM eroded a v-shaped, 2 m deep channel. Vegetation on the right bank of the stream in the runout zone consists of an open forest of mature *Abies balsamea*, whereas the left bank is covered by a denser forest of younger balsam fir.

3.2.2 Sites HH, LH and HUR

Hillman's Highway (HH) and South Gully (HUR) are located in Tuckerman and Huntington Ravines, respectively, whereas Lion's Head (LH) is an avalanche path that traverses a summer trail on a ridge between the two ravines mentioned above (Figure 3.1). Avalanche activity of lower magnitude (i.e., of class < 4 on the Canadian avalanche danger scale) is important at HH and HUR as reported by the USFS Snow Rangers, who recorded respectively 42 and 32 avalanches at these sites between 2006 and 2012 (Table 3.2). 13 events were recorded at LH during this period. The starting zones of these three sites are located downhill from a large alpine plateau, which makes them prone to important snow drifting accumulation from the

westerlies. During hurricane Irene in 2011, a debris flow occurred in HH, but turned left and avoided the avalanche runout zone, which makes it suitable to dendrogeomorphic reconstruction of avalanches. The vegetation in the runout zone of HH and LH is similar to GS. The runout zone of HUR is covered by a dense forest of heavily impacted *Abies balsamea* without a clear opening in the forest like at the precedent sites.

3.2.3 Sites K7 and AR

One avalanche path (K7) is located in King's Ravine and another (AR) in Amoonosuc Ravine, which are respectively on the northern and western sides of the Presidential Range (Figure 3.1). The runout zone of K7 is covered by an open forest of *Abies balsamea*, *Populus tremuloides* Michx. and *Betula papyrifera* Marsh. The extensive runout zone of AR follows the drainage of the Amoonosuc River where the center is colonized by shrubs and sparse heliophilic deciduous trees (*Betula papyrifera* and *Populus tremuloides*). The sides are covered by a closed forest dominated by *Abies balsamea* with few *Tsuga Canadensis* (L.) Carr.

On the summit of Mt. Washington, the average winter temperature (from December to April) is -11.8 °C. With such cold temperatures, almost the entirety of the precipitations from November to April is solid, with an average annual snowfall of 714.2 cm on the summit. Severe winds are characteristic of the Presidential Range. Record peak gusts above 200 km/h were measured for every month and gusts of hurricane strength (above 119 km/h) are recorded two days out of three during winter (Gordon, 1989). It is therefore frequent that the USFS Snow Rangers forecast a high avalanche danger with low-density snowfalls of only 5-7 cm (Joosen, 2008).

3.3 Methods

3.3.1 Site selection

An inventory of the major avalanche paths of the range was created following a discussion with the USFS Snow Rangers. Amongst this inventory, seven sites were selected primarily based on the presence of a runout zone that extends below the treeline with trees exhibiting signs of impacts by snow avalanches. Other criteria were the absence of other geomorphological or ecological processes that could cause similar damages to the trees (Stoffel *et al.*, 2013), the ease of access by foot travel and the location outside of a zone where sampling was restricted for conservation issues.

3.3.2 Sample collection and preparation

The physiographic characteristics of the avalanche paths were measured using topographic maps and aerial photographs. The runout zones of each site were identified as the boundary between open land and closed forest at the lower limit of the avalanche paths. Since this paper focuses on low-frequency, high-magnitude events, most of the trees were sampled along or beyond this boundary, with the exception of AR where most of the trees were sampled on the northern trimline, because this avalanche path follows a catchment where an important flood due to hurricane Irene in August 2011 acted as a major ecological disturbance in the runout zone. Living trees showing external damages (impact scars, loss of apical dominance, broken branches, tilting or topping) were sampled. Stem discs were collected at the level of the impacts on trees with a diameter smaller than 20 cm. The larger trees

were cored at the level of the damage or at the lowest possible height if the latter was too high. At least one core was taken uphill and downhill. When coring a tree with a scar, a core was taken each side of the scar and one core was taken downhill. A minimum of 59 and a maximum of 78 trees were sampled at each sites. In total, 456 discs and 350 cores were taken from 450 trees (Table 3.3).

In the lab, samples were dried and sanded before being analyzed under a binocular microscope to determine the age at sampling height and to identify any growth disturbance (hereafter labelled GD). Cross-dating was performed using characteristic tree-rings caused by different climatic (e.g., frost rings) and ecological events (Filion *et al.*, 1986). False rings and pale coloured tree-rings were almost inexistent in our samples. The occurrence of a GD was inferred using these four proxies: i) the presence of scar tissue; ii) significant growth reduction; iii) the presence of tangential rows of traumatic resin ducts (TRD); or iv) the onset of compression wood. Each GD was then assigned a score according to the quality of the indicator following a standard approach in dendrogeomorphologic studies (e.g., Germain *et al.*, 2005; Luckman and Fraser, 2001; Reardon *et al.*, 2008; Schläppy *et al.*, 2013). The system used in this study is derived from Corona *et al.* (2010):

Class 5: Clear impact scar associated with compression wood or the presence of TRD or a significant major growth reduction.

Class 4: Clear scar without any other indicator, compression wood filling the entire tree-ring width and lasts for at least 3 successive years or significant growth reduction.

Class 3: Compression wood that fills the entire width of the tree-rings and that lasts 1 or 2 growth years.

Class 2: Compression wood that does not fill the tree-ring width or a complete sequence of compression wood on a tree younger than 10 years old.

Class 1: Compression wood that is poorly defined.

3.3.3 Dendrochronological reconstitution

To minimize the noise caused by other processes leaving lower-intensity impacts on trees than high-magnitude snow avalanches, such as snow creeping (Stoffel and Corona, 2013) or snow loading (Bégin and Boivin, 2000), GDs of classes 1, 2 and 3 were discarded for further analysis. With the remaining GDs, at each site, an index I_t was calculated as the ratio of trees recording a GD over the number of trees that were alive at year t following the equation (Shroder, 1978):

$$I_t = \left(\frac{\sum_{i=1}^{n}(R_t)}{\sum_{i=1}^{n}(A_t)}\right) \times 100 \quad (1)$$

Where R_t represents the number of trees showing a response at year t and At represents the total number of trees that were alive at year t.

Different qualitative, semi-qualitative or quantitative methods exist to discriminate years of snow avalanche activity from the noise caused by other ecological disturbances (cf Butler and Sawyer (2008) and Corona *et al.* (2012) for thorough reviews). The modern GD-I_t method —using a different double threshold for sample sizes of 10–20 (GD $\geq$ 3 and $I_t \geq$ 15%), 21–50 (GD $\geq$ 5 and $I_t \geq$ 10%), and $\geq$ 51 trees (GD $\geq$ 7 and $I_t \geq$ 7%)— was preferred for its capacity to reduce noise by adapting the threshold to the sample size (Chiroiu *et al.*, 2015). However, this procedure is quite strict and does not take into account the spatial distribution of the impacted trees, which can lead to misclassify avalanche years (Schläppy *et al.*, 2013). We therefore improved the modern method by considering if a spatial autocorrelation exists between impacted trees, since it is likely that an avalanche impacts trees in a specific region of the runout zone (Corona *et al.*, 2010; Lopez Saez *et al.*, 2012; Schneuly-Bollschweiler *et al.*, 2013). Using the projected coordinates, we placed every sampled tree as a point object in ArcGIS 10.1. In the event of a year that exceeds the I_t

threshold but does not meet the GD threshold, the Moran index (Moran, 1950) was calculated to evaluate whether the impacted trees were randomly distributed (Moran I = 0), dispersed (Moran I moving toward -1) or clustered (Moran I moving toward 1). Random or dispersed years were disregarded and years with a statistically significant (using the Z-score with a *p-value* < 0.1) Moran I > 0 were included in the avalanche chronology.

For each avalanche path, the annual probability of recording an avalanche was calculated using the following equation:

$$AP_i = \left(\frac{A_i}{L_i}\right) \quad (2)$$

Where A represents the number of reconstructed events at site i and L is the length of the chronology at site i, defined as the number of years where the sample size was large enough ($n \geq 10$ trees) to assess avalanche activity (Germain *et al.*, 2009, Casteller *et al.*, 2011). The return period (RP) was calculated as the inverse of the annual probability (RP=1/AP).

3.3.4 Weather data processing

Meteorological variables, such as snow, rain, temperature and wind velocity were considered as potential triggers for avalanches. Daily data were obtained from two weather stations. First, the dataset from Mount Washington Observatory (1,917 m a.s.l.), a non-profit recording the weather on the summit of Mt. Washington, includes precipitation, temperature and wind from 1936-2012. Second, a National Weather Service (NWS) cooperative station operated by the Appalachian Mountain Club (AMC; COOP #276818, NCDC station ID 20018701, NWS Location ID

HGMN3) located at Pinkham Notch, at the base of Mt. Washington (619 m a.s.l.), provided data on precipitation and temperature from 1931-2012. All the variables were computed from these daily data and were standardized prior to being used as predictor variables.

Since tree-ring analysis provides avalanche data with an annual resolution, in order to minimize temporal scale and aggregation problems, weather variables were created by calculating monthly values from December to April and winter values (encompassing all data from December to April) using the daily data aforementioned. Except for the snowpack variables, which were unavailable for the present study region, the predictors were created following Schläppy *et al.* (2015) and are summarized in Table 3.4. In total, 24 annual and 120 monthly (24 variables calculated for the five months) predictors were created. Precipitation and temperature values were calculated using the data from both weather stations. However, in the analysis mentioned below, predictors from Pinkham Notch weather station gave better fits. Wind values were calculated using data from the Mount Washington Observatory data. Each variable was standardized to facilitate the interpretation of the different coefficients and the comparison with other studies using the following equation:

$$x_{it}^{norm}(t) = \frac{x_{it} - \mu_i}{\sigma_i} \quad (3)$$

where i represents the variable and t, the year. Although some avalanche chronologies extend beyond 1936, only the period from 1936-2012 were considered in the following analysis because of weather data availability.

3.3.5 Logistic regressions

The logistic regression is a type of generalized linear model where the response variable is categorical, often binary. It is commonly used as a framework to examine the relationship between a discrete dependant variable (such as occurrence and non-occurrence) and a set of predictors. The link function allowing the transfer of the predictions at the scale of the independent variables is the natural logarithm of the odds ratio such as:

$$\text{logit}(p_t) = \ln\left(\frac{p_t}{1-p_t}\right) = \beta_0 + \beta_1 X_1 + \cdots + \beta_n X_n \quad (4)$$

where p_t is the probability of occurrence of an event at time t, β is the coefficients of the regression and X, the meteorological predictors.

One major challenge is the high number of predictors given the scarcity of avalanche years. The procedure used to select the most significant predictors was based on the method developed by Schläppy *et al.* (2015) and is only summarized here. The computation was performed using the GLM package of R software. All covariates were tested individually in a logistic regression to keep only the predictors with a p-value ≤ 0.2. To avoid creating redundancy in the final logit model, correlation coefficients were calculated between every remaining covariate. When two variables had an $r \geq 0.5$, the one with the smallest p-value was kept. A stepwise regression procedure was then implemented with the remaining set of variables. Based on two initial models, one containing no covariates (*null* model) and the other one containing every covariate, the procedure combines forward selection and backward elimination of variables using the Akaike Information Criteria (AIC) as a metric to compare the relative quality of the different models. Because of the relatively low number of avalanche events (1) relatively to the amount of non-events (0) at every study sites,

we kept models with a maximum of four predictors significant at the 10% level. This procedure was repeated for every study site using the monthly, the annual and the combined sets of variables. The performance of the model was assessed in three different ways. The significant of the intercept and individual predictors was calculated using the Wald chi-square statistic to make sure they were all significant at the 0.1 level (Peng *et al.*, 2002). We then used Nagelkerke's pseudo-R^2 (Nagelkerke, 1991) to verify the goodness-of-fit. This metric reflects the improvement of the full model over the intercept model in the reproduction of the actual outcomes, which is the occurrence or absence of avalanche events in the present case. Finally, we checked whether the model's high value (≥ 0.5) were associated with avalanche years and low values (< 0.5) with non-avalanche years. This allowed calculating the sensitivity (i.e., the ratio of correctly classified avalanche events), the specificity (i.e., the ratio of correctly classified non-avalanche events) and the overall performance of the model (i.e., the ratio of correctly classified years).

3.3.6 Classification trees

Classification trees (CTs) are a data mining method to study the relationships between a dependant variable (here the occurrence of snow avalanches) and a large number of predictors. At each step, the algorithm produces a binary split of the dataset into the two most uniform subsets using the value of a single predictor. It also produces a list of surrogate splits. The CTs are non-parametric and insensitive to the distributions of the predictors. A more thorough description of the CTs is given by Breiman *et al.* (1984). As stated earlier, compared to logistic regressions, CTs have the advantage of providing multiple scenarios leading to the triggering of avalanches. Moreover, compared to other classification algorithms such as neural networks or random forest that function like a black box, the binary split approach of CT analysis

provides a clear and easily understandable interpretation of complex interactions between weather predictors (Davis *et al.*, 1999). While CTs have thus been used for meteorological data analysis in relation to short-term avalanche activity with a daily resolution by different authors (Davis *et al.*, 1999; Hendrikx *et al.*, 2005, 2014; Peitzch *et al.*, 2012), this procedure has never been applied to explore the weather scenarios responsible for years of high-magnitude avalanche activity.

First, CTs were built using the covariates of the logit models for every site. However, since the architecture of a classification algorithm differs completely from the one of a regression model, CTs were also made from the complete set combining the meteorological variables at the monthly and annual scale. Given the high autocorrelations between many of the predictor variables, identification of important variables to retain in the CT model was made prior to the tree construction. For each site, a bootstrap procedure was first implemented to select the most important variables. 10,000 CTs were constructed using a random selection of 30 variables chosen amongst the available predictor variables. Variable importance is measured as a score that describes the relative impact of a given variable on the decrease of the deviance at each node. For every tree, the three most important variables are recorded separately with their scores. We extracted the 60 variables that had the highest total score. This method differs slightly than the bootstrap procedure proposed by Lagadec *et al.* (2015) who chose seven variables based on the importance score instead of its ranking. Given the high autocorrelation rate amongst the meteorological dataset used in this study, we chose to extract a higher number of variables in a first step and then computed the autocorrelation between remaining predictors. If a couple of variables had a Pearson $r \geq 0.5$, the variable that was most frequently present in the bootstrap procedure was retained and the other was discarded. For each site, the final dataset contained approximately 15 meteorological variables that were used to build three different CTs, integrating 1) every covariate, 2) only the predictors related to the precipitation, and finally 3) only the predictors related to the temperature and the

wind. Because of the small size of the sample, a cross-validation procedure was implemented in order to estimate the error rates for each CT model. The dataset was iteratively divided into ten equal parts. For a given iteration, the model is calibrated on nine parts and validated on the last division. The cross-validation error is the averaged error rate computed for the ten iterations. A sensitivity analysis was performed with the CTs, for which we performed 5-, 10- and 50-fold cross-validation. The performance of the different CT models was evaluated using the same sensitivity, specificity and overall prediction ratios that were described in the previous section. This allowed comparing the regression and the classification frameworks.

3.4 Results

3.4.1 Avalanche chronology

2,251 GDs were identified, 960 of which were considered strong avalanche indicators (Class 4 or 5) (Table 3.3). The average amount of GDs per tree is 5.0. The tree-ring chronology begins in 1889 (at site SM). In total, 45 avalanches were above the I_t and GD threshold (Figure 3.2). Using the Moran index allowed to add 9 events to the chronology (Table 3.5). Within the 77-year bracket for which weather data were available (1936-2012), avalanches were identified in 19 different years, whereas the tree-ring procedure did not allow the assessment of avalanche activity during the 58 remaining years. Identifying avalanches at different sites during a same year was considered an indicator of the intensity of snow avalanche activity at the regional scale, which was particularly important for years where an event was recorded in at least 5 sites: 1952, 1958, 1969 and 1982. 1969 is the only year where avalanches

were identified in every studied path; it also is the only year that was identified by the active and retired Snow Rangers as a winter of extreme avalanche activity in the Presidential Range. The return period for the different paths varies from 7 to 18 years.

3.4.2 Logistic regressions

Logistic regression models were established for each path using monthly and annual data. Using the annual covariates, the different models included either one (2 models) or two (5 models) variables that were all related to precipitation with the exception of two (Table 3.6). All models passed the likelihood ratio test at the $\alpha = 0.05$ level. However, for six paths, the pseudo-R^2 value is under 0.5. Moreover, the sensitivity of the different models is low (< 43% for 6 paths), indicating their low ability to determine avalanche years. These deceptive results suggest that the annual covariates were inadequate to predict years of high-magnitude avalanche activity within the logistic regression framework.

Using the monthly covariates, the logistic regression models were all highly significant based on the likelihood ratio test with pseudo-R^2 coefficients varying from 0.57 to 0.73 (Table 3.7). Each model comprises 3 or 4 predictors. The sensitivity of the models ranges from 50.0% to 71.4%, which is superior to the results obtained with the annual variables. The higher specificity rates, all above 95%, suggest that the models are still better to predict non-event years than years with avalanche occurrence. Regression models built with a starting dataset containing both annual and monthly covariates gave the same models than with the exclusive use of the monthly data.

3.4.3 CT analysis

The construction of CT for every site allowed identifying scenarios explaining the occurrence of snow avalanches of a sufficient magnitude to trigger an ecological response. With the exception of site HUR, every CT model constructed with the bootstrap procedure described above uses a combination of one to three precipitation covariates coupled with one or two temperature/wind covariates to provide two scenarios of high-magnitude avalanche triggering (Figure 3.3). In their trimmed versions, the CTs use two (four sites), three (two sites) or four (one site) meteorological predictors.

3.4.4 Accuracy and performance metrics of the different CT models

3.4.4.1 CT cross-validation prediction error

Figure 3.4 presents the averaged cross-validation prediction error for the CTs using either the variables from the logit models (CT_logit), as well as the different cases with variables selected from the bootstrap procedure: all covariates (CT_all), precipitation covariates (CT_snow) and wind/temperature covariates (CT_temp). The sensitivity analysis (5-, 10- and 50-fold cross-validation) is only presented for the complete bootstrap dataset (CT_all) to improve readability. Every dataset and every sensitivity scenario produced an average cross-validation prediction error value between 0.10 and 0.16 with a 90% confidence interval on the mean between 0.01 and 0.03. Therefore, no dataset produced a significantly different cross-validation prediction error. However, the CT built with the covariates from the logit (CT_logit)

seems a bit more robust since its value is the lowest. Following the same logic, the CT built with the temperature and wind predictors (CT_temp) looks like the less performing. The sensitivity analysis between 5-, 10- or 50-fold cross-validation (CT_all_5, CT_all_10, CT_all_50) did not produce significant changes in the prediction error values.

3.4.4.2 Success of the classification rates

The average sensitivity, specificity and overall prediction were used as metrics to compare the performance of the different CTs with the logit models (Figure 3.5). The specificity and overall prediction rate yield similar results, but they were more stable for the logit models and the CTs using the variables of the logit model, as it is demonstrated by the substantially lower confidence intervals around the means. The variability between the sensitivity is greater, with the logit models having the lowest average value. The only set of models that produce a significantly superior average sensitivity was the CTs with all covariates selected with the bootstrap procedure. The average sensitivity of the CTs built with either the precipitation or the temperature and wind variables is almost identical. Their confidence intervals around the mean are also similar and are the highest of the tested models, which signifies highest standard deviations.

3.5 Discussion

3.5.1 Tree-ring reconstruction

Through this tree-ring based chronology, the return period of high-magnitude snow avalanches with an important ecological impact is approximately 7 years, with 4 years being especially noticeable for the high avalanche activity at the range scale (1952, 1958, 1969 and 1982). Although in the Presidential Range, snow avalanches of lower magnitude occur yearly in many avalanche paths, only a handful is of sufficient size to break trees (class-3 according to the Canadian avalanche danger scale (Schaerer and McClung, 2006). Indeed, the only event recorded in the tree-ring chronology of HH during the period 2006-2012 was in 2008, which corresponds to the highest magnitude event of the USFS Snow Rangers' short-term archive, where a class-4 avalanche destroyed 16 000 m^2 of forest. Figure 3.6 shows the magnitude of the 1969 runout zone compared to its extension in 2008 at site HH. These limits were inferred by the extent of the area cleared by trees on aerial photographs from 1973 and 2010. Trees that were disturbed in 1969 are located just outside of the runout extension. Because of their proximity with the trimline (< 15 m), and the fact that trees are widely spaced at this site, we attributed these damages to material (snow, rocks, trees) transported by the avalanche beyond the boundary of the forest that was cleared. If this material were big enough and still moving with sufficient speed, it is probable that it caused damages to trees in the vicinity of the clearing. Compared to many other studies where the tree-ring based chronology of snow avalanche activity was compared to existing archives to maximize the amount of events reconstructed (Chiroiu *et al.*, 2015; Corona *et al.*, 2012; Schläppy *et al.*, 2013), the present paper focuses on creating a chronology of the high-magnitude snow avalanches with a low return period and important ecological impacts. The sampling effort at the downslope

limit of the runout zone as well as strict thresholds to identify snow avalanches were selected accordingly to meet the objectives of this paper.

The latter example in HH demonstrates that the threshold used to assess avalanche activity is appropriate for the reconstruction of high-magnitude events in the Presidential Range. While Chiroiu *et al.* (2015) argue that a method where the intensity of the recorded GDs is weighted (Kogelnig-Mayer *et al.*, 2011) allow a reduction of the noise and may yield better results for older periods or smaller sample size, this method was rejected, since its implementation would have resulted in the inclusion of avalanche years with only GDs of intensity 1 or 2 being recorded. However, the modern GD-I_t method proved to be effective in recording older events. For example, during winter 1939, an historical avalanche with a crown width of the whole headwall in Tuckerman Ravine ran past the corrie lip out of the cirque. This rare event (which is known to have happened only in 1969 since) suggests that 1939 was a year of important avalanche activity; it is therefore expected that it be recorded as an avalanche year at one site (GS). The inclusion of a second criterion based on the Moran's index whenever only the I_t was above the threshold seems to be a statistically robust method to complete the avalanche chronology. Indeed, most of the avalanches identified with this method were synchronous with events reconstructed in other sites using the modern threshold (Figure 3.2). Since snow avalanches respond to weather triggers, it seems logical that high-magnitude events were often recorded at a wider scale than the individual avalanche path. Moreover, the acknowledged 2008 event in HH was identified as a result of a significant Moran's I above 0.

The longest period of inactivity in this tree-ring based chronology (11 years) occurs between the two biggest avalanche years recorded; 1958 and 1969. The only site where an avalanche was identified between these two years being at LH where no events were recorded in 1958, this suggests that avalanche activity that year was of sufficient magnitude resulting in an ecological disturbance of enough amplitude to

delay the regeneration of the subalpine forest in the runout zone. Hence, there is a lack of trees that could record events between these two avalanche years. Trees that were sufficiently strong to survive the first high-magnitude avalanche year were probably able to survive the 1969 cycle as well. However, given the potential of these two events to destroy tree-ring based evidences of avalanches, the chronology presented in this article should be regarded as the minimum frequency of natural snow avalanches.

The USFS Snow Rangers mention that according to their experience, events are less frequent at sites where the avalanche regime is sensitive to easterly snowfalls such as AR. It is interesting to note that the high-magnitude avalanche return period for this site was similar to the others. While events of lower magnitude might indeed be less frequent since westerly snowfall and drifting are the prevailing conditions in the Presidential Range, our data suggest that extreme events occur with similar recurrence in cirques of every aspects. The authors did not push this analysis further, but this finding advocates for a comparison of the distribution of the synoptic systems responsible for the most extreme snowfall in order to verify whether there is a shift between the proportions of storms origins at different magnitudes.

3.5.2 Logistic regressions

The highly significant levels of the logistic regression models based on the monthly resolved variables are consistent with results from Schläppy *et al.* (2015) and thus demonstrate a strong relationship between climate and high-magnitude avalanche activity. While one should be cautious to infer causality between predictors and a dependant variable in any statistical model, the covariates that were selected for the different paths are still generally consistent with the conditions that could lead to

avalanches of high magnitude, namely: 1) high rate of solid precipitation; 2) low temperatures favouring the creation of weak layers and the preservation of fragile layers deep in the snowpack, and 3) high winds provoking important snow drifting and the creation of wind slabs. These conditions were similar to logistic regression models found in other studies with different spatiotemporal resolutions (Jomelli *et al.*, 2007; Corona *et al.*, 2010; Schläppy *et al.*, 2015), as well as to the CT models presented above. Almost all predictors selected by the different logistic regression models vary coherently with these conditions. The case of the wind is interesting since average windspeed from December exhibits a positive relationship in HH, while the average windspeed from March and January exhibits negative relationships in HUR and AR, respectively. This is consistent with the exposition of the different path to prevailing winds. HH is on the lee aspect from the prevailing westerlies usually blowing from the WNW and therefore is prone to accumulation from drifting, whereas AR is located on the windward side of the Presidential and higher wind blow more snow away from the starting zone. As for HUR, even if it is on the lee side of the range, its northward-dominated aspect makes it less prone to accumulation from drifting in the starting zone than HH.

3.5.3 Classification trees

As expected, for every avalanche path, the prevailing scenarios necessitate important precipitation to trigger high-magnitude avalanches. Indeed, the root node of every CT is split by a snow or precipitation variable. Moreover, five CT models use a snowstorm predictor as their primary split, which could describe a high-magnitude direct action avalanche regime. This would be coherent with the fact that most lower-magnitude avalanches of the study region are produced by direct weather events, as reported by personal communications with the USFS snow rangers and scientific

literature (Joosen, 2008). Despite this conjecture, given the fact that snowstorm and snowfall covariates should be highly autocorrelated, the annual resolution of tree-ring data and absence of snowpack data, it is impossible to draw any conclusion whether the identification of these different snow variables at the root node of the CTs represent different avalanche triggering conditions.

However, as shown on Figure 3.5, the exclusive use of precipitation or temperature predictors led to CT models that did not performed as well. This statistical observation demonstrates that the inclusion of predictors from this second category highly improves the quality and performance of the models. Indeed, cold spells (Figure 3.3 a, b and d) can favour the persistence of weak layers in the snowpack or the development of a sufficient snowpack temperature gradient for the formation of faceted crystal and depth hoar (Haegeli and McClung, 2007). In a windy environment such as this study region, high velocity winds (Figure 3.3 c, f and g) have the potential to favour the triggering of avalanches through the creation of slabs either by snow drifting or snow sublimation. Therefore, the high-magnitude avalanche regime of these paths in the Presidential Range not only depends upon important snowfalls, but also on atmospheric conditions that favour the construction of fragile layers within the snowpack.

Comparing these results with other studies, it is interesting to notice that three of the five meteorological scenarios elaborated for the nearby Chic-Chocs Range (Québec, Canada) by Germain *et al.* (2009) could apply to the present CTs, namely 1) high frequency of snowstorms, 2) years with above-average snowfalls and 3) early-season weak layer of faceted crystals and depth hoar. The latter authors also identified avalanche events that followed sequences of freezing-rain and strong winds as well as the development of facet-crust following rain episodes. The weather data available for the Presidential Range did not allow to determine the occurrence of freezing rain, making it impossible to consider this variable in the CT analysis. As for the second

scenario, it seems unlikely that it is adapted to the avalanche regime of the present study region. Whenever one of the rain variables could be used as a surrogate split in the CT models, the relationship between the avalanche activity and liquid precipitation was negative. The maritime setting of the Chic-Chocs in the Gaspé Peninsula can account for these differences.

3.5.4 Comparison of logistic regression and CT models applied to avalanches

As stated before, the logistic regression models were highly significant and therefore demonstrate the presence of a statistical relationship between weather predictors and snow avalanches as inferred by dendrogeomorphology. However, these models are difficult to interpret especially because of the absence of splits in the dataset. Indeed, different weather events can provoke snow avalanches. On the contrary, the CT method provides insights into the weather triggers of high-magnitude snow avalanche years in the Presidential Range. The high classification rates and the low cross-validation prediction error rates are arguments in favour of the robustness of the models. The CTs also had similar or superior classification rates than different logistic regression models applied to avalanches found in the literature, whether daily (Jomelli *et al.*, 2007) or annually (Corona *et al.*, 2010; Castebrunet *et al.*, 20120; Schläppy *et al.*, 2015) resolved. The superior capacity of these models to identify avalanche years reinforces the idea that the CT method can be applied to annually resolved, long-term avalanche chronologies as well as to daily chronologies following the procedure proposed by Hendrikx *et al.* (2005, 2014). Comparing with previous tree-ring based studies that have linked punctual meteorological events or winter climatic conditions, either qualitatively (Germain *et al.*, 2009; Corona *et al.*, 2012; Decaulne *et al.*, 2014) or quantitatively (Corona *et al.*, 2010, Schläppy *et al.*, 2015), the coupling of CTs with tree-ring records provides a tool to gather together

both types of data in statistically robust models that are easier to interpret than logit models. This is an especially promising venue in the understanding of long-term avalanche regimes, because the triggering of an event can be the result of a direct action (e.g., important snowfall) and/or of a cascade of environmental conditions leading to the formation of a fragile layer in the snowpack.

Finally, we acknowledge the risk of overfitting the data in the CTs presented above, especially in the context of the scarcity of the years with avalanche activity identified. Despite the efforts of the authors to limit the number of predictors and to avoid any autocorrelation amongst them, with an avalanche chronology containing few avalanche years amongst many non-event years, there is always a possibility that the strong statistical relationships are random. Moreover, the superior classification rates from the CT models can be the result of their more flexible architecture rather than an increased capacity to provide insights into the physics of avalanche activity. However, the results of the cross-validation coupled with the coherence between the selected predictors, the physics of avalanche activity and the peculiarity of the smaller-magnitude direct avalanche regime of the study region bring confidence that the CTs capture, at least partially, the climate-avalanche dynamics of the study region. Indeed, the fact that, contrary to the logit models, the predictors used in the CT models for the sites HH, LH and HUR (Figure 3.3) are associated with the most active months in the recent archives by the snow rangers (Table 3.2) suggests that the identified weather-avalanche relationships are indeed but also significant for avalanches of smaller size. In any case, the CT procedure presented here should be reproduced elsewhere, especially on sites with a higher return period of high-magnitude snow avalanches, in order to corroborate the findings of this study.

3.6 Conclusions

In a study region where no records of past snow avalanche activity exists, the use of different proxies is the only way to gain insights in the long-term dynamics of the process. Using the dendrogeomorphological procedures, we reconstructed 19 years of avalanche activity at seven different study sites in the Presidential Range since 1930. The application of the modern threshold coupled with the Moran Index proved to be appropriate to maximize the identification of avalanche years while minimizing the noise in the tree-ring chronology. This paper then compared the use of different statistical methods to better understand the climate-avalanche relationship. The logistic regression models were statistically significant and were especially robust in their prediction of avalanche events with monthly resolved data. However, comparing their performance with CTs, the latter were significantly superior in assessing avalanche years.

Despite that dendrogeomorphology limits the resolution of the chronology to an annual time step, the analysis of the results using the CT algorithm highlighted probable weather drivers responsible for the occurrence of high-magnitude avalanche years at different spatiotemporal scales. In the present case, this statistical procedure was especially useful for its capacity to integrate meteorological data at two different timescales, namely monthly and annually resolved predictors. The CT method looks like a promising venue that could be applied in tree-ring snow avalanche records elsewhere, as well as tree-ring records of different weather-triggered geomorphological processes on steep slopes. Finally, the selected covariates are not only related to the amount of precipitations, but also to low temperatures and high winds. This corroborates that high-magnitude events do not necessarily follow a direct action avalanche regime due solely to important snowfalls, like most higher-frequency lower-intensity avalanches in this study region. It is the hope of the

authors that this article provides a better understanding of the relationship between climate and long-term avalanche activity in the Presidential Range of New Hampshire that will assist the USFS Snow Rangers in their daily avalanche forecasting activity.

Tableau 3.1 Main geomorphic characteristics of the different avalanche paths.

Path name	Starting zone (m)	Runout zone (m)	Track length (m)	Mean slope angle (°) Starting zone	Runout zone	Dominant aspect
GS	1450	1200	600	30	15	E
SM	1450	1100	1000	40	25	SE
HH	1550	1200	1050	40	10	ENE
LH	1375	1150	475	40	30	SE
HUR	1575	1250	625	40	25	NNE
K7	1550	1150	775	40	20	NNW
AR	1600	1025	1650	35	15	WSW

Tableau 3.2 Cumulative monthly snow avalanches recorded by the USFS snow rangers from 2006-2012. The other paths are not monitored. S: dry slab WL: wet loose WS: wet slab.

Path	December			January			February			March			April			Total		
	S	WL	WS	S	WL	WS	S	WL	WS	S	WL	WS	S	WL	WS	S	WL	WS
HH	7	-	-	11	-	1	9	1	-	4	2	-	5	-	-	36	3	1
LH	-	-	-	3	-	-	3	-	-	7	-	-	-	-	-	13	-	-
HUR	4	1	1	7	-	1	9	1	-	3	2	1	2	-	-	25	4	3

Tableau 3.3 Sample depth and intensity class for GDs assessed at different sites.

Site	Beginning of chronology	Trees	Discs	Cores	Samples	Classes 1,2,3	GDs Classes 4,5	Total	Avalanches identified
GS	1937	67	45	82	127	159	103	262	7
SM	1889	63	75	39	114	232	191	423	7
HH	1903	62	52	57	109	242	125	367	6
LH	1920	78	77	90	167	172	170	342	9
HUR	1943	59	81	20	101	223	158	381	10
K7	1954	60	55	36	91	83	92	175	7
AR	1950	61	73	26	99	180	121	301	8
Total		**450**	**458**	**350**	**808**	**1291**	**960**	**2251**	**54**

Tableau 3.4 Predictors used in this study. Weather station: P = Pinkham Notch, S = Mt. Washington Observatory.

Category	Variable	Description	Weather station
Precipitation	Snow_month	Sum of snowfall	P
	Ppt_month	Sum of precipitation (rain + snow)	P
	Snow_Xcm_24h_month	Nb of events of 10, 15, 20 or 25 cm snowfall in 24 hours	P
	Snow_Xcm_72h_month	Nb of events of 25, 50, 75 or 100 cm snowfall in 72 hours	P,
	$Snow\_24h\_month_{>1SD}$	Nb of events of 24h snowfall > 1 SD* from the mean	P
	$Snow\_24h\_month_{>2SD}$	Nb of events of 24h snowfall > 2 SD from the mean	P
	$Snow\_72h\_month_{>1SD}$	Nb of events of 72h snowfall > 1 SD from the mean	P
	$Snow\_72h\_month_{>2SD}$	Nb of events of 72h snowfall > 2 SD from the mean	P
Temperature	Tmin_month	Mean of the daily min temperature	P
	Tmax_month	Mean of the daily max temperature	P
	Tmean_month	Mean of the daily average temperature	P
	$Tmin\_month_{<-1SD}$	Nb of days with a min temperature < -1 SD from the mean	P
	$Tmin\_month_{<-2SD}$	Nb of days with a min temperature < -2 SD from the mean	P
	$Tmax\_month_{>1SD}$	Nb of days with a max temperature > 1 SD from the mean	P
	$Tmax\_month_{>2SD}$	Nb of days with a max temperature > 2 SD from the mean	P
	$Tmean\_month_{>1SD}$	Nb of days with an average temperature > 1 SD from the mean	P
	$Tmean\_month_{>2SD}$	Nb of days with an average temperature > 2 SD from the mean	P
Wind	Wind_month	Mean of the daily average windspeed	S

Tableau 3.5 Avalanches identified with the Moran I of the trees recording high-intensity GDs. The *p*-values of the Z scores were < 0.01 (bold), < 0.05 (italic) or <0.1 (regular).

Site	Year	Trees	GD	I_t	Moran I	Z score
GS	1999	67	5	7.46%	0.155	**2.83**
	2008	66	6	9.09%	0.372	**6.30**
SM	1943	33	3	9.09%	0.355	**2.81**
HH	1943	37	3	8.11%	0.188	*2.02*
	1958	53	4	7.55%	0.100	1.59
	2008	62	6	9.68%	0.148	*2.26*
LH	2001	78	7	7.69%	0.169	*2.53*
HUR	1952	26	3	11.54%	0.346	*2.55*
K7	2010	60	5	8.33%	0.125	*2.52*
AR	1958	28	3	10.71%	0.233	1.69

Tableau 3.6 Logistic regression models at the path scale using annually resolved predictors.

Site	Variable	*p*-value	β	R^2	Sensitivity	Specificity	Overall prediction
GS	Intercept	0.000	-3.22	0.49	57.1%	100.0%	96.1%
	Snow_75cm_72h_yr	0.026	1.16				
	$Snow\_72h\_yr_{>1SD}$	0.015	1.18				
SM	Intercept	0.000	-2.95	0.36	28.6%	98.6%	92.2%
	Snow_20cm_24h_yr	0.003	1.36				
HH	Intercept	0.000	-2.99	0.28	33.3%	100.0%	94.8%
	Snow_20cm_24h_yr	0.006	1.12				
LH	Intercept	0.000	-3.01	0.36	12.5%	97.1%	88.3%
	Snow_yr	0.009	1.09				
	Tmax_yr	0.062	-0.96				
HUR	Intercept	0.000	-2.36	0.43	40.0%	98.3%	90.0%
	$Snow\_72h\_yr_{>1SD}$	0.007	1.30				
	Snow_50cm_72h_yr	0.047	1.16				
K7	Intercept	0.000	-3.41	0.63	42.9%	96.2%	89.8%
	Ppt_yr	0.020	1.59				
	Snow_15cm_24h_yr	0.028	1.42				
AR	Intercept	0.000	-3.00	0.46	37.5%	96.4%	88.9%
	Snow_20cm_24h_yr	0.003	1.62				
	$Tmax\_yr_{>2SD}$	0.018	1.32				

Tableau 3.7 Logistic regression models at the path scale using monthly resolved predictors.

Site	Variable	*p*-value	β	R^2	Sensitivity	Specificity	Overall prediction
GS	Intercept	0.000	-4.05	0.57	57.1%	98.6%	94.7%
	$Snow\_72h\_dec_{>1SD}$	0.011	1.73				
	$Tmean\_dec_{>2SD}$	0.018	1.28				
	$Tmin\_feb_{<-1SD}$	0.066	-1.42				
	Snow_20cm_24h_feb	0.057	1.13				
SM	Intercept	0.000	-3.88	0.61	71.4%	98.6%	96.1%
	Snow_50cm_72h_feb	0.026	1.38				
	$Snow\_72h\_dec_{>1SD}$	0.007	1.69				
	Snow_50cm_72h_mar	0.099	0.90				
HH	Intercept	0.008	-6.83	0.69	66.7%	98.6%	96.1%
	Snow_15cm_24h_feb	0.040	3.26				
	W_dec	0.088	3.19				
	Tmax_dec	0.075	-1.36				
	Snow_10cm_24h_jan	0.099	1.68				
LH	Intercept	0.003	-5.82	0.73	62.5%	95.7%	92.2%
	Snow_dec	0.025	2.33				
	Snow_15cm_24h_mar	0.019	2.43				
	$Tmin\_dec_{<-1SD}$	0.024	1.76				
	$Tmin\_apr_{<-2SD}$	0.024	1.42				
HUR	Intercept	0.000	-3.70	0.64	50.0%	96.7%	90.0%
	Snow_20cm_24h_feb	0.021	1.92				
	$Snow\_24h\_mar_{>2SD}$	0.017	1.23				
	$Snow\_72h\_dec_{>1SD}$	0.049	1.34				
	W_mar	0.007	-1.63				
K7	Intercept	0.001	-4.41	0.67	71.4%	100.0%	96.6%
	$Snow\_72h\_feb_{>1SD}$	0.077	1.26				
	$Snow\_72h\_dec_{>1SD}$	0.018	2.25				
	Ppt_apr	0.011	2.27				
AR	Intercept	0.009	-5.94	0.61	62.5%	98.2%	93.7%
	$Tmax\_feb_{>1SD}$	0.002	-5.28				
	$Snow\_24h\_mar_{>2SD}$	0.034	1.52				
	W_jan	0.054	-1.61				

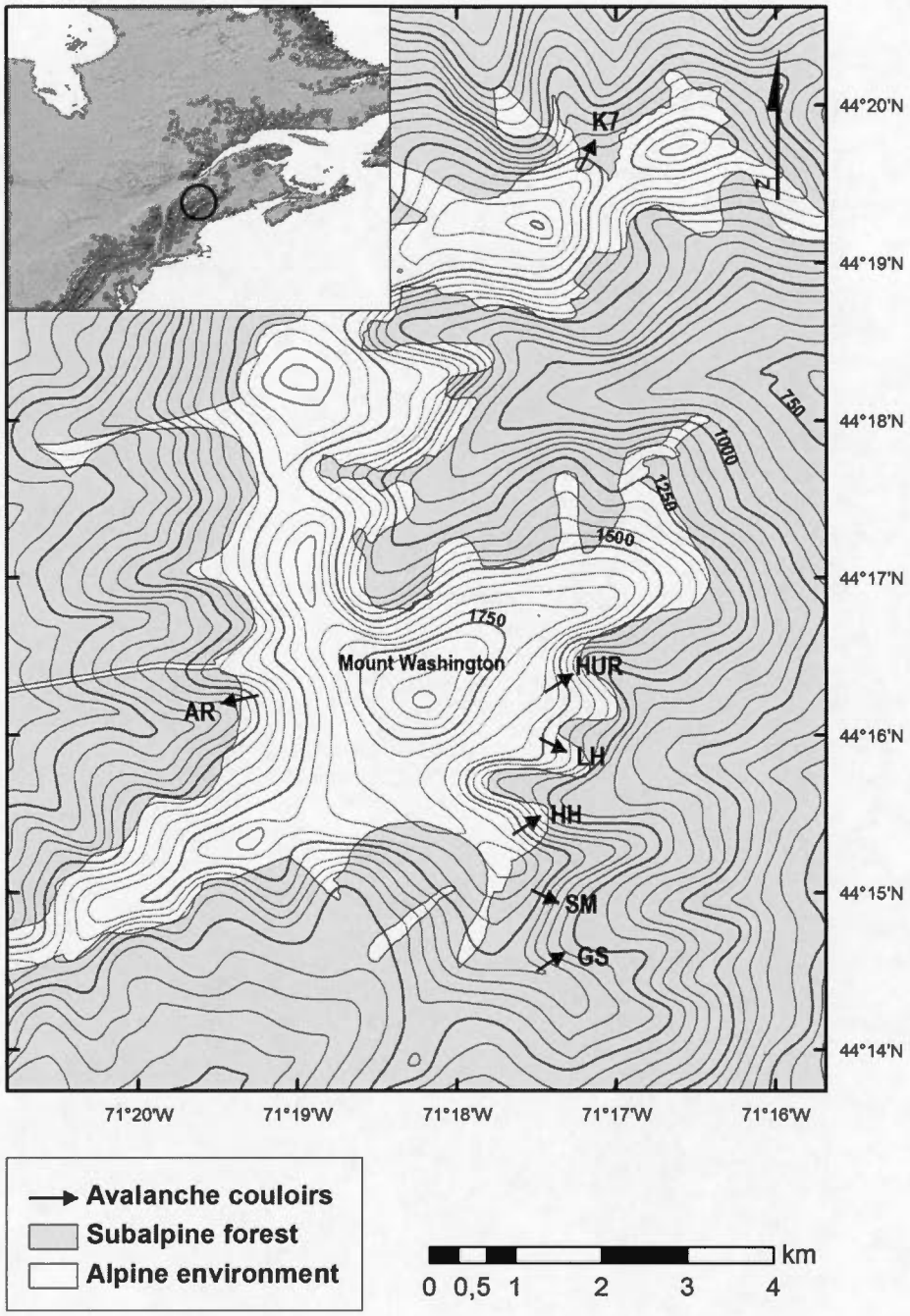

Figure 3.1 Map of the Presidential Range showing the localisation of the different avalanche paths investigated in this study. Contour intervals are 50 m.

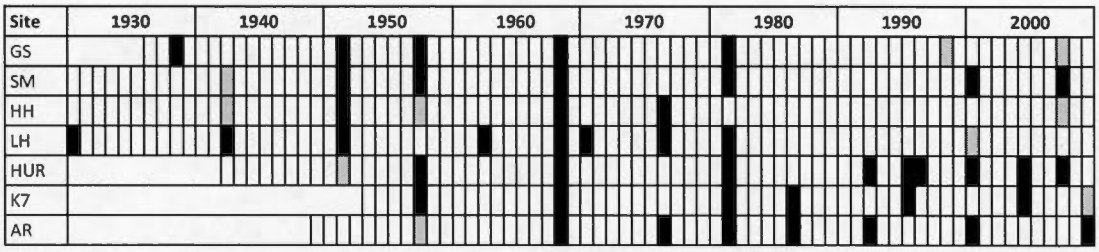

Figure 3.2 Spatiotemporal distribution of high-magnitude avalanches at the different study sites. Black squares represent avalanches identified following the modern GD-I_t threshold. Grey squares represent avalanches identified with the Moran I.

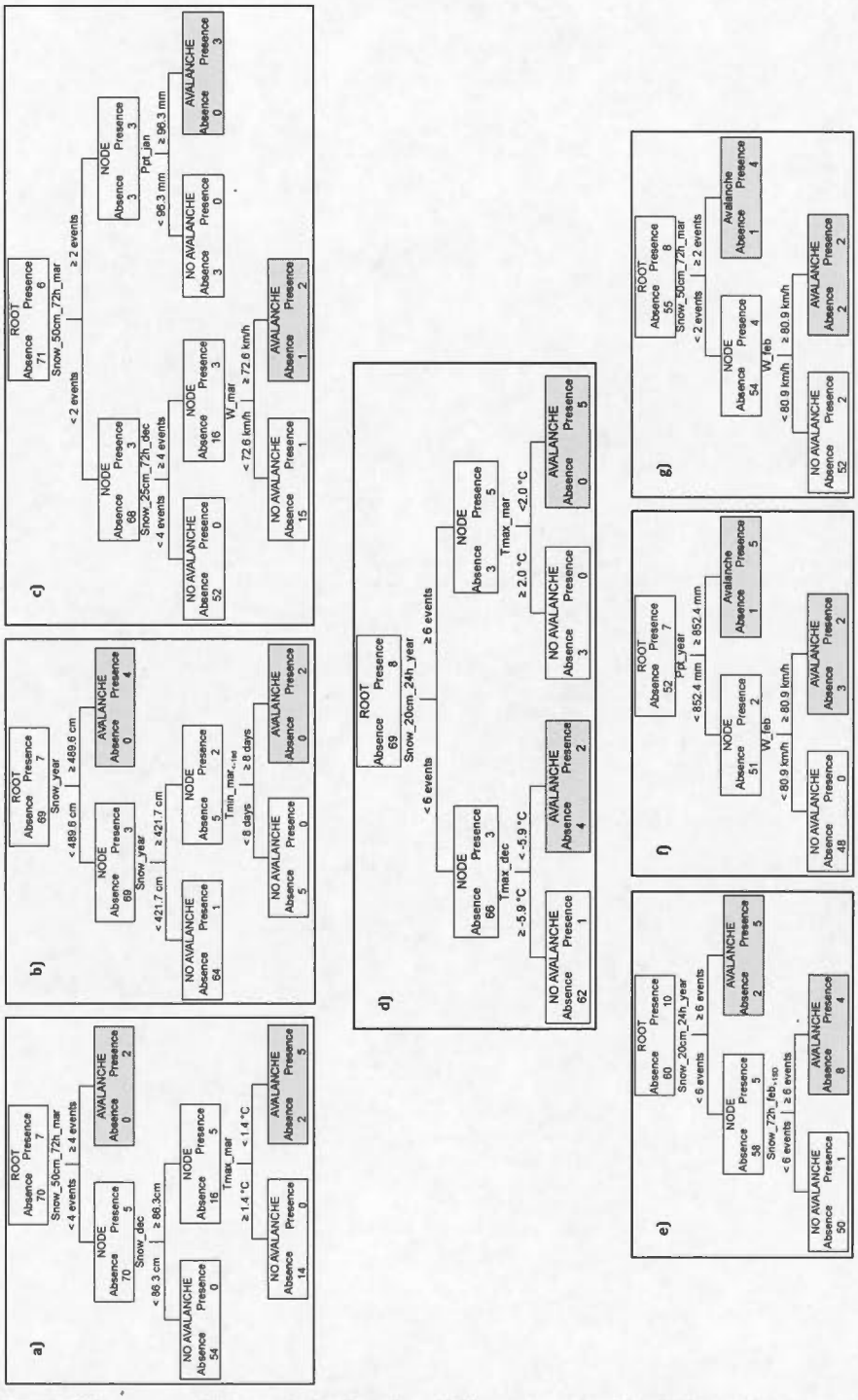

Figure 3.3 CT models for the different paths, based on the bootstrap procedure using the complete dataset. (a) GS (b) SM (c) HH (d) LH (e) HUR (f) K7 (g) AR

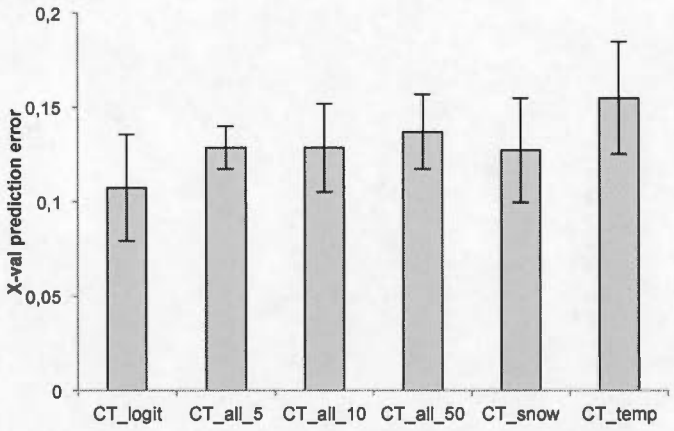

Figure 3.4 Comparison of the mean cross-validation prediction errors of the different CT models using the covariates from the logit models (*CT_logit*) or the predictors selected by the bootstrap procedure (*CT_all*: precipitation, temperature and wind predictors; *CT_snow*: precipitation predictors; *CT_temp*: temperature and wind predictors). 5, 10 and 50 refers to the number of cross-validations used in the sensitivity analysis, which is only presented for *CT_all* models. Error bars present the Student's *t* 90% confidence interval around the mean.

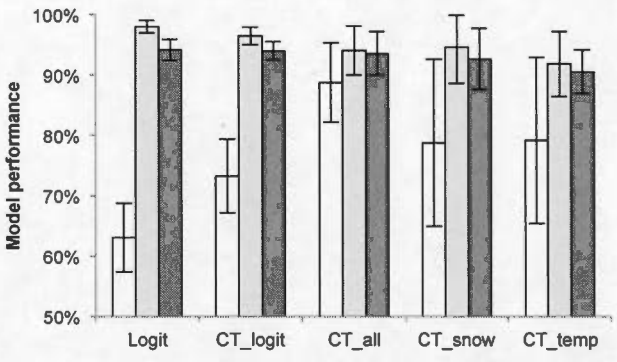

Figure 3.5 Comparison of the performance of the logistic regression (*Logit*) with the different CT models using the same covariates than the logistic regression models (*CT_logit*) or the variables selected using the bootstrap procedure (*CT_all*: precipitation, temperature and wind predictors; *CT_snow*: precipitation predictors; *CT_temp*: temperature and wind predictors). The mean sensitivity (white), specificity (pale grey) and overall prediction (dark grey) are presented as indicators of their ability to assess avalanche activity. Error bars present the Student's *t* 90% confidence interval around the mean.

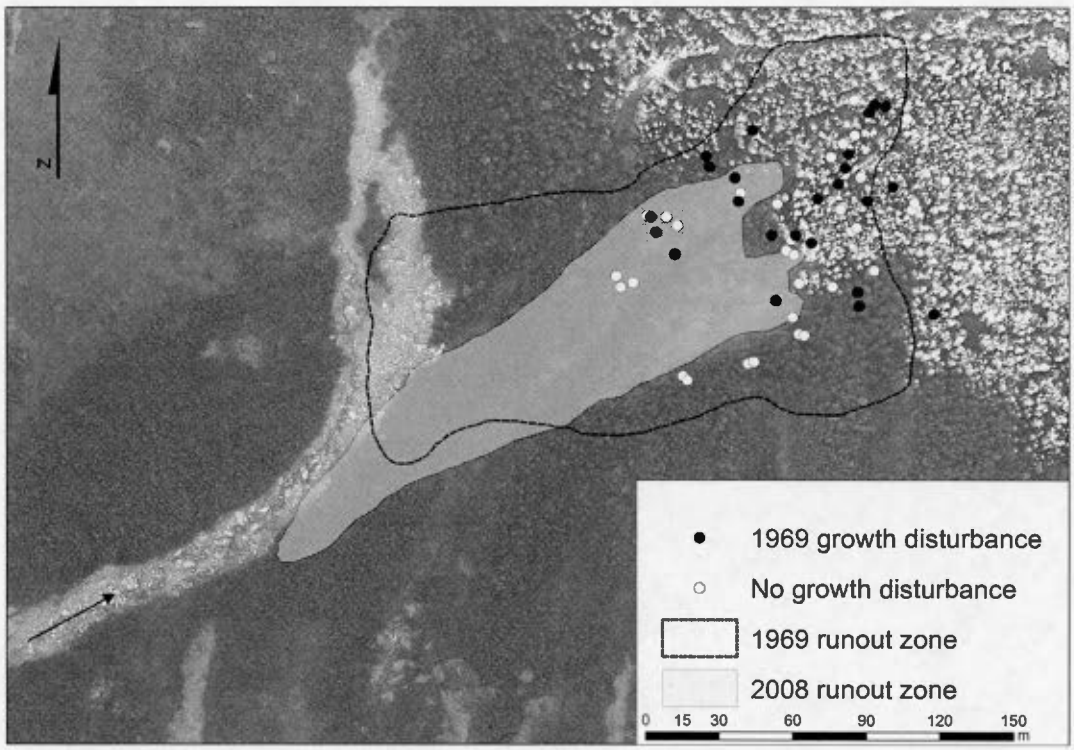

Figure 3.6 Map illustrating the ecological impact of the high-magnitude avalanches of 1969 and 2008 at site HH. The runout extensions were drawn according to the clearing of trees on orthorectified aerial photographs. Trees could therefore exhibit growth disturbance outside of this zone if material (snow, rocks, trees) flowed beyond the boundary of the forest that was cleared. The arrow shows the direction of the flow. The zone without vegetation was affected by a debris flow during the passage of hurricane Irene in 2011. The runout zone of the debris flow did not follow the same trajectory as the high-magnitude avalanches.

CHAPITRE IV

LARGE-SCALE TELECONNECTION PATTERNS AND SYNOPTIC CLIMATOLOGY OF MAJOR SNOW-AVALANCHE WINTERS IN THE PRESIDENTIAL RANGE (NEW HAMPSHIRE, USA)

Jean-Philippe Martin[1] and Daniel Germain[2]

[1]Environmental sciences Institute, Université du Québec à Montréal, C.P. 8888 Succursale Centre-Ville, Montréal, Québec, Canada.

[2]Geography Department, Université du Québec à Montréal, C.P. 8888 Succursale Centre-Ville, Montréal, Québec, Canada.

Article soumis à la revue *International Journal of Climatology.*

Résumé

Les relations entre la météorologie synoptique, les téléconnexions à grande échelle et l'indice d'activité avalancheuse régionale (RAAI) reconstituée par dendrochronologie ont été évaluées dans la Chaîne Présidentielle des White Mountains (New Hampshire, États-Unis). Lors de la période 1936-2012, 18 années d'activité avalancheuse à l'échelle régionale ont été comparées aux modes climatiques hivernaux conjoints températures/précipitations (froid et humide (FH), froid et sec (FS), chaud et humide (CH), chaud et sec (CS)), à l'Oscillation de l'Atlantique Nord (NAO), à l'Oscillation du Pacifique Sud (ENSO), aux cartes des anomalies composites à 500-mbar, ainsi qu'à la proportion de la neige provenant de différentes trajectoires de tempêtes. Les chutes de neige annuelles et la NAO sont corrélées avec le RAAI. Il y a une différence significative dans l'activité avalancheuse des années avec une NAO inférieure à -3. Les hivers avalancheux sont présents dans les quatre modes climatiques, mais en proportion supérieure dans les hivers FH comparativement aux trois autres modes, ainsi que dans les hivers humides comparativement aux hivers secs. Les hivers FH, FS et CH présentent toutes une NAO négative, située davantage à l'est pour les modes humides. Les hivers froids reçoivent une part plus importante de neige de dépressions en provenance des Grands Lacs, comparativement aux dépressions côtières pour les hivers humides. La NAO semble être un prédicteur adéquat des chutes de neige, sans toutefois informer sur les trajectoires de tempêtes dominantes. À l'opposé, il y a absence de corrélation entre les chutes de neige et l'ENSO, mais ce dernier montre une relation significative avec les proportions de neige issues de dépression en provenance de la côte (relation positive) et des Grands Lacs (relation négative). Cette étude présente les premiers résultats détaillant les mécanismes à l'échelle synoptique expliquant la variabilité de l'activité avalancheuse issue des fluctuations dans les téléconnexions à l'échelle globale. Ces résultats suggèrent également que l'occurrence d'années extrêmes en terme d'activité avalancheuse est atribuable au phasage entre la NAO négative et l'ENSO positif.

Mots clés :

Avalanches de neige; Dendrochronologie; Oscillation de l'Atlantique Nord; Oscillation du Pacifique Sud; Météorologie synoptique; Chaîne Présidentielle

Abstract

The relationships between the synoptic climatology, large-scale teleconnections and the regional avalanche activity index (RAAI) inferred from tree-rings were evaluated for the Presidential Range in the White Mountains (New Hampshire, USA). During the period 1936-2012, 18 years of regional avalanche activity were compared with the winter-scale prevailing joint temperature/precipitation modes (Cold Wet (CW), Cold Dry (CD), Warm Wet (WW) and Warm Dry (WW)), the North Atlantic Oscillation (NAO), the El Niño-Southern Oscillation (ENSO), the 500-mbar composite anomaly maps and the ratio of snow from different storm tracks. The total winter snowfall and the NAO negatively correlate with the RAAI. A Chi-square test allowed to infer that there was a difference in the RAAI between winters with a NAO under or above -3. Winters of avalanche activity were present in the four climatic modes, albeit the ratio of avalanche/non-avalanche years is superior for CW winters compared to the three other modes, as well as for wet winters compared to dry winters. CW, CD and WW winters exhibit a negative NAO anomaly, which is eastbound for the wet years. Cold winters receive more snow from the Great Lakes, whereas coastal depressions are more important during wet winters. The NAO is an adequate predictor of snowfall, but does not provide information about the storm tracks. On the contrary, the ENSO is poorly correlated with snowfall, but its relationship is significant with the ratio of snow produced by coastal depressions (positive relationship) and Great Lakes storms (negative relationship). These are the first results detailing the mechanisms at the synoptic scale that could account for the variability in the avalanche dynamics following the fluctuations in large-scale teleconnections, and suggest that the most extreme avalanche years in the region occur during the phasing between a positive ENSO and a negative NAO at the winter scale.

Keywords

Snow avalanche; Tree-ring; North Atlantic Oscillation; El Niño-Southern Oscillation; Synoptic climatology; Presidential Range

4.1 Introduction

Since 1951, in the United States (US), snow avalanches account for more than 1,000 fatalities (Colorado Avalanche Information Center, 2015). This death toll increased in the last decade, especially because of the development of backcountry activities on avalanche-prone steep slopes (Logan and Witmer, 2012). While most of these accidents occur in western US, it still is an important natural hazard in Northeastern North America. In Quebec (eastern Canada), it is the second deadliest natural hazard since 1825 (Hétu *et al.*, 2011; Germain, 2016). In the White Mountains of New Hampshire, avalanche-related accidents occur yearly, accounting for 15 fatalities since 1954 (CAIC, 2015).

Because the triggering of snow avalanches is related to the characteristics of the snowpack, they are sensitive to the variations in climate like the majority of cryogenic land surface processes (Eckert *et al.*, 2010; Haeberli *et al.*, 2010; Jomelli *et al.*, 2011). In recent years, there have been an increasing number of studies on the climate-avalanche relationship. From an operational standpoint, scientists have applied statistical frameworks such as, among others, logistic regressions (Castebrunet *et al.*, 2012; Jomelli *et al.*, 2007), classification trees (Hendrikx *et al.*, 2005, 2014; Martin and Germain, *in press*), nearest neighbour (Singh *et al.*, 2015) or ensemble forecasting (Vernay *et al.*, 2015), to improve the forecasting of snow avalanches using weather predictors at different spatiotemporal scales. From a phenomenological point of view, recent papers explored, among other subjects, the temporal trends in avalanche activity with the ongoing climate changes (Eckert *et al.*, 2013) or the relationship between climate and snowpack characteristics (Conlan *et al.*, 2014).

The characteristics of the snowpack evolve following the fluctuations in synoptic-scale atmospheric circulation, and therefore the latter affect the spatiotemporal pattern of avalanche activity (Fitzharris and Schaerer, 1980; Ferguson *et al.*, 1990; Mock and Birkeland, 2000). In a descriptive fashion, early studies present the different synoptic-scale atmospheric circulation patterns prevailing during periods of avalanche activity in Norway (Fitzharris and Bakkehøi, 1986), in Iceland (Bjornsson, 1980), in the Indian Himalayas (Rangachary and Bandyopadhyay, 1987) or in the Austrian Alps (Hächler, 1987). Early results in the Canadian Rockies provide quantitative evidences that many atmospheric circulation patterns are needed to explain avalanche activity at the winter scale (Fitzharris, 1987). In recent years, Birkeland *et al.* (2001) statistically demonstrated that high snow water equivalent and high snowfall conditions corresponding to days of high avalanche activity were linked to characteristic anomalies of the 500-mbar heights. Many studies also used synoptic-scale meteorology to determine its relationship with snowfall (Birkeland and Mock, 1996; Esteban *et al.*, 2005). More recent results succeeded in linking the synoptic atmospheric conditions to the formation of extensive surface hoar (Yokley *et al.*, 2014), which is a crystal type that can cause a weak layer within the snowpack.

On a larger scale, Mock *et al.* (2000) investigated the relationship between synoptic-scale meteorology, avalanche activity and larger-scale teleconnections, namely the Pacific-North American (PNA) and the Pacific Decadal Oscillation (PDO). Indeed, given the local influence on weather of global climatic systems, they can have a significant influence on the avalanche regimes. In Western North America, the impacts of El Niño-Southern Oscillation (ENSO) as well as other global teleconnections on snow avalanches has been investigated. Dixon *et al.* (1999) first reported a significant decrease in avalanche activity during El Niño years for Glacier National Park (US). The authors attributed this relationship to the below-average precipitations characteristic of the positive phases of ENSO, but did not corroborate their findings with weather or snow data. In British-Columbia (BC, Canada),

McClung (2013) succeeded in linking the ENSO to the type of avalanche. His results show that La Niña winters were colder and produced more snow, thus causing more snow avalanches and a higher proportion of dry snow avalanches. Bellaire (2013 *in* Thumlert *et al.*, 2014) also recognized the greater impact of the global climatic systems on avalanche activity at Roger's Pass (BC) when the ENSO and the Pacific Decadal Oscillation (PDO) are in phase. Still in BC, Thumlert *et al.* (2014) made an exploratory analysis correlating different compositions of the ENSO, the PDO, the Arctic Oscillation (AO) and the North Atlantic Oscillation (NAO) with avalanche activity. In their study, most of their indices correlated with either the quantity of dry or wet snow avalanches. In Europe, the NAO is the major large-scale atmospheric circulation pattern affecting the climate (Casanueva *et al.*, 2014). Keylock (2003) first established a connection between the positive phase of NAO and snow avalanches in Iceland, and postulated that the recent rise in NAO could have implications on return periods and runout distances. Using the same method as the former author, Garcia *et al.* (2009) found a negative relationship between avalanche activity and the NAO in the Eastern Pyrenees, but could not identify the process of the NAO governing avalanche activity. However, in the French Alps, no correlations were found between avalanche activity and the NAO (Jomelli *et al.*, 2007).

All the aforementioned studies were conducted on large-scale historic databases that could include up to approximately 25,000 snow avalanches at the daily scale (McClung, 2013). In the White Mountains of New Hampshire, and to a greater extent Northeastern North America, where no such archives exist, the use of tree-rings has been recognized as a valid proxy to reconstruct snow avalanche activity with an annual resolution (Germain *et al.*, 2009; Corona *et al.*, 2013). However, the potential for this lower resolution chronology to identify relationship between snow avalanches, the global climatic systems and synoptic meteorology has never been tested. Yet, in New England, the relationship between winter conditions and NAO has been acknowledged (Hartley and Keables, 1998). A negative relationship

between snowfall and NAO is indeed the product of characteristic synoptic conditions during heavy snowfall winters. During a negative NAO year, anomalously positive 700-hPa heights over Greenland indicate more frequent blocking thus favouring the occurrence of "Nor'easters" which tend to result in heavy snowfalls over New England (Bradbury *et al.*, 2002*a*). Moreover, Huntington *et al.* (2004) found a significant negative correlation between the NAO and the winter ratio between snow and rain in northern New England. However, in the nearby Gaspé Peninsula, studies show an absence of significant relationship between this index and snow cover (Fortin and Hétu, 2014) or avalanche activity (Germain et al., 2009). As for ENSO, results from the same authors indicate that no clear links exist between this teleconnection and the climate of New England. However, recent studies have identified linkages between this index and the prevalent synoptic scale meteorology: coastal storms are more frequent during El Niño years (Bradbury *et al.*, 2003). Germain *et al.* (2009) suspected a relation between ENSO and regional avalanche activity in the Chic-Chocs Range (Quebec, Canada), but could not provide a significant statistical relationship or link ENSO to the climatic drivers of avalanche activity.

It is the aim of this paper to provide the first study linking a tree-ring based regional avalanche chronology to the global climatic indices and the ensuing synoptic climatology. The objectives are the following: i) to identify the prevailing weather scenarios during the major avalanche years identified from tree-rings in the Presidential Range of the White Mountains (New Hampshire); ii) to explore the impact of large-scale teleconnection patterns on the regional avalanche activity and the alpine weather of the study region, and iii) to analyse the synoptic climatology of avalanche activity.

4.2 Study sites

The Presidential Range of the White Mountains (New Hampshire, United States, 44°16' N 71°18' W; Figure 4.1) includes different peaks along a North to South ridge. Avalanches mostly occur on the steep slopes of the twelve Pleistocene glacial cirques located above the treeline all around this ridge (Goldthwait *et al.*, 1987). The whole range in general is one if not the most important destination of the Northeast for the practice of winter activities on the steep slopes (alpine climbing and backcountry skiing). Most of this activity is located in two cirques – Tuckerman and Huntington Ravines – hence the start of a daily avalanche forecasting program by the United States Forest Service (USFS) in 1959. Nowadays, given the small area covered by the forecast and the high spatial variability of the snowpack, the USFS Snow Rangers produce a daily advisory for every avalanche path in these two cirques. During the 2007 winter, the forecasters started to archive every avalanche observation. However, no previous records exist.

The avalanche paths concerned by the present study are located on Figure 4.1. All of these paths have a starting zone above the alpine limit (between 1,375 and 1,600 m a.s.l.), a runout zone fragmenting the subalpine forest (between 1,025 and 1,250 m a.s.l.) and an average slope between 30° and 40°. A detailed description of these sites is available in Martin and Germain (*in press*).

Despite its low altitude, the Presidential Range is known for his extreme weather. On the summit of Mount Washington (highest summit of the Northeast, 1,917 m a.s.l.), the average winter temperature (winter is hereafter defined as the period from December 1st of the preceding year to April 30th of a given year) is -11.8 °C. The average annual snowfall is 714.2 cm and most of the winter precipitations are solid. Severe winds are characteristic of Mount Washington summit, which held for many decades the record for directly measured surface wind speed (372 km/h). The record

peak gust for every month is above 200 km/h and gusts of hurricane strength (i.e., above 119 km/h) are recorded two thirds of the days during winter (Gordon, 1989). At the timescale of the present study, Mount Washington summit did not exhibit any significant trend in temperature or snowpack duration, albeit the records from a station at lower altitude did show a significant warming and a decrease in continuous snow cover (Seidel *et al.*, 2009). The authors explain this lack of trend for the summit by the fact that the summit of Mount Washington is subject to boundary layer and free troposphere conditions (Grant *et al.*, 2005).

4.3 Methods

4.3.1 Tree-ring analysis and regional avalanche activity reconstruction

The dendrochronological procedure used here is summarized. A more thorough description is available in Martin and Germain (*in press*). The seven avalanche paths were selected based on recommendations from the USFS snow rangers, the extension of the runout zone below the treeline with the presence of trees damaged by previous snow avalanches, the simplicity of access and the location outside of a strict conservation zone.

Considering the objective of working with high-magnitude avalanches, at each site, trees were sampled along or beyond the boundary between open land and closed forest at the lower limit of the runout zone. Site AR is an exception where the sampling effort was concentrated on the northern trimline because an important flood during the passage of hurricane Irene disturbed the rest of the runout zone. Trees showing external damages were sampled by collecting stem discs at the level of the

disturbances for smaller trees (diameter < 20 cm) or wood cores, either at the level of the apparent damage or as low as possible if the latter was too high. Depending on the availability of healthy trees showing external damages in the runout zone, between 59 and 78 individuals were sampled at each site. Laboratory work consisted first in drying and sanding the samples. Under a binocular microscope, the age at sampling height of every tree was assessed as well as the date of the different growth disturbances (GD). To avoid recording other disturbances of lower magnitudes (e.g., snow creeping), only high-quality GDs were recorded, namely: i) clear impact scars, ii) the presence of traumatic resin ducts (TRD), iii) major growth reductions or iv) compression wood sequences lasting > 3 successive years.

At each site, the ration of trees recording a GD over the number of samples alive at year t gave the index I_t (Shroder, 1978):

$$I_t = \left(\frac{\sum_{i=1}^{n}(R_t)}{\sum_{i=1}^{n}(A_t)}\right) \times 100 \quad (1)$$

Where R_t is the number of trees exhibiting a GD at year t and A_t represents the number of trees alive at year t. The modern *GD-I_t* method (Chiroiu *et al.*, 2015) was used to discriminate years of avalanche activity at the path scale. This method uses a different double threshold according to sample sizes of 10–20 (GD $\geq$ 3 and $I_t \geq$ 15%), 21–50 (GD $\geq$ 5 and $I_t \geq$ 10%), and $\geq$ 51 trees (GD $\geq$ 7 and $I_t \geq$ 7%). Since trees impacted by an avalanche are usually spatially clustered (Corona *et al.*, 2010), for a given year, if a site is above the I_t threshold but below the GD threshold, avalanche activity was inferred if the impacted trees had a Moran's I significantly above 0 (using the Z-score with a p-value < 0.1).

Avalanche activity indices are commonly used to quantify the degree of avalanche activity at different spatiotemporal scales, by weighting the number of events by its size, using the Canadian avalanche classification (McClung and Schaerer, 2006). However, avalanche size is not available from tree-ring data. To estimate the

avalanche activity at the scale of the Presidential Range, a regional avalanche activity index (RAAI) was calculated as followed (Germain *et al.*, 2009):

$$RAAI_t = \left(\frac{\sum_{i=1}^{n} I_t}{P_t}\right) \quad (2)$$

Where I_t represents the avalanche index for site i for year t and P_t the number of sites that could record an avalanche at year t (defined as the period from December of year t-1 to April of year t) based on a minimum sample size of 10 trees. The assumption behind the RAAI is that high-magnitude avalanches should damage more trees hence a higher probability of being recorded in the tree-ring chronology (Germain *et al.*, 2009). The RAAI was then compared to the percentage of active avalanche paths (PAAP) for each year to assess its representativeness. A major difficulty is to discriminate significant avalanche activity at the range scale from noise caused by other disturbance. In the literature, Germain *et al.* (2009) propose a RAAI threshold of 10% to infer activity at the regional scale in the Chic-Chocs Range, but mention that this threshold could change according to the ecological context. The extreme values of the probability distribution of the RAAI are therefore the focus of interest. The behaviour of extreme values being different from the rest of the distribution, Picklands (1975) argued that the tail of an extreme value parent distribution, above a certain threshold, should follow a generalized Pareto distribution. We identified the threshold above which the RAAI followed a generalized Pareto distribution using the Peaks Over Threshold (POT) method (Embrecht *et al.*, 1997), using different graphical and statistical indicators. Ouellet and Germain (2014) previously used the POT method to discriminate hyperconcentrated flow activity in tree-ring data.

4.3.2 Climate data processing

Daily weather data were obtained from two weather stations. The first dataset came from Mount Washington Observatory, a station located on the summit of Mount Washington, which recorded weather data from 1936. Given that snowfall is recorded at this station using a snow gauge despite the high winds, the accuracy of snow data is doubtful. However, since the avalanche starting zones are located in the alpine environment, and given that the quantity of precipitation increases with altitude, our assumption is that the meteorological conditions are probably more similar to this station than lower elevations stations. Therefore, we consider that if a recorded daily snowfall is above 10 cm, it can be considered as a snowstorm that deposited a substantial precipitation quantity in the avalanche starting zones. Daily temperatures from this station were also used. Second, at Pinkham Notch, at the base of Mount Washington (619 m asl), the Appalachian Mountain Club operates a National Weather Service cooperative station (COOP #276818, NCDC station ID 20018701, NWS Location ID HGMN3). Being more sheltered from the high winds, total snowfall and maximum snowdepth were recorded at this station.

Weather variables were created at different resolutions (Table 4.1). Since the Presidential Range is known for the prevalence of direct action avalanches, at the daily scale for every avalanche year, winter snowstorms (i.e., consecutive days with > 10 cm snowfall) were identified. At the monthly scale, total storm snow was calculated. At the winter scale, total storm snow, total snowfall and maximum snowdepth were recorded. To model the atmospheric temperature over larger timescales, the number of freezing degree-days (FDD) and thawing degree-days (TDD) were computed at the monthly and winter scale.

For every snowstorm, the prevailing low-pressure system was identified, following the storm track classification used by Collins *et al.* (2014; Figure 4.1a): 1) Canada if

the system passes North of the Great Lakes, 2) Great Lakes when the storm passes over the Great Lakes, 3) Ohio for the systems that follow the Ohio valley between the Appalachian Mountains and the South of the Great Lakes, 4) Coastal for the depressions that move northward on the Atlantic Coast. The Great Lakes and Coastal storm tracks were responsible for most of the snowstorms. Daily synoptic maps from the National Oceanic and Atmospheric Administration (NOAA) Central Library were used to identify the storm tracks. For the avalanche year, 500-mbar geopotential height anomalies were computed for the winter period using NCEP/NCAR composite maps (Kalnay *et al.*, 1996).

The NAO and ENSO indices were included as well. Station-based winter (December through March) and monthly (December through April) NAO data were available from Hurrell and NCAR (2014). Station-based data were favoured over PC-based since they extend prior to 1950. For ENSO, we used the Oceanic Niño Index for the 3.4 region (ONI 3.4). Because of the lag between the ONI 3.4 value and the climatic response (Fründt *et al.*, 2013), the previous 3 month sea surface temperatures (SSTs) moving average provided by USNWS (2015) was used as the monthly value from December to April (e.g., December value was given by the average from October to December), which was then averaged to provide the winter index. The ENSO data extend from 1950 to 2012.

4.3.3 Climate data analysis

First, the relationships between the RAAI and climate were investigated using different statistical methods. At the global scale, a *t*-test and a Mann-Whitney rank-sum test were performed to verify whether the difference in the average winter NAO index was significant between years of RAAI above or below the threshold. Chi-

square tests were then calculated to assess whether there was a significant difference in avalanche activity for winters experiencing either a positive or negative NAO or ENSO. Since many datasets did not meet the assumption of normality, we used Spearman rank correlations to investigate the dependency between different weather variables, avalanche activity and the teleconnections. The correlations with a p-value < 0.05 on the Spearman's rho were then bootstrapped 1000 times to make sure that their statistical significance was not the result of the few extreme data points.

In order to investigate the prevailing scenarios of regional avalanche activity, we used a joint temperature/precipitation modes approach (Beniston, 2009; López-Moreno *et al.*, 2011; Fortin and Hétu, 2014). We first determined the threshold that corresponded to the 40% and 60% quantiles of solid precipitation and temperature. We then defined the quantiles as follow: dry (if precipitation is below 40% quantile), wet (if precipitation is above 60% quantile), cold (if temperature is below 40% quantile) and warm (if temperature is above 60% quantile). For each year, this allowed to count the number of days in four different modes: Cold/Dry (CD), Cold/Wet (CW), Warm/Dry (WD) and Warm/Wet (WW). For each year, from the defined quantiles, we calculated precipitation (PI) and temperature (TI) indices as follow:

$$PI = \frac{N_{P60} - N_{P40}}{N} \quad (3)$$

$$TI = \frac{N_{T60} - N_{T40}}{N} \quad (4)$$

Where N_{P60} and N_{P40} are the number of days with precipitations above 60% and below 40%, respectively, N is the number of days. N_{T60} and N_{T40} are the number of days with temperatures above 60% and below 40%, respectively. The 40 and 60 percentiles were selected on the basis to have sufficient number of days for each winter mode to investigate whether the difference in climate and synoptic parameters were significant (López -Moreno *et al.*, 2011). Indeed, the 25 and 75 percentiles

would have resulted in scarce wet days. These indices were then compared with the 500-mbar geopotential heights anomaly composite maps. Spearman's correlations were also computed between the modes and the indices on one side and winter NAO, ENSO, RAAI and PAAI on the other side.

Since snow avalanches respond to weather variables, we also investigated the relationships between teleconnections, the weather and the prevailing storm tracks at different scales during avalanche years. At the winter scale, *t*-tests were performed to verify whether the difference between the means of total snowfall and maximum snowdepth was significant for winters of positive and negative NAO and ENSO. At the winter and month scales, we assessed whether one could project the winter weather from the NAO and ENSO values by using the latters as predictors of total snowfall and snowfall from the two primary storm tracks (Coastal and Great Lakes) in linear regression models. Given that the solid precipitation in 1969 was exceptional with a return period well above 100 years, data from that winter were sometimes considered as outliers to compare the validity of the models with and without an extreme data point.

4.4 Results

4.4.1 Regional avalanche activity

The avalanche chronology for every site is presented and discussed in Martin and Germain (*in press*). For regional activity, the best fit with the generalized Pareto distribution was obtained with a threshold of 4%. Based on this value, 18 years of regional avalanche activity were identified in total from 1936 to 2012, which is the

length of the weather record (Table 4.2). The PAAP explained most of the variance in the RAAI (R^2 = 0.91; p < 0.001). Given the assumption of tree-rings as being an indicator of snow avalanche activity, this suggests that most high-impact GDs were caused by avalanche activity. This strong relationship also enables us to identify 6 years with less than two active avalanche paths as high-magnitude avalanche years at the regional scale (1937, 1939, 1963, 1971, 1997 and 1999).

4.4.2 Relationships between RAAI and climate

The winter snowfall proved to be a significant predictor of the regional avalanche activity in a linear regression model (R^2 = 0.489; p < 0.0001), but the quality of the relationship decreases significantly if the most extreme data points are removed (R^2 = 0.1855; p < 0.0001). In both cases, the Durbin-Watson d-statistic > 2.0 implied that the residuals were not autocorrelated. While it is expected that avalanches be conditioned by snow, this result reinforces that the RAAI represents adequately the regional avalanche dynamics.

Table 4.3 presents the Spearman's rho values for correlations between RAAI, PAAI and different climatic variables. The rank correlation between NAO and the regional avalanche activity is significant (p < 0.05), which suggests that higher avalanche activity will be recorded on years with a negative winter NAO index. However, the 95% confidence interval on the bootstrapped correlations was not significant. The Chi-square test allowed to reject the null hypothesis that there were no differences in the regional annual avalanche activity between years of winter NAO under or above -3 (X^2 = 6.49; p < 0.05; Table 4.4), but failed to reject the same null hypothesis with other thresholds (NAO under or above -2, -1, 0, 1, 2, or 3). Moreover, the average NAO for years with or without avalanche activity was significantly different

according to a two-sample *t*-test (t = -1.83; $p < 0.05$) or the Mann-Whitney non-parametric test (W = 423; $p < 0.1$). The average snowfall and snowdepth was significantly superior for years of negative NAO as well ($t = 2.34$; $p < 0.05$). The rank correlation, the Chi-square, the *t*-test and the Mann-Whitney test were not significant between avalanches or snowfall and ENSO data.

Years of high-magnitude regional avalanche activity were present in the four prevailing modes (Figure 4.2). The ratio of avalanche/non-avalanche year is significantly superior for CW mode compared to the three other modes ($X^2 = 6.72$; $p < 0.01$) as well as the wet (CW-WW) modes compared to the dry (CD-WD) modes ($X^2 = 3.68$; $p < 0.1$). The 500-mbar geopotential heights composite anomalies for the years of each mode are presented on Figure 4.3. Three modes exhibit a negative NAO composite anomaly (CW, CD and WW), but its longitudinal position varies, the strongest anomaly being over or west of Greenland for the wettest year and east of Greenland for the CD mode. The WW mode is characterized by a positive NAO in phase a positive anomaly centered on the Gulf of Alaska, qualitatively identified as a cold PDO on Figure 4.3c. The ratio of snow accumulated following the different storm tracks differs considerably between the four modes (Figure 4.4). Cold (CW-CD) years exhibit a higher proportion of storm snow coming from the Great Lakes and Canada. Snow brought by coastal depressions is more important during wet (CW-WW) years. A higher relative quantity of snow comes from Ohio lows during WD years.

4.4.3 Relationships between weather, teleconnections and synoptic meteorology

For high-magnitude avalanche years at the regional scale, linear regressions were calculated to verify whether the NAO and ENSO could be adequate predictors of the

total quantity of storm snow as well as the amount of snow deposited by the main two synoptic systems (Coastal Low and Great Lakes Low). Significant linear regressions ($p < 0.01$) suggest a negative relationship between the monthly NAO index and total snow as well as snow from Coastal Low storms (Figure 4.5). The presence of outliers can alter the strength of the relationship. Indeed, the lowest monthly NAO index was in December 1963 where the Mount Washington Observatory weather station only recorded 50.29 cm of snow. In February 1969, two extreme Coastal Low storms deposited respectively 107 and 231 cm of snow. When these two outliers are removed, the regression coefficients slightly increase. The NAO does not however influence the quantity of snow from Great Lakes Low storms. No relationships between ENSO and storm snow, either total, from Coastal Lows or from Great Lakes Lows, were significant. At the winter scale, the regression model predicting the cumulative storm snow from NAO is highly significant ($R^2 = 0.48$; $p < 0.01$; Figure 4.6). This strong relationship is probably caused by the scarce dataset (18 data points), but it should be noted that the removal of the upper left outlier does not alter considerably the regression coefficient (data not presented). However, regression models of the NAO with the ratio of snow coming either from Coastal Lows or Great Lake Lows were not different from the null model. The inverse situation occurred with ENSO (Figure 4.6), where the variance in the winter ONI could not be used to predict the variance in the total snow. However, this index is positively correlated to the ratio of snow from Coastal Lows ($R^2 = 0.44$; $p < 0.01$) and negatively correlated to the ratio of snow from Great Lake Lows ($R^2 = 0.34$; $p < 0.05$). These results suggest that while the NAO can provide insights in the quantity of storm snow that will receive the Presidential Range, the prevailing storm tracks are better defined by the variations in the ENSO.

4.5 Discussion

4.5.1 Regional snow avalanche activity of the Presidential Range

In this study, we provide the first long-time chronology of avalanche activity at the regional scale for the Presidential Range. The RAAI allowed identifying 18 years of avalanche activity of sufficient magnitude to produce an ecological impact over a period of 77 years. This index is not widely used in the literature, and therefore arguments should be made of its ability to capture the dynamics of snow avalanche. In the present case, the strong relationship between the RAAI, the PAAP and snowfall variables in a mountain range where avalanches result mostly from the direct action of snow (Joosen, 2008) corroborate its relevance to assess the avalanche activity at larger spatial scales in regions where no historical archives exist.

The average return interval of 4.28 years for the period 1936-2012 is close to but slightly shorter than the 5.5-year interval calculated by same method in the nearby Chic-Chocs Range for the period 1895-1999 (Germain *et al.*, 2009). This slight difference can be attributed to the shorter record period in this study, because the latter authors mention a higher number of snow avalanches recorded by tree-rings since 1950. The data presented above also show an increase in the frequency of high-magnitude activity since 1990. However, given the short timespan of the study and the fact that older avalanches tend to be erased from the tree-ring record, for example by natural tree mortality or more recent extreme avalanches that can destroy evidence of former events, we do not believe that this increase can be attributed to a climatic trend, especially that the only slightly significant climatic trends observed locally (Seidel *et al.*, 2009) were in support of conditions unfavourable to snow avalanching at the path scale (Martin and Germain, *in press*).

4.5.2 Climatology of regional avalanche activity

The data presented above show that the regional avalanche activity responds to climatic variables at different spatial scales. The RAAI value is correlated positively with the snow (snowfall) and negatively with the temperature, namely the number of TDD (Table 4.3). This is also observable in the high ratio of avalanche/non-avalanche years for winters with a prevailing CW scenario. However, despite this higher ratio for the CW scenario, avalanche years were identified for winters witnessing preferentially any weather mode (Figure 4.2). This finding was expected given the complexity of the snowpack evolution that is influenced by a myriad of explanatory variables not mentioned in this study (e.g., solar radiation, wind, topographic characteristics, aspect, etc.). Nonetheless, the classification of avalanche years in different precipitation/temperature modes allowed to better apprehend the relationship between weather, the synoptic anomalies, the prevailing storm tracks and the global scale teleconnections.

Wet modes (CW and WW) are both characterized with a strong positive anomaly over Greenland, characteristic of a negative NAO. The resulting blocking above the Atlantic Ocean favours the creation of a trough above the East Coast as well as a southward shift of the polar jet, especially during CW years. Under these conditions, Coastal storms are expected to be more frequent in New England (Jones and Davis, 1995; Thomspon and Wallace, 2001). The relationship between avalanches, snow and the NAO were further corroborated by the other statistical tests produced above (i.e., Chi-square, Mann-Whitney). These results are also in agreement with the significant albeit weak negative correlations between the NAO and the quantity of snow from coastal storms or, to a lesser extent, the ratio of snow from coastal storms. However, the local impacts of global circulation patterns are more intricate; while in a negative NAO phase, the CD mode years were characterized by a positive anomaly located

East of Greenland as well as the lowest ratio of storm snow coming from Coastal Lows. The global NAO index is solely based on a latitudinal gradient, but its longitudinal position has been demonstrated to have an impact on the climate of New England. Bradbury *et al.* (2002*b*) showed that the longitudinal position of the East Coast trough significantly influences the winter precipitation regime, since an eastward displaced trough would direct the Coastal Low above the Atlantic Ocean, with our study region remaining outside or at the western edge of the storm track. The 500-mbar anomalies of the CD year are therefore favourable to the storms following a more zonal (East-West) flow, which is coherent with the high relative frequency of storm tracks from the Great Lakes or following the Ohio Valley during these years. WD years were characterized by a positive NAO and a strong positive anomaly above the Northern Pacific (Figure 4.3d), which qualitatively suggests a cold PDO. Both the positive NAO and the negative PNA/PDO favour zonal flow, the latter being negatively correlated with the precipitations in the Ohio Valley (Coleman and Rogers, 2003), hence the higher proportion of Ohio Valley snowstorms during WD years. The connection between NAO and avalanche activity is therefore in agreement with the synoptic-scale meteorology studies of the region. Since the NAO generally produces the inverse meteorological conditions than for Northern Europe, our findings also corroborate the results of Keylock (2003) who identified a positive relationship between NAO and avalanche activity in Iceland. Coupled with the more widely studied ENSO-avalanche teleconnection in Western North America, this study also contributes to the argument that snow avalanches are sensitive to global atmospheric circulation patterns. Given the modulating effect of the Northern Pacific oscillations on the climate patterns resulting from ENSO (Gershunov and Barnett, 1998) and the qualitative observation about the PDO during the WD and WW years, further analysis should include other teleconnections to better nuance the variability in avalanche regimes caused by large-scale circulation patterns. Moreover, at the regional scale for New England or Quebec, studies suggest strong linkages between hydroclimatic parameters and large scale indices such as the Baffin Island-West

Atlantic index (Shabbar *et al.*, 1997; Coulibaly *et al.*, 2000), the Pacific North American Pattern (Hartley and Keables, 1998; Huntington *et al.*, 2004; Morin *et al.*, 2007), the US East Coast Trough index (Bradbury *et al.*, 2002*b*) or the Atlantic sea surface temperature (Bradbury *et al.*, 2003). However, the scarcity of avalanches in the chronology led us to focus solely on the NAO and ENSO to compare with previous aforementioned studies.

Even if the teleconnection between ENSO and New England climate is unclear, we observed a significant weak positive correlation between this index and the temperature. Contrarily to Germain *et al.* (2009) for the Chic-Chocs Range, there was no relationship between ENSO and the avalanche activity in the Presidential Range, nor between ENSO and the quantity of snowfall in this region. However, during avalanche years, the ratio of snow coming from coastal storms was positively correlated with ENSO at the winter scale, which suggests that the preferential storm tracks will be influenced by this global climatic pattern. These results are in agreement with Hirsch *et al.* (2001) who also observed that years with a positive ENSO were characterized by more important Coastal Low storms. While the sole ENSO index does not provide much information with regards to avalanche activity, its phasing with NAO might. A negative NAO bringing important snowfalls in phase with a positive ENSO increasing the ratio of snow following the coastal track of the notorious Nor'Easters should create conditions favourable to an important avalanche activity at the regional scale. Indeed, the two extreme years in terms of RAAI and snowfall, 1958 and 1969, both were characterized by a negative winter NAO (-2.14 and -4.89), a positive ENSO (0.66 and 0.84) and extreme coastal snow storms (data not presented). The return period of the snowfall for the years 1958 and 1969 were estimated to 100 and 325 years, respectively. The scarcity of avalanche years and the short period of this study limit our ability to push the relationships between the phasing different indices and snow avalanches further, but these two cases provide

evidence that winters witnessing a negative NAO and a positive ENSO could trigger avalanche activity of high-magnitude at the regional scale.

4.6 Conclusions

This paper is the first to suggest an avalanche pattern resulting from the variation of NAO and its phasing with ENSO and illustrated with the influence of these indices on the prevailing storm tracks. It also shows that tree-ring data are of sufficient resolution to get statistically significant results between regional avalanche activity and climate over a multidecadal timespan. As the database of snow avalanches recorded by the USFS snow rangers at the daily scale further grow, we believe that it should provide a great opportunity to corroborate these findings of this study over a smaller spatiotemporal scale. Moreover, in a region where the snow variability is very high (Joosen, 2008), considering this parameter would allow to verify and better understand in which part and on which aspect of the range is the regional avalanche activity prevailing under different climate scenarios.

The results of this study are also in agreement with those of aforementioned studies about the relationship between NAO/ENSO, the synoptic scale meteorology and the hydroclimatic conditions in Northeastern North America. Therefore, in the light of the ongoing climate change, contrary to previous studies on the climatology of this study region (Grant *et al.*, 2005; Seidel *et al.*, 2009), our results support the conclusion that the alpine environment of the Presidential Range is sensible to large-scale climatic fluctuations, and therefore the avalanche activity should follow the suggested trends in the ENSO (Collins and the CMIP Modelling Groups, 2005) or the projected trends in the NAO (Ning and Bradley, 2015). In this regard, a better understanding of the future evolution in the magnitude and expected displacement of

the centers of action of these indices could allow to better apprehend the response of the high magnitude regional avalanche activity of the Presidential Range to the projected climatic change.

From an operational point of view, as suggested by McClung (2013) the relationship between NAO/ENSO and avalanche activity in the Presidential Range should not be regarded as dominant, since avalanche forecasting is based on present snow and weather conditions rather than climate (Schaerer and McClung, 2006). However, considering that the general occurrence of positive/negative NAO and ENSO can be predicted, it is our hope that these findings could facilitate avalanche hazard planning in the Presidential Range, through the assessment of the expected prevailing weather scenario for the winter, the identification of the storm tracks most likely to bring considerable amount of snow and the expectation of a winter of high or low avalanche activity at the regional scale.

Acknowledgements

This work was supported through a doctoral grant accorded to Jean-Philippe Martin from the Fonds de Recherche Québécois Nature et Technologies (FRQNT). The laboratory work was carried in the Tree-Ring laboratories of the Geography Department and the Centre for Forest Research (Université du Québec à Montréal). Eric Kelsey from the Mount Washington Observatory provided the weather data. Many thanks to Mathieu Gratton, Jean-François Milot and Jean-François Jasmin for the fieldwork assistance. The authors are especially grateful to, Jeffrey Lane, Frank Carrus and Brad Ray, active and retired USFS Snow Rangers, for the generous sharing of their extensive knowledge of the avalanche dynamics on Mount Washington.

Tableau 4.1 Weather and climatic variables used in this study. MW: Mount Washington Observatory. PN: Pinkham Notch.

Category	Resolution	Variable	Station/Source	Period
Precipitation	Day	Snowstorm	MW	1936-2012
	Month	Total storm snow	PN	1936-2012
	Winter	Total storm snow	PN	1936-2012
		Total snowfall	PN	1936-2012
		Maximum snowdepth	PN	1936-2012
Temperature	Month	Number of freezing degree-days (°C)	MW	1936-2012
		Number of thawing degree-days (°C)	MW	1936-2012
	Winter	Number of freezing degree-days (°C)	MW	1936-2012
		Number of thawing degree-days (°C)	MW	1936-2012
Teleconnection	Month	NAO	Hurrell, NCAR	1936-2012
		NAO	Hurrell, NCAR	1936-2012
		ENSO ONI 3.4	USNWS	1950-2012
	Winter	NAO (December-March)	Hurrell, NCAR	1936-2012
		ENSO ONI 3.4 (December-April)	USNWS	1950-2012
Synoptic data	Day	Storm track	NOAA	1936-2012
	Winter	500 mbar composite anomaly	NCEP/NCAR	1948-2012

Tableau 4.2 Regional avalanche activity index (RAAI) for the Presidential Range based on tree-ring data. Bold indicates year above the 4% threshold for which high-magnitude regional avalanche activity was inferred.

Year	RAAI (%)	Year	RAAI (%)	Year	RAAI (%)	Year	RAAI (%)
1969	**39.5**	1984	3.7	1970	1.6	2004	0.8
1958	**15.6**	1936	3.2	1980	1.4	1986	0.8
1952	**14.8**	1942	3.2	2002	1.4	1960	0.7
1982	**14.6**	2003	2.9	1975	1.3	2011	0.7
2001	**12.6**	1953	2.8	1990	1.2	1962	0.6
2008	**10.6**	1973	2.7	1972	1.2	1946	0.6
1977	**10.0**	2006	2.7	1961	1.2	1967	0.6
1943	**9.3**	1991	2.5	2000	1.2	1955	0.6
1987	**7.8**	2007	2.5	1938	1.1	1945	0.5
1996	**7.5**	1974	2.4	1989	1.1	1964	0.5
1939	**7.1**	1949	2.4	1944	1.1	1968	0.5
1993	**6.6**	1940	2.2	1950	1.1	1959	0.4
2005	**5.6**	1947	2.2	1956	1.1	1976	0.2
1937	**5.4**	1978	2.1	1988	1.1	1941	0.0
1999	**4.8**	1998	2.0	1951	0.9	1948	0.0
1963	**4.7**	1995	1.9	1985	0.9	1957	0.0
1997	**4.6**	1979	1.6	1965	0.9	2012	0.0
1971	**4.2**	1994	1.6	1992	0.9		
2010	3.9	2009	1.6	1966	0.9		
1954	3.7	1983	1.6	1981	0.9		

Tableau 4.3 Spearman's rank correlation rho values and significance at different thresholds (**$p < 0.01$; *$p < 0.05$; !$p < 0.1$). Bold indicates correlations that were significant at a 95% confidence interval using the bootstrap. RAAI: regional avalanche activity index; PAAP: percentage of active avalanche path; FDD: number of freezing degree-days; TDD: number of thawing degree-days; NAO: North Atlantic Oscillation winter index; ENSO: El Niño Southern Oscillation winter index.

	RAAI	PAAP	Snowfall	Snowdepth	FDD	TDD	NAO	ENSO
RAAI	1	**0.73**	0.37**	0.11	-0.09	-0.21!	-0.27*	-0.11
PAAP	-	1	**0.42****	0.30**	0.06	-0.23*	-0.20!	0.01
Snowfall	-	-	1	**0.74****	0.17	**-0.41****	**-0.39****	0.01
Snowdepth	-	-	-	1	0.27*	-0.32**	**-0.43****	-0.04
FDD	-	-	-	-	1	**-0.39****	-0.25*	0.35**
TDD	-	-	-	-	-	1	**0.45****	-0.00
NAO	-	-	-	-	-	-	1	0.01
ENSO	-	-	-	-	-	-	-	1

Tableau 4.4 Contigency table of avalanche activity during years of extreme negative NAO.

	NAO ≤ -3	NAO > -3
Avalanche year	4	15
Non-avalanche year	1	57

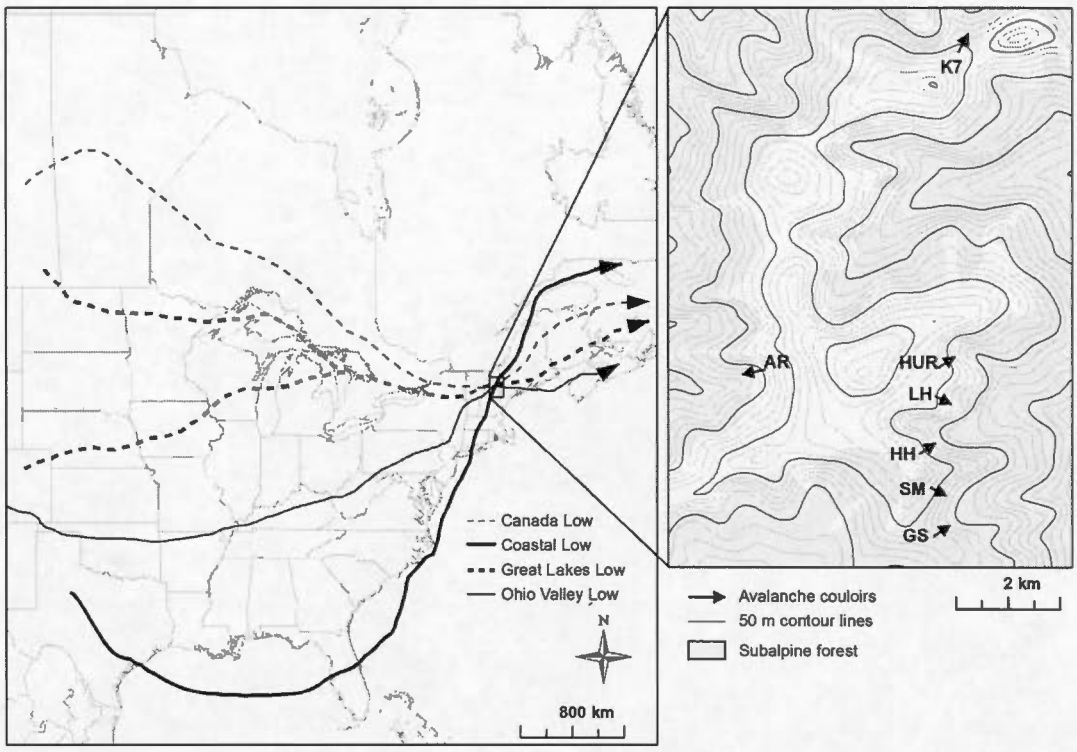

Figure 4.1 Localisation of the study region showing a) examples of potential trajectory of the different storm track classifications and b) the avalanche paths from which was derived the regional avalanche activity index based on tree-ring analysis. AR: Amoonosuc Ravine; K7: King's Ravine; HUR: Huntington Ravine; LH: Lion's Head; HH: Hillman's Highway; SM: Gulf of Slides (site #1); GS: Gulf of Slides (site #2).

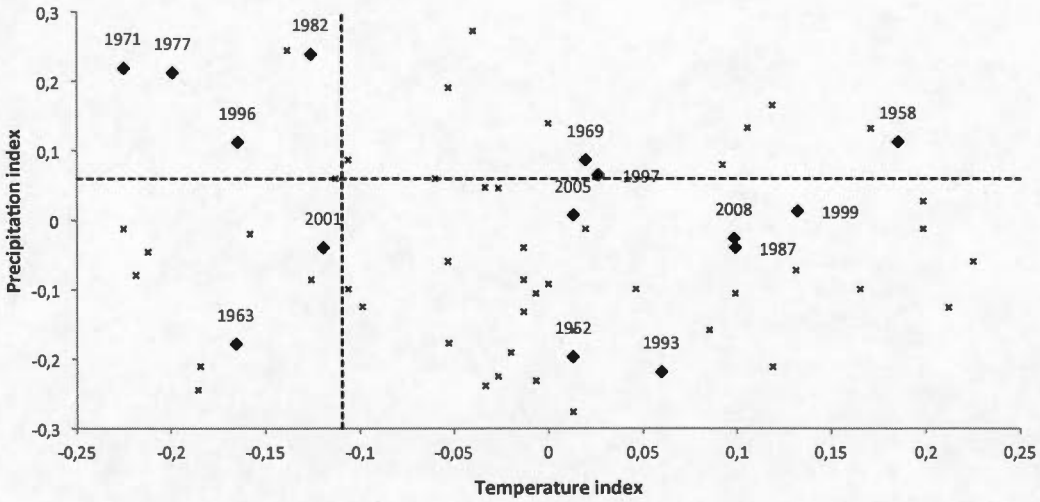

Figure 4.2 Classification of 1936-2012 winters in the different prevailing weather modes. Diamonds represent years of high-magnitude regional avalanche activity.

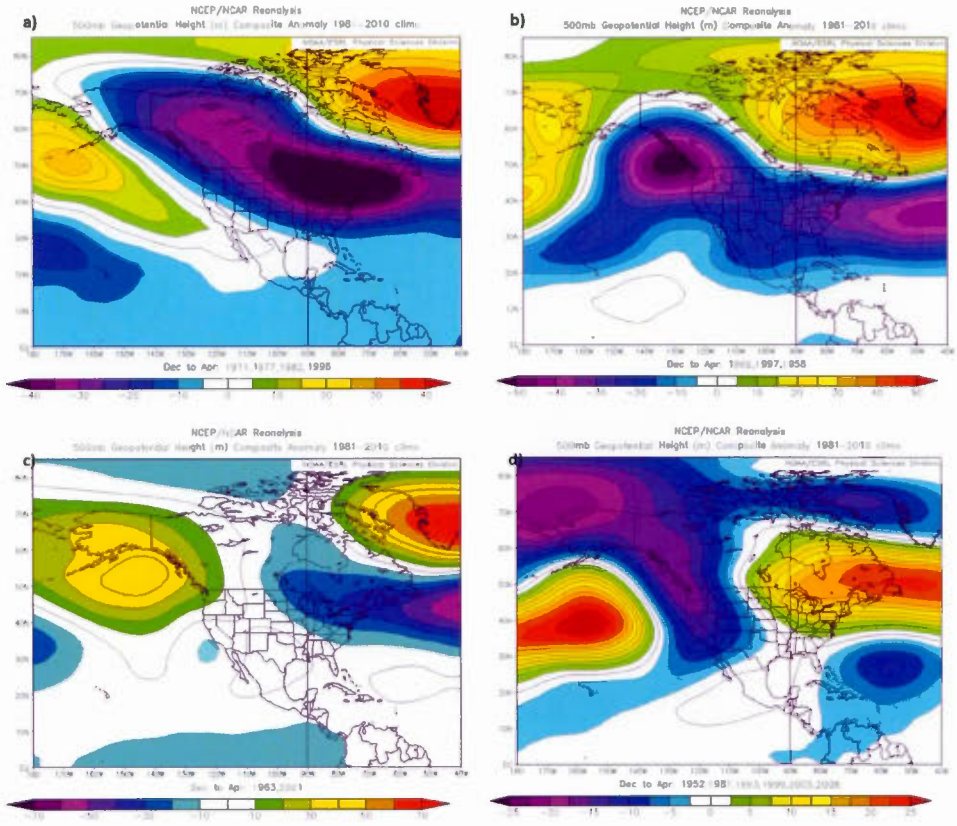

Figure 4.3 500-mbar geopotential height composite anomaly maps of the regional avalanche years classified according to the prevailing weather mode: a) CW, b) WW, c) CD and d) WD. Images provided by the NOAA/ESRL Physical Sciences Division, Boulder Colorado from their Web site at http://www.esrl.noaa.gov/psd/.

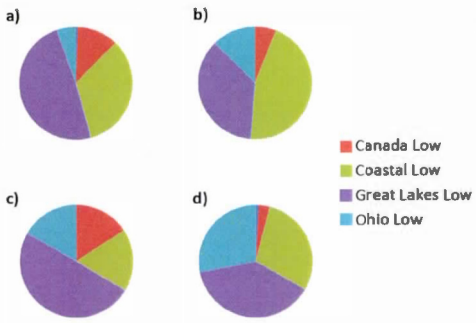

Figure 4.4 Distribution of the storm snow in the different storm tracks during a) CW, b) WW, c) CD and d) WD winters.

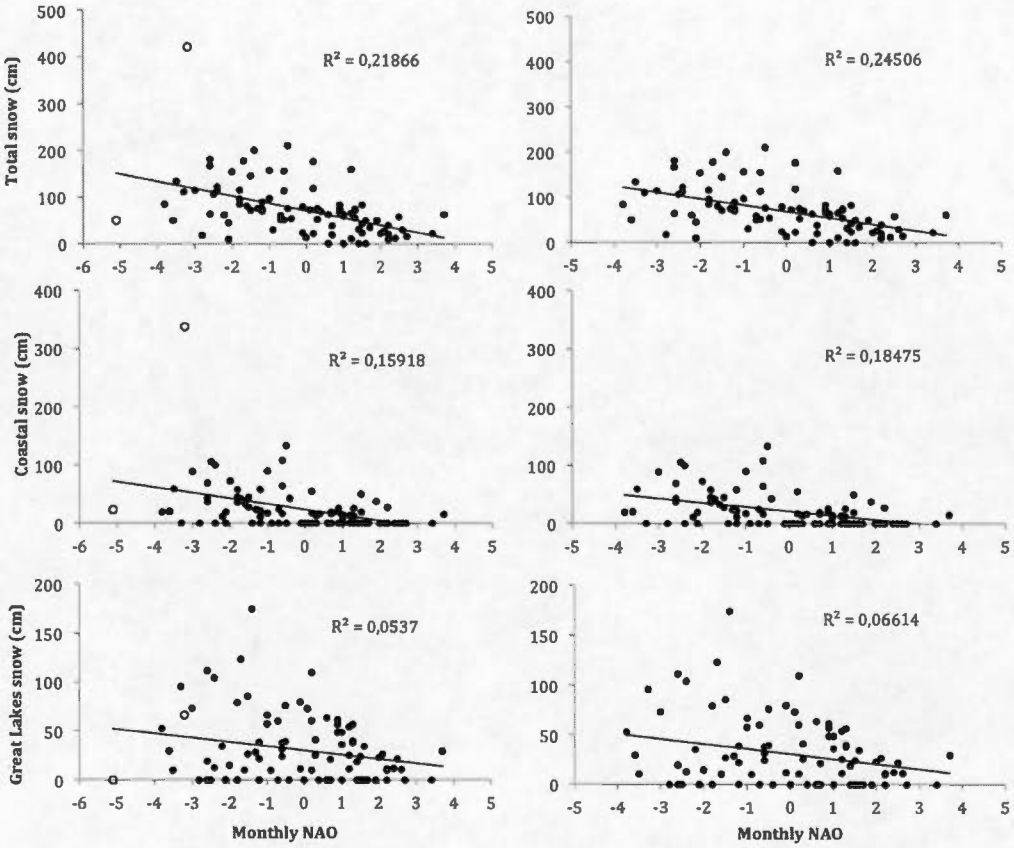

Figure 4.5 Linear regression models showing the relationship between monthly total, Coastal and Great Lakes snowfalls with NAO, including (left column – hollow circles) or excluding (right column) the two outliers discussed in section 4.3.

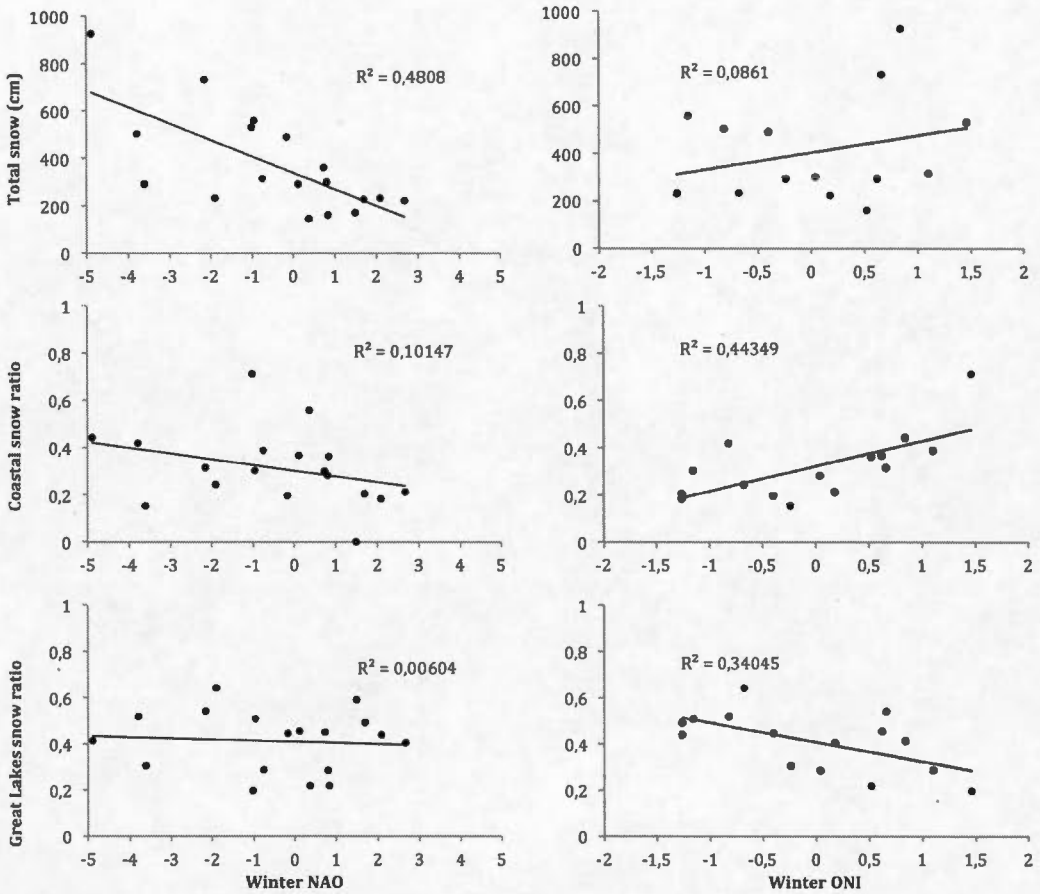

Figure 4.6 Linear regression models showing the relationship between winter total, Coastal and Great Lakes snowfalls with NAO (left column) or ENSO (right column).

CONCLUSION

Cette thèse avait pour objectif principal de documenter la dynamique des avalanches de neige dans la Chaîne Présidentielle au New Hampshire (États-Unis) selon une démarche rétrospective basée sur la dimension historique des avalanches de forte intensité. Les analyses dendrochronologiques effectuées dans le cadre de cette étude fournissent les premières archives de l'activité avalancheuse s'étendant sur une période approximative d'un siècle pour la région d'étude. À cet effet, il a été démontré que dans un milieu dynamique où la forêt subalpine est affectée par une multitude de perturbations climatiques, écologiques et géomorphologiques, il est possible de discriminer le signal inhérent aux avalanches de neige grâce aux patrons spatiaux dans la réponse des arbres. Les séries temporelles de l'activité avalancheuse ainsi créées ont permis de mettre en relief les mécanismes climatiques de déclenchement des mouvements de neige de forte intensité.

Une partie importante de cette recherche avait pour but de mieux comprendre la relation entre l'activité avalancheuse et les variables météorologiques et climatiques à différentes échelles d'investigation. À cet égard, il s'agit de la première étude dendrochronologique proposant des résultats aussi probants sur cette question. D'un point de vue météorologique, les arbres de classifications présentés dans le troisième chapitre, en plus d'avoir un pouvoir prédictif légèrement supérieur aux régressions logistiques, permettent d'identifier quatre scénarios expliquant l'occurrence des avalanches de forte intensité dans la Chaîne Présidentielle, soit :

1) *Fréquence importante des tempêtes de neige*. Corroborant les observations des *Snow Rangers* quant à la prédominance des avalanches à action directe, les modèles de cinq des sept couloirs utilisent une variable associée avec le nombre de tempêtes durant l'hiver. De plus, celles-ci sont toujours situées au nœud racine des arbres de classification concernés, ce qui signifie qu'elles sont les variables proposant la séparation la plus homogène dans le jeu de données. Il est intéressant de mentionner que dans chacun des modèles, la quantité d'évènements nécessaires au déclenchement des avalanches de forte intensité est au-delà d'un écart-type au-dessus de la moyenne. Ainsi, la plupart des années d'occurrence d'avalanches de forte intensité dans la Chaîne Présidentielle sont caractérisées par une quantité de tempêtes de neige largement supérieure à la moyenne.

2) *Hivers avec un enneigement supérieur à la moyenne*. Le meilleur nœud racine pour les deux autres modèles provient des chutes totales de neige durant l'hiver. Indépendamment si le régime des avalanches est à action directe ou indirecte, une quantité de neige supérieure augmentera le potentiel pour la formation de plaques de neige plus profondes et donc des avalanches de plus forte intensité.

3) *Températures favorisant la formation de couches fragiles ou de givre de profondeur*. Une vague de froid précoce sur un faible couvert nival peut favoriser le développement d'un gradient de température dans le manteau neigeux supérieur au seuil de 10°C m^{-1} nécessaire à la formation de gobelets et de givre de profondeur (Haegeli et McClung, 2007). Un tel scénario est présent au site LH où dans l'éventualité d'un faible enneigement, une période froide au mois de décembre peut expliquer l'occurrence d'avalanches importantes. Une vague de froid tardive peut également expliquer la formation de couches fragiles qui ne supporteront pas de surcharges nivales ultérieures.

Un tel scénario est d'ailleurs présent dans les arbres de classification des sites GS, SM et LH.

4) *Présence de vents violents*. Ce scénario se retrouve dans trois arbres de classification. En effet, le vent a le potentiel de favoriser le déclenchement des avalanches par deux mécanismes. Premièrement, des vents importants peuvent causer une déflation éolienne favorisant la surcharge nivale sur les pentes abritées. Ce phénomène est caractéristique de notre région d'étude. En effet, dans le Tuckerman Ravine, la moyenne de l'épaisseur maximale de la neige se situe autour de 16 m alors qu'au sommet du mont Washington, on enregistre en moyenne 7 m de précipitations solides. De plus, dans des conditions d'humidité relative basse, de forts vents peuvent également sublimer la neige et créer une plaque à vent d'envergure.

Ces résultats démontrent que la Chaîne Présidentielle, à l'instar du Québec, semble susceptible au risque associé aux avalanches de forte intensité à action directe à la suite d'un épisode important de précipitations solides. En effet, la fréquence élevée des tempêtes est un des scénarios retenus par Germain *et al.* (2009) pour expliquer l'activité avalancheuse régionale de forte intensité dans les Chic-Chocs en Gaspésie. Il est d'ailleurs intéressant de remarquer que les trois premiers scénarios élaborés dans le cadre de cette thèse et décrits précédemment corroborent ceux obtenus par ces derniers auteurs. À l'extérieur du milieu alpin des Chic-Chocs, un tel scénario a également été mis en relief sur la côte septentrionale gaspésienne, où les chutes de neige supérieures à la moyenne (Dubé *et al.*, 2004) et l'occurrence d'une tempête de neige (Hétu, 2007 ; Fortin *et al.*, 2011 ; Graveline et Germain, 2016) ont été identifiées comme des conditions de déclenchement d'avalanches de forte intensité. À plus grande échelle, d'importantes précipitations solides dans les 48 heures précédant l'évènement couplées à une forte déflation éolienne expliquent également les avalanches responsables de la tragédie de Blanc-Sablon en 1995 (Germain, 2016)

ainsi que de la plupart des accidents mortels liés aux mouvements de neige sur les courts versants raides du Québec (Hétu *et al.*, 2015) et de Terre-Neuve (Liverman *et al.*, 2001). Ainsi, la présente thèse permet de corroborer la tendance à l'échelle du Nord-Est nord-américain quant à l'importance de tenir compte des avalanches à action directe dans la gestion des risques liés aux mouvements de neige, voire de l'élargir non seulement aux courts versants raides, mais également aux pentes à plus forte dénivelée en milieu alpin.

Cependant, les études citées ci-dessus s'intéressant à l'activité avalancheuse en Gaspésie ou à Terre-Neuve ont pour la plupart identifié un second régime où le déclenchement faisait suite à un évènement de pluie sur le manteau neigeux couplé à des températures positives. Selon les *Snow Rangers*, un tel scénario semble peu probable pour la Chaîne Présidentielle. En effet, lorsqu'une variable de pluie était utilisée comme variable de substitution dans un arbre de classification modélisé dans le chapitre 3, la relation entre celle-ci et l'activité avalancheuse était négative. Vraisemblablement, le contexte maritime de ces sites serait la source de cette différence. Bien que le manteau neigeux dans la Chaîne Présidentielle soit classé comme étant de type maritime (Allen, 2000), les conditions climatiques extrêmes, comme en fait foi la présence de la superficie floristique arctique-alpine la plus extensive au sud du Labrador (Bliss, 1963), feraient en sorte que les processus de déclenchement analogues se situeraient à de plus hautes latitudes. En effet, la tragédie de Kangiqsualujjuaq en 1999 aurait été causée par la surcharge d'une couche fragile de cristaux à facettes datant du début de décembre (Germain, 2016), ce qui concorde avec le troisième scénario élaboré ci-dessus. Or, des recherches plus approfondies sur le manteau neigeux dans ces différentes régions, telle que celle entreprise par Fortin et Hétu (2009) en Gaspésie, s'avèrent nécessaires pour corroborer ces conclusions.

À plus grande échelle, il s'agit de la première étude qui met en relief les relations entre les avalanches de neige dans le Nord-Est nord-américain et les patrons de circulation atmosphérique. De plus, contrairement aux autres recherches sur ce sujet, les résultats présentés dans le quatrième chapitre montrent que la variabilité dans les conditions climatiques et la météorologie synoptique lors des années avalancheuses sont cohérentes avec les fluctuations et le phasage entre la NAO et l'ENSO.

Nous sommes conscients que la portée des résultats énumérés ci-dessus est limitée par la faible quantité des avalanches reconstituées. En effet, sur la période à l'étude, les séries temporelles discrètes reconstituant les mouvements de neige de forte intensité comportaient davantage de 0 (année non-avalancheuse) que de 1 (année avalancheuse). Or, les relations avalanche-météorologie proposées sont cohérentes avec la physique du processus, la reconnaissance par les prévisionnistes locaux d'un régime d'avalanches à action principalement direct, les principaux mois d'activité avalancheuse dans les archives à court terme (cf. chapitre 3) et les scénarios climatiques proposés par Germain *et al.* (2009), soit la seule autre étude sur ce sujet à proximité de notre région d'étude. Cependant, en terme statistique, un tel déséquilibre entre occurrence et absence peut engendrer des biais dans le pouvoir prédictif des modèles proposés, surtout en considérant la multitude de variables météorologiques prédictives utilisées. C'est ainsi que dans le quatrième chapitre, nous nous sommes attardés à l'étude des patrons synoptiques et climatiques en utilisant exclusivement les données positives, c'est-à-dire les années avalancheuses, car comme le mentionne McClung (2002), dans une optique de prévision du risque, il est essentiel d'accorder davantage d'importance aux données positives (années avalancheuses) qu'aux données négatives (années non-avalancheuses). Bien que les résultats de cette thèse gagneraient à être corroborés par des études ultérieures, nous espérons qu'ils outilleront davantage les *Snow Rangers* de la Chaîne Présidentielle dans une perspective de diminution du risque avalancheux sur un massif où l'affluence à

l'extérieur des zones de prévision est appelée à croître considérablement dans les années à venir.

Perspectives futures de recherche

Nous avons entrepris cette thèse dans une optique d'analyse multi-scalaire de la dynamique des avalanches de neige. Bien que cette étude contribue à l'avancement des connaissances à différentes échelles spatiotemporelles, autant au niveau du processus (couloir, Chaîne Présidentielle, milieu alpin du Nord-Est nord-américain) que du climat (local, régional et global), l'utilisation d'un tel cadre conceptuel permet d'entrevoir une multitude de perspectives futures en terme de recherche :

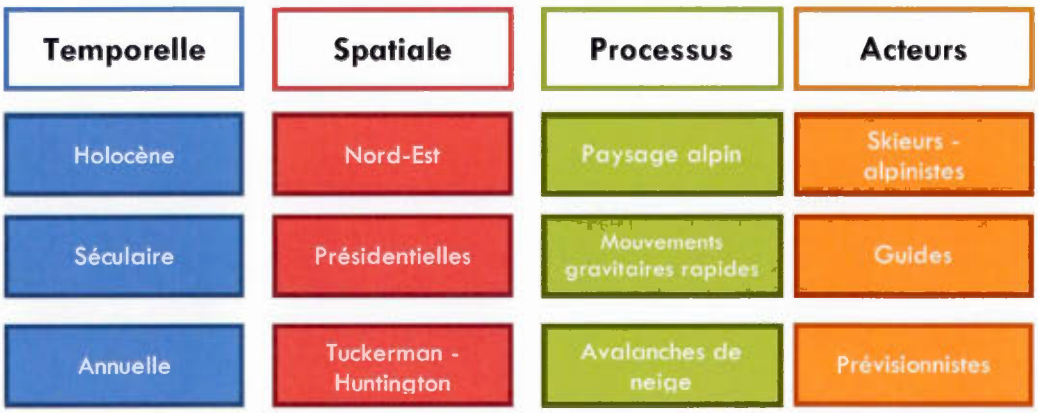

Milieux alpins

Tel que mentionné par Capers *et al.* (2013), il y a un manque de coordination et d'interdisciplinarité dans l'étude des milieux alpins du Nord-Est nord-américain. La méta-analyse du premier chapitre propose trois cadres conceptuels pour intégrer les éléments de la biosphère, de l'atmosphère et de la géosphère afin d'appréhender la dynamique de cet environnement exceptionnel. Or, puisque cette étude tentait d'intégrer des données issues de différents milieux, récoltées selon différentes méthodes et à différentes époques, les conclusions ne passent pas pour l'instant le test de la réplicabilité. L'intérêt croissant pour cet environnement fragile mentionné antérieurement par des scientifiques de différents horizons disciplinaires et professionnels permettrait la mise en place de projets permettant de valider l'importance de ces trois concepts dans la mise en place et la préservation des milieux alpins du Nord-Est nord-américain.

Dynamique des versants

D'autre part, au niveau de la dynamique des versants à plus grande échelle spatiale, nous avons remarqué que dans un gradient du sud-ouest au nord-est, on note une transition dans la contribution des différents mouvements gravitaires rapides à la fragmentation de la forêt d'interface. En effet, dans les Adirondacks (New York, États-Unis), les glissements pelliculaires et les coulées de débris représentent des perturbations écologiques majeures (Bogucki, 1977). L'occurrence des avalanches de neige semble uniquement préserver la fragmentation de la forêt à la suite d'une ouverture créée par un glissement ou une coulée. À l'opposé, dans les Chic-Chocs

(Gaspésie, Canada), nous posons l'hypothèse d'une importance croissante des processus cryogéniques tels que les avalanches de neige (Germain *et al.*, 2005, 2009) et les coulées de neige liquéfiée (Larocque *et al.*, 2001) dans la fragmentation de la forêt subalpine.

Dans un contexte de gestion et de cartographie du risque, il importe de connaître la distance d'arrêt des avalanches. Bien qu'il existe une vaste littérature sur différentes méthodes déterministes et empiriques de détermination de la distance d'arrêt des avalanches, peu d'études s'intéressent à cette question sur les versants de faible dénivelé ou sur les versants forestiers (Jones et Jamieson, 2004). Or, dans la Chaîne Présidentielle, les zones d'arrêt se situent généralement sur une pente supérieure à 10°, inclinaison communément utilisée afin de définir le début de la zone de décélération et d'arrêt (cf McClung et Schaerer, 2006 pour une discussion approfondie sur cette question). L'utilisation de séries temporelles dendrochronologiques a déjà été utilisée afin de valider la distance d'arrêt déterminée par des modèles statistiques-dynamiques calibrés sur des données historiques (Schläppy *et al.*, 2014). Or, en l'absence d'archives, il serait pertinent de parvenir à calibrer un tel modèle à partir de périodes de retour inférées par la dendrochronologie.

Relations avalanche-climat

De plus, bien que les résultats de la présente thèse montrent une relation significative entre l'activité avalancheuse et le climat, il apparaît pertinent de s'intéresser à cette question à différentes échelles. Par exemple, pourrait-on appliquer les arbres de classification en Gaspésie ou dans un autre massif du Nord-Est nord-américain afin de valider les scénarios proposés pour les reconstructions dendrochronologiques des

avalanches dans les Chic-Chocs (Germain *et al.*, 2009) et pour le milieu côtier (Dubé *et al.*, 2004 ; Graveline et Germain, 2016)? De plus, dans ce dernier massif, aucune relation statistique entre la NAO ou ENSO et l'activité avalancheuse régionale a été notée (Germain *et al.*, 2009). Cette dernière observation est cohérente avec l'absence de relation entre ces indices et le couvert nival (Fortin et Hétu, 2014), contrairement aux massifs de la Nouvelle-Angleterre. Cependant, devant la vaste étendue spatiale couverte par la prévision des avalanches en Gaspésie, il serait d'autant plus pertinent de valider la présence ou l'absence de relation entre les mouvements de neige, la météorologie synoptique et les patrons de circulation atmosphérique globaux. Pour ce faire, il importerait de faire la discrimination entre les couloirs d'avalanches situés à l'intérieur des terres de ceux situés directement sur la côte, puisque les couloirs situés directement en bordure du Golfe du Saint-Laurent semblent répondre à des situations météorologiques différentes des couloirs situés à quelques kilomètres dans ces mêmes vallées. Finalement, l'omniprésence de relations entre les avalanches et la NAO dans l'Atlantique Nord, tel que démontré par cette étude, mais également en Islande (Keylock, 2003) et au Portugal (Garcia *et al.*, 2009) combiné à l'impact de cet indice sur les inondations (Collins, 2009 ; Armstrong *et al.*, 2012, Mazouz *et al.*, 2013), nous questionne sur l'impact global des patrons de circulation atmosphérique sur les risques hydroclimatiques à l'échelle de l'Atlantique Nord.

À plus petite échelle spatiotemporelle, les résultats de la présente étude ne permettent pas de dégager un modèle quotidien de prévision des avalanches pour les différents couloirs. Dans les sites pour lesquels il existe aujourd'hui un relevé systématique de l'activité avalancheuse, soit le Tuckerman et le Huntington Ravines, l'accumulation de données pourrait permettre de mettre en relief une relation entre les variables météorologiques et l'activité avalancheuse, surtout qu'un régime avalancheux à action directe quasi-exclusive est tout indiqué pour cela. À cet égard, avec une accumulation suffisante de données, il convient de s'interroger sur le potentiel de l'apprentissage supervisé (réseaux de neurones, classification naïve bayésienne,

machines à vecteur de support, etc.) pour développer des modèles prédictifs. Bien que ces techniques statistiques agissent comme une boîte noire apportant peu d'éclairage au niveau de la compréhension du processus, elles pourraient être d'un grand support opérationnel. De plus, devant les limites temporelles imposées par la thèse, il nous a été impossible de réaliser une étude sur la détermination de seuils nivologiques empiriques de déclenchement des avalanches, à l'instar des seuils pluviométriques développés pour d'autres mouvements de masse à des échelles locales (Guzzetti *et al.*, 2005) à globales (Caine, 1980). Puis, la proximité des couloirs d'avalanche dans les sites les plus fréquentés dans la Chaîne Présidentielle couplée à leur facilité d'accès en feraient un lieu de prédilection afin de tester différentes méthodes de détermination de la variabilité spatiale du manteau neigeux par échantillonnage (Schweizer *et al.*, 2008), modélisation (Kronholm et Birkeland, 2005) ou télédétection (Dozier et Painter, 2004).

Facteurs humains

La présente discussion serait incomplète si on passait sous silence les facteurs humains d'exposition au risque avalancheux. En effet, avec notre connaissance exhaustive des avalanches de neige et la forte capacité des prévisionnistes d'offrir un bulletin de risque intelligible et complet, et dans une optique où la plupart des accidents en Amérique du Nord surviennent dans un cadre récréatif, il importe de mieux comprendre ces facteurs humains de vulnérabilité. À cet effet, nos discussions avec les *Snow Rangers* ont fait état de cette lacune pour la région d'étude, ce qui rejoint également les résultats démontrant que la quasi-totalité des accidents de ski liés aux avalanches sont causés par les facteurs humains (Atkins, 2000) ainsi que la tendance à l'augmentation des articles sur cette dimension du risque, notamment dans

les actes du colloque *International Snow Science Workshop* des dernières années. De plus, parmi les facteurs humains, les questions liées au manque de jugement semblent primordiales (Atkins, 2000). À cet effet, McCammon (2002) a proposé une piste de solution en appliquant le concept de trappes heuristiques au risque avalancheux. Cependant, cette question a été exclusivement traitée de façon isolée et *post hoc* grâce à des comptes-rendus d'accidents (Hendrikx *et al.*, 2013). La question des trappes heuristiques devrait également être intégrée dans un cadre d'analyse plus large s'intéressant notamment au processus de prise de décision ainsi qu'au rôle que joue la perception du risque dans le niveau de préparation (Wachinger *et al.*, 2013). L'affluence importante des skieurs et des alpinistes dans la Chaîne Présidentielle en ferait un lieu particulièrement propice à la réalisation d'une telle étude.

En conclusion, cette discussion démontre que la présente thèse sur la dynamique des avalanches de neige dans la Chaîne Présidentielle n'est pas une fin, mais bien l'ouverture sur une multitude d'opportunités dans un vaste champ de recherche pluridisciplinaire. En effet, la plupart de la littérature scientifique portant sur les avalanches de neige provient de l'Ouest nord-américain ou des Alpes européennes. Or, les particularités régionales, qu'elles soient de nature topographique, géomorphologique, écologique, climatique ou humaine, appellent à la promotion d'une recherche multidisciplinaire de l'activité avalancheuse dans le Nord-Est nord-américain afin d'accroître notre compréhension du phénomène, mais également de diminuer le risque inhérent à ce processus.

APPENDICE A

SUPPLEMENTARY MATERIAL 1. BIBLIOGRAPHIC DATABASE SORTED BY RANGE, FROM SOUTH TO NORTH.

Northeastern North America

Ackerly, S.C. (1989) Reconstructions of mountain glacier profiles, northeastern United States. *Geological Society of America Bulletin*, 101(4), 561-572. http://dx.doi.org/10.1130/0016-7606

Antevs, E. (1928) The last glaciation, with special reference to ice retreat in northeastern North America. *American Geography Society Research Service*, 17.

Brown, R.J.E. (1976) *Études du pergélisol au Québec et à Terre-Neuve (Labrador)*. N.R.C.C. n°14966F. Ottawa : National Research Council of Canada.

Clark, P.U. et Mix, A.C. (2000) Global change: Ice sheets by volume. *Nature*, 406, 689-690. http://dx.doi.org/10.1038/35021176

Davis, R.B. et Jacobson, G.L.Jr. (1985) Late glacial and early Holocene Landscapes in northern New England and adjacent areas of Canada. *Quaternary Research*, 23(3), 341-368. http://dx.doi.org/10.1016/0033-5894(85)90040-7

Dyke, A.S. (2004) An outline of North American Deglaciation with an emphasis on central and northern Canada. Dans Ehlers, J. et Gibbard, P.L. (dir), *Quaternary Glaciations – Extent and Chronology, Part II: North America* (p.373-424). *Developments in Quaternary Science, 2b*. Amsterdam : Elsevier.

Flint, R.F. (1929) The stagnation and dissipation of the Last Ice Sheet. *Geographical Review*, 19(2), 256-289. http://dx.doi.org/10.2307/208535

Flint, R.F. (1951) Highland centers of former glacial outflow in northeastern North America. *Geological Society of America Bulletin*, 62(1), 21-38.

Flint, R.F. (1953) Probable Wisconsin substages and Late-Wisconsin events in northeastern United States and southeastern Canada. *Geological Society of America Bulletin*, 64(8), 897-920.

Gannett, H. (1899) The Timber Line. *Journal of the American Geographical Society of New York*, 31(2), 118-122. http://dx.doi.org/10.2307/196931

Gaudreau, D.C., Jackson, S.T. et Webb, T. III (1989) Spatial scale and sampling strategy in paleoeoclogical studies of vegetation patterns in mountainous terrain. *Plant Biology*, 38(4), 369-390. http://dx.doi.org/10.1111/j.1438-8677.1989.tb01370.x

Kimball, K.D. et Weihrauch, D.M. (2000) Alpine vegetation communities and the alpine-treeline ecotone boundary in New England as biomonitors for climate change. *USDA Forest Service Proceedings*, 3(5), 93–101.

Munroe, J.S. (2008) Alpine soils on Mount Mansfield, Vermont, USA: pedology, history, and intraregional comparison. *Soil Science Society of American Journal*, 72(2), 524-533. http://dx.doi.org/10.2136/sssaj2006.0430

Waitt, R.B. et Davis, P.T. (1988) No evidence for post-icesheet cirque glaciations in New England. *American Journal of Science*, 288(5), 495-533.

Catskills (New York, USA)

Kirkland, J.T. (1979) Deglaciation events in the western Catskill Mountains, New York. *Geological Society of American Bulletin*, 90(6), 521-524.

Kudish, M. (2013) History of the spruce-fir forest in the Catskill Mountains of New York. *Annals of the New York Academy of Sciences*, 1298, 78-85. http://dx.doi.org/10.1111/nyas.12274

Maenza-Gmelch, T.E. (1997) Late-glacial – early Holocene vegetation, climate, and fire at Sutherland pond, Hudson Highlands, southeastern New York, U.S.A. *Canadian Journal of Botany*, 75(3), 431-439. http://dx.doi.org/10.1139/b97-045

Menking, K.M., Peteet, D.M. et Anderson, R.Y. (2012) Late-glacial and Holocene vegetation and climate variability, including major droughts, in the Sky lakes region

of southeastern New York State. *Palaeogeography, Paleoclimatology, Palaeoecology*, 353-355, 45-59. http://dx.doi.org/10.1016/j.palaeo.2012.06.033

Adirondack (New York, USA)

Bogucki, D.J. (1977) Debris slide hazard in the Adirondack Province of New York State. *Environmental Geology*, 1, 317-328. http://dx.doi.org/10.1007/BF02380500

Whitehead, D.R. et Jackson, S.T. (1990) The Regional Vegetational History of the High Peaks (Adirondack Mountains), New York. *New York State Museum Bulletin*, 478.

White Mountains (New Hampshire, USA)

Agassiz, L. (1870) On the former existence of local glaciers in the White Mountains. American Naturalist, 4, 550-558.

Alexander, C. (1940) The Presidential Range of New Hampshire as a biological environment, with particular reference to the insects. *American Midland Naturalist*, 24,104-132.

Antevs, E. (1932) *Alpine zone of Mt. Washington Range*. Auburn: Merrill & Webber.

Bailey, S.W., Hornbeck, J.W., Martin, C.W. et Buso, D.C. (1987) Watershed factors affecting stream acidification in the White Mountains of New Hampshire, USA. *Environmental Management*, 11, 53-60. http://dx.doi.org/10.1007/BF01867179

Bliss, L. (1963) Alpine Plant communities of the Presidential Range, New Hampshire. *Ecology*, 44(4), 678-697. http://dx.doi.org/10.2307/1933014

Bliss, L. (1966) Plant productivity in alpine microenvironments on Mt. Washington, New Hampshire. *Ecological Monographs*, 36(2), 125-155. http://dx.doi.org/10.2307/1942152

Brackley, F.E. et Kacprzynski, F.T. (1989) *Establishment Record of Alpine Gardens Research Natural Area within the White Mountain National Forest, Coös County, New Hampshire*. United States Forest Service.

Buso, D.C., Martin, C.W. et Hornbeck, J.W. (1984) *Potential for acidification of six remote ponds in the White Mountains of New Hampshire*. Research Report Number, 43:1984. Durham : Water Resources Research Center.

Crosby, I.B. (1924) The physiographic history of Pinkham Notch. *Appalachia*, 15(4), 462-468.

Crosby, I.B. (1928) Potholes on Mount Jefferson. *Appalachia*, 17, 44-45.

Crosby, W.O. (1890) The Madison Boulder. *Appalachia*, 6, 61-70.

Davis, P.T. (1999) Cirques of the Presidential Range, New Hampshire, and surrounding alpine areas in the Northeastern United States. *Géographie physique et Quaternaire*, 53(1), 25-45. http://dx.doi.org/10.7202/004784ar

Dennys, C.S. (1940) Stone-rings on New Hampshire mountains. *American Journal of Science*, 238(6), 432-438.

Emerson, P. (1900) Glacial erosion in the White Mountain notches. *Science*, 11, 911-912. http://dx.doi.org/10.1126/science.11.284.911

Fowler, B.K. (1984) Evidence for a late-Wisconsinan cirque glacier in King Ravine, northern Presidential Range, New Hampshire, U.S.A.: Alternative interpretations. *Arctic and Alpine Research*, 16(4), 431-437. http://dx.doi.org/10.2307/1550905

Fowler, B.K. (1999) Pre-Late Wisconsinan age for part of the glaciolacustrine stratigraphy, lower Peabody valley, northern White Mountains, Gorham, New Hampshire. *Géographie physique et Quaternaire*, 53(1), 109-116. http://dx.doi.org/10.7202/004817ar

Flaccus, E. (1959) Revegetation of landslides in the White Mountains of New Hampshire. *Ecology*, 40, 692-703. http://dx.doi.org/10.2307/1929821

Goldthwait, J.W. (1913*a*) Glacial cirques near Mount Washington. *American Journal of Science, 4th series*, 35(205), 1-19.

Goldthwait, J.W. (1913*b*) Following the trail of ice sheet and valley glacier on thePresidential Range. *Appalachia*, 13, 1-23.

Goldthwait, J.W. (1914) Remnants of an old graded upland on the Presidential Range of the White Mountains. *American Journal of Science*, 37, 451-463. http://dx.doi.org/10.2475/ajs.s4-37.221.451

Goldthwait, J.W. (1915) The origin of Lost River and its giant potholes. *Science*, 41, 834-836.

Goldthwait, J.W. (1916) Glaciation in the White Mountains of New Hampshire. *Geological Society of America Bulletin*, 27, 263-294.

Goldthwait, J.W. (1939) Mount Washington in the great ice age. *New England Naturalist*, 5, 12-19.

Goldthwait, J.W. (1970) Mountain glaciers of the Presidential Range. *Arctic and Alpine Research*, 2(2), 85-102. http://dx.doi.org/10.2307/1550345

Goldthwait, R.P. (1970) Mountain glaciers of the presidential Range in New Hampshire. *Arctic and Alpine Research*, 2(2), 85-102. http://dx.doi.org/10.2307/1550345

Goldthwait, R.P. et Mickelson, D.M. 1982. Glacier Bay: A model for the deglaciation of the White Mountains in New Hampshire. Dans Larson, G.J. et Stone, B.D. (dir), *Late Wisconsinan glaciation of New England* (p.167-181). Dubuque : Kendall/Hunt.

Hadley, E. et Bliss, L. (1964) Energy relationships of alpine plants on Mt. Washington, N.H. *Ecological Monographs*, 34(4), 331-357. http://dx.doi.org/10.2307/2937067

Hattin, D.E. (1958) New evidence of high-level glacial drainage in the White Mountains, N.H. *Journal of Glaciology*, 3(24), 315-319.

Hitchcock, C.H. (1878) Glacial markings among the White Mountains. *Appalachia*, 1(4), 423-426.

Johnson, D.W. (1917) Date of local glaciation in the White, Adirondack, and Catskill Mountains. *Geological Society of America Bulletin*, 28, 543-553. http://dx.doi.org/10.1130/GSAB-28-543

Johnson, D.W. (1933) Date of local glaciation in the White Mountains. *American Journal of Science*, 225, 399-405.

Miller, G.S.Jr. (1985) On a collection of small mammals from the New Hampshire mountains. *Proceedings of the Boston Society of Natural History*, 26: 177-197.

Miller, N.G. et Spear, R.W. (1999) Late-Quaternary history of the alpine flora of the New Hampshire White Mountains. *Géographie physique et Quaternaire*, 53(1): 137-157. http://dx.doi.org/10.7202/004854ar

Packard, A.S.Jr. (1867*a*) Ice-marks and ancient glaciers in the White Mountains. *American Naturalist*, 1, 260-269.

Packard, A.S.Jr. (1867*b*) Evidences of the existence of ancient local glaciers in the White Mountain valleys. *American Journal of Science, 2nd Series*, 43(127), 42-43.

Reiners, W.A. et Lang, G.E. (1979) Vegetational patterns and processes in the balsam fir zones, White Mountains, New Hampshire. *Ecology*, 60, 403-417. http://dx.doi.org/10.2307/1937668

Ridge, J.C., Bensonen, M.R., Brochu, M., Brown, S.L., Callahan, J.W., Cook, G.J., Nicholson, R.S. et Toll, N.J. (1999) Varve, paleomagnetic, and ^{14}C Chronologies for late Pleistocene events in New Hampshire and Vermont (U.S.A.). *Géographie physique et Quaternaire*, 53(1), 79-107. http://dx.doi.org/10.7202/004864ar

Stone, G.H. (1880) Note on the Androscoggin glacier. *American Naturalist*, 14: 299-302.

Thompson, D.J. (1999) Talus fabric in Tuckerman Ravine, New Hampshire: Evidence for a tongue-shaped rock glacier. *Géographie physique et Quaternaire*, 53(1): 47-57. http://dx.doi.org/10.7202/004881ar

Thompson, W.B. (1983) Large glacial moraine discovered in the White Mountains. *Appalachia, New Series*, 44(4), 186-188.

Thompson, W.B. (1999) History of the research on glaciation in the White Mountains, New Hampshire (U.S.A.). *Géographie physique et Quaternaire*, 53(1), 7-24. http://dx.doi.org/10.7202/004879ar

Thompson, W.B., Fowler, B.K. et Dorion, C.C. (1999) Deglaciation of the northwestern White Mountains, New Hampshire. *Géographie physique et Quaternaire*, 53(1), 59-77. http://dx.doi.org/10.7202/004882ar

Tiffney, W.Jr. (1972) Snow cover and the Diapensia lapponica habitat in the White Mountains, New Hampshire. *Rhodora*, 74, 358-377.

Vose, G.L. (1868) Traces of ancient glaciers in the White Mountains of New Hampshire. *American Naturalist*, 2, 281-291.

Mount Katahdin and other Maine mountain ranges (USA)

Anderson, R.S. et Davis, R.B. (1985) History of late- and post-glacial vegetation and disturbance around Upper South Branch Pond, northern Maine. *Canadian Journal of Botany*, 64, 1977-1986. http://dx.doi.org/10.1139/b86-262

Borns, H.W.Jr. et Calkin, P.E. (1977) Quaternary glaciation, west-central Maine. *Geological Society of America Bulletin*, 88(12), 1773-1784. http://dx.doi.org/10.1130/0016-7606

Davis, P.T. et Davis, R.B. (1980) Interpretation of minimum-limiting radiocarbon dates for deglaciation of Mount Katahdin area, Maine. *Geology*, 8(4), 396-400. http://dx.doi.org/10.1130/0091-7613

Shreve, R.L. (1985) Late Wisconsin ice-surface profile calculated from esker paths and types, Katahdin esker system, Maine. *Quaternary Research*, 23(1), 27-37. http://dx.doi.org/10.1016/0033-5894(85)90069-9

Stone, B.D. et Borns, H.W.Jr. (1986) Pleistocene glacial and interglacial stratigraphy of New England, Long Island, and adjacent George Bank and Gulf of Maine. *Quaternary Science Reviews*, 5, 39-52. http://dx.doi.org/10.1016/0277-3791(86)90172-1

Charlevoix and Laurentian Highlands (Quebec, Canada)

Allard, M. et Fortier, R. (1990) The thermal regime of a permafrost body at Mont du Lac des Cygnes, Quebec. *Canadian Journal of Earth Sciences*, 27, 694-697. http://dx.doi.org/10.1139/e90-067

Grumich, J. et Thériault, L. (1979) *Projet Lac Louis – centrale à réserve pompée : Investigation géologique 1977-78*. Québec : Hydro-Québec.

Occhietti, S. (2007) The Saint-Narcisse morainic complex and early Younger Dryas events on the southeastern margin of the Laurentide Ice Sheet. *Géographie physique et Quaternaire*, 61(2-3), 89-117. http://dx.doi.org/10.7202/038987ar

Payette, S. (1984) Un îlot de pergélisol sur les hauts sommets de Charlevoix, Québec. *Géographie physique et Quaternaire*, 38(3), 305-307. http://dx.doi.org/10.7202/032570ar

Chic-Chocs (Quebec, Canada)

Archambault, B. (1991) *Étude d'un glacier rocheux relique de la vallée de Mont Saint-Pierre, Gaspésie, Québec.* (Mémoire de maîtrise). Montréal, Université de Montréal.

Asnong, H. et Richard, P.J.H. (2003) La végétation et le climat postglaciaires du centre et de l'est de la Gaspésie, au Québec. *Géographie physique et Quaternaire*, 57(1): 37-63. http://dx.doi.org/10.7202/010330ar

Baron-Lafrenière, L. (1983) *Géomorphologie glaciaire de la région du mont Jacques-Cartier, Gaspésie.* (Mémoire de maîtrise). Montréal, Université de Montréal.

Bédard, P. (1993) Postglacial and pre-last-glacial weathering of till on the high plateaus of central Gaspésie, Québec, Canada. *Canadian Journal of Earth Sciences*, 30, 1853-1860. http://dx.doi.org/10.1139/e93-163

Bédard, P. et David, P.P. (1991) La météorisation sur les hauts plateaux de la Gaspésie (Québec): quelques aspects. *Géographie physique et Quaternaire*, 45(2), 195-211. http://dx.doi.org/10.7202/032860ar

Boucher, D., Filion, L. et Hétu, B. (2003) Reconstitution dendrochronologique et fréquence des grosses avalanches de neige dans un couloir subalpine du mont Hog's Back en Gaspésie central (Québec). *Géographie physique et Quaternaire*, 57(2-3), 159-168. http://dx.doi.org/10.7202/011311ar

Charbonneau, R. et David, P.P. (1993) Glacial dispersal of rock debris in central Gaspésie, Québec, Canada. *Canadian Journal of Earth Sciences*, 30, 1697-1707. http://dx.doi.org/10.1139/e93-148

Coleman, A.P. (1922) Physiography and glacial geology of Gaspé Peninsula, Québec. *Geological Survey of Canada Museum Bulletin*, 34.

David, P.P. et Lebuis, J. 1985. Glacial maximum and deglaciation of western Gaspé, Québec, Canada. [Chapitre de livre]. Dans Borns, H.W.Jr., LaSalle, P. et Thompson, W.B. (dir) *Late Pleistocene History of Northern New England and adjacent Quebec. Geological Society of America, Special paper*, 197.

De Römer, H.S. (1977) *Région des monts McGerrigle.* Québec : Ministère des Richesses naturelles.

Dubé, S., Filion, L. et Hétu, B. (2004) Tree-Ring Reconstruction of High-Magnitude Snow Avalanches in the Northern Gaspé Peninsula, Québec, Canada. Arctic, *Antarctic and Alpine Research*, 36(4), 555-564. http://dx.doi.org/10.1657/1523-0430

Flint, R.F., Demorest, M. et Washburn, A.L. (1942) Glaciation of Shickshock Mountains, Gaspe Peninsula. *Geological Society of America Bulletin*, 53(8), 1211-1230. http://dx.doi.org/10.1130/GSAB-53-1211

Germain, D. et Voiculescu, M. (2007) Les avalanches de neige dans les Chic-Chocs (Canada) et les Carpates Méridionales (Roumanie): Bilan des connaissances et perspectives futures. *Revista de geomorfologie*, 9, 17-31.

Germain, D., Filion, L. et Hétu, B. (2005) Snow avalanche activity after fire and logging disturbances, northern Gaspé Peninsula, Quebec, Canada. *Canadian Journal of Earth Sciences*, 42, 2103-2116. http://dx.doi.org/10.1139/e05-087

Germain, D., Filion, L. et Hétu, B. (2009) Snow avalanche regime and climatic conditions in the Chic-Choc Range, eastern Canada. *Climatic Change*, 92(1-2), 141-167. http://dx.doi.org/10.1007/s10584-008-9439-4

Hétu, B. (1990) Évolution récente d'un talus d'éboulis en milieu forestier, Gaspésie, Québec. *Géographie physique et Quaternaire*, 44(2), 199-215. http://dx.doi.org/10.7202/032818ar

Hétu, B. (1991) Active stratified scree deposits near Manche-d'Épée Gaspesia, Quebec, Canada. *Zeitschrift fur Geomorphologie*, 35(4), 439-461.

Hétu, B. (1992) Coarse cliff-top aeolian sedimentation in northern Gaspesie, Quebec (Canada). *Earth Surface Processes and Landforms*, 17(1), 95-108. http://dx.doi.org/10.1002/esp.3290170108

Hétu, B. (1995) Bedding of stratified talus deposits in Gaspesie, Quebec, Canada. The role of nivo-aeolian sedimentation and supranival transitions. *Permafrost and Periglacial Processes*, 6(2), 147-171. http://dx.doi.org/10.1002/ppp.3430060211

Hétu, B. et Gray, J.T. (2000) Les étapes de la déglaciation dans le nord de la Gaspésie (Québec): les marges glaciaires des dryas ancien et récent. *Géographie physique et Quaternaire*, 54(1), 5-40. http://dx.doi.org/10.7202/004831ar

Hétu, B. et Vandelac, P. (1989) La dynamique des éboulis schisteux au cours de l'hiver, Gaspésie septentrionale, Québec. *Géographie physique et Quaternaire*, 43, 389-406. http://dx.doi.org/10.7202/032791ar

Hétu, B., Van Steijn, H. et Vandelac, P. (1994) Les coulées de pierres glacées: un nouveau type de coulées de pierraille sur les talus d'éboulis. *Géographie physique et Quaternaire*, 48, 3-22. http://dx.doi.org/10.7202/032969ar

Larocque, S.J., Hétu, B. et Filion, L. (2001) Geomorphic and dendroecological impacts of slushflows in central Gaspé Peninsula (Québec, Canada) *Geografiska Annaler*, 83A(4), 191-201. http://dx.doi.org/10.1111/j.0435-3676.2001.00154.x

Payette, S. et Boudreau, F. (1984) Évolution postglaciaire des hauts sommets alpins et subalpins de la Gaspésie. *Canadian Journal of Earth Sciences*, 21, 319-335. http://dx.doi.org/10.1139/e84-034

Richard, P.J.H. et Labelle, C. (1989) Histoire postglaciaire de la végétation au lac du Diable, mont Albert, Gaspésie, Québec. *Géographie physique et Quaternaire*, 43(3), 337-354. http://dx.doi.org/10.7202/032787ar

Cape Breton (Nova Scotia, Canada)

Barr, S.M. et Raeside, P.R. (1989) Tectono-stratigraphic terranes in Cape Breton Island, Nova Scotia: Implications for the configuration of the northern Appalachian orogen. *Geology*, 17(9), 822-825. http://dx.doi.org/10.1130/0091-7613

Borns, H.W.Jr. (1965) Late-glacial ice-wedge casts in Northern Nova Scotia, Canada. *Science*, 148, 1223-1225. http://dx.doi.org/10.1126/science.148.3674.1223

Livingstone, D.A. et Estes, A.H. (1967) A carbon-dated pollen diagram from the Cape Breton plateau, Nova Scotia. *Canadian Journal of Botany*, 45(3), 339-359. http://dx.doi.org/10.1139/b67-032

Miller, R.F. (1996) Allerød-Younger Dryas coleoptera from western Cape Breton Island, Nova Scotia, Canada. *Canadian Journal of Earth Sciences*, 33, 33-41. http://dx.doi.org/10.1139/e96-004

Miller, R.F. (1997) Late-glacial (Allerød-Younger Dryas) coleoptera from central Cape Breton Island, Nova Scotia, Canada. *Canadian Journal of Earth Sciences*, 34, 247-259. http://dx.doi.org/10.1139/e17-

Mott, R.J. et Prest, V.K. (1967) Stratigraphy and palynology of buried organisc deposits from Cape Breton Island, Nova Scotia. *Canadian Journal of Earth Sciences*, 4(4), 709-724. http://dx.doi.org/10.1139/e67-047

Mott, R.J. (1994) Wisconsinan Late-glacial environmental change in Nova Scotia: A regional synthesis. *Journal of Quaternary Science*, 9(2), 155-160.

Long Range (Newfoundland, Canada)

Anderson, T.W. et Macpherson, J.B. (1994) Wisconsinan late-glacial environmental change in Newfoundland : A regional synthesis. *Journal of Quaternary Science*, 9(2), 171-178.

Batterson, M.J. et Catto, N.R. 2001. Topographically-controlled Deglacial history of the Humber River Basin, Western Newfoundland. *Géographie physique et Quaternaire*, 55(3), 213-228. http://dx.doi.org/10.720/006851ar

Brookes, I.A. (1970) New evidence for an independant Wisconsin-age cap over Newfoundland. *Canadian Journal of Earth Sciences*, 7(6), 1374-1382. http://dx.doi.org/10.1139/e70-133

Brookes, I. (1971) Fossil ice wedge casts in western Newfoundland. *Maritime Sediments*, 7, 118-122.

Grant, D.R. (1969*a*) Surficial Deposits, Geomorphic Features, and Late Quaternary History of the Terminus of the Northern Peninsula of Newfoundland and Adjacent Quebec-Labrador. *Maritime Sediments*, 5(3), 101-112.

Grant, D.R. (1969*b*) Late Pleistocene re-advance of Piedmont glaciers in Western Newfoundland. *Maritime Sediments*, 5(3): 126-128.

Macclintock, P. et Twenhofel, W.H. (1940) Wisconsin Glaciation of Newfoundland. *Geological Society of America Bulletin*, 51(11), 1729-1756. http://dx.doi.org/10.1130/GSAB-51-1729

Osborn, G., Spooner, I., Gosse, J. et Clark, D. (2007) Alpine glacial geology of the Tablelands, Gros Morne National Park, Newfoundland. *Journal Canadien des Sciences de la Terre*, 44, 819-834. http://dx.doi.org/10.1139/E07-016

Shaw, J. (2003) Submarine moraines in Newfoundland coastal waters: implications for the deglaciation of Newfoundland and adjacent areas. *Quaternary International*, 99-100, 115-134. http://dx.doi.org/10.1016/S1040-6182(02)00125-8

Shaw, J., Piper, D.J.W., Fader, G.B.J., King, E.L., Todd, B.J., Bell, T., Batterson, M.J. et Liverman, D.G.E. (2006) A conceptual model of the deglaciation of Atlantic

Canada. *Quaternary Science Reviews*, 25(17-18), 2059-2081. http://dx.doi.org/10.1016/j.quascirev.2006.03.002

Tanner, V. (1940) The glaciations of Long Range of western Newfoundland. *Geologiska Föreningen i Stockholm Förhandlingar*, 62(4), 361-368. http://dx.doi.org/10.1080/11035894009445041

Waitt, R.B.J. (1981) Radial outflow and unsteady retreat of late Wisconsin to early Holocene icecap in the northern Long Range Upland, Newfoundland. *Geological Society of America Bulletin*, 92, 834-838. http://dx.doi.org/http://dx.doi.org/10.1130/0016-7606(1981)

LISTE DES RÉFÉRENCES

Alestalo, J. (1971) Dendrochronological interpretation of geomorphic processes. *Fennia*, 105, 1-139.

Allen, K.U. (2000, octobre) Avalanche terrain and condition in the Presidential Range. *Proceedings of the International Snow Science Workshop.* Actes du colloque, à Big Sky, États-Unis, du 2 au 6 octobre 2000.

Ancey, C., Gervasoni, C. et Meunier, M. (2004) Computing extreme avalanches. *Cold Regions Science and Technology*, 39(2-3), 161-180. http://dx.doi.org/10.1016/j.coldregions.2004.04.004

Anderson, R.S. et Davis, R.B. (1986) History of late- and post-glacial vegetation and disturbance around Upper South Branch Pond, northern Maine. *Canadian Journal of Botany*, 64, 1977-1986. http://dx.doi.org/10.1139/b86-262

Anderson, T.W., Levac, E. et Lewis, M.C.F. (2007) Cooling in the Gulf of St. Lawrence and estuary region at 9.7 to 7.2 ^{14}C ka (11.2–8.0 cal ka): Palynological response to the PBO and 8.2 cal ka cold events, Laurentide Ice Sheet air-mass circulation and enhanced freshwater runoff. *Palaeogeography, Palaeoclimatology, Palaeoecology*, 246, 75-100. http://dx.doi.org/10.1016/j.palaeo.2006.10.028

Armstrong, W. H., Collins, M. J. et Snyder, N. P. (2012) Increased frequency of low-magnitude floods in New England. *JAWRA: Journal of the American Water Resources Association*, 48, 306–320. http://dx.doi.org/10.1111/j.1752-1688.2011.00613.x

Asnong, H. et Richard, P.J.H. (2003) La végétation et le climat postglaciaires du centre et de l'est de la Gaspésie, au Québec. *Géographie physique et Quaternaire*, 57(1), 37-63. http://dx.doi.org/10.7202/010330ar

Atkins, D. (2000, octobre) Human factors in avalanche accidents. *Proceedings of the International Snow Science Workshop.* Actes du colloque, à Big Sky, États-Unis, du 2 au 6 octobre 2000.

Bailey, S.W., Hoy, J. et Cogbill, C.V. (2015) Vascular flora and geoecology of Mont de la Table, Gaspésie, Québec. *Rhodora*, 117(969), 1-40. http://dx.doi.org/10.3119/14-07

Ballantyne, C.K. (2002) Paraglacial geomorphology. *Quaternary Science Reviews*, 21, 1935–2017. http://dx.doi.org/10.1016/S0277-3791(02)00005-7

Bebi, P., Kulakowski, D. et Rixen, C. (2009) Snow avalanche disturbances in forest ecosystems – State of research and implications for management. *Forest Ecology and Management*, 257(9), 1883-1992. http://dx.doi.org/10.1016/j.foreco.2009.01.050

Beckage, B., Osborne, B., Gavin, D.G., Pucko, C., Siccama, T. et Perkins, T. (2008) A rapid upward shift of a forest ecotone during 40 years of warming in the Green Mountains of Vermont. *Proceedings of the National Academy of Science*, 105(11), 4197-4202. http://dx.doi.org/10.1073/pnas.0708921105

Bégin, Y. et Boivin, S. (2000) Tree-ring dating of past snow regimes. [Chapitre de livre]. Dans Jones, H.G., Pomeroy, J.W., Walker, D.A. et Hohman, R.W. (dir.), *Snow Ecology – An Interdisciplinary Examination of Snow-Covered Ecosystems* (p.323-344). Cambridge : Cambridge University Press.

Bellaire, S. (2013) Relating avalanche activity to climate change and coupled ocean – atmospheric phenomena. Abstract du *Davos Atmosphere and Cryosphere Assembly*, à Davos, Suisse, 2013.

Bellaire, S., Jamieson, B.J., Thumlert, S., Goodrich, J. et Statham, G. (2016) Analysis of long-term weather, snow and avalanche data at Glacier National Park, B.C., Canada. *Cold Regions Science and Technology* 121, 188-125. http://dx.doi.org/10.1016/j.coldregions.2015.10.010

Beniston, M. (2009) Trends in joint quantiles of temperature and precipitation in Europe since 1901 and projected for 2100. *Geophysical Research Letters*, 36, L07707. http://dx.doi.org/10.1029/2008GL037119

Birkeland, K.W. et Mock, C.J. (1996) Atmospheric circulation patterns associated with heavy snowfall events, Bridger Bowl, Montana, U.S.A. *Mountain Research and Development*, 16, 281-286. http://dx.doi.org/10.2307/3693951

Birkeland, K.W. (1997) *Spatial and temporal variations in snow stability and snowpack conditions throughout the Bridger Mountains, Montana.* (Thèse de doctorat). Arizona State University.

Birkeland, K.W., Mock, C.J. et Shinker, J.J. (2001) Avalanche extremes and atmospheric circulation patterns. *Annals of Glaciology*, 32(1), 135-140. http://dx.doi.org/10.3189/172756401781819030

Bjornsson, H. (1980) Avalanche activity in Iceland, climatic conditions, and terrain features. *Journal of Glaciology*, 26, 13-23.

Birks, H.H. et Birks, H.J.B. (2000) Future uses of pollen analysis must include plant macrofossils. *Journal of Biogeography*, 27(1), 31-35. http://dx.doi.org/10.1046/j.1365-2699.2000.00375.x

Bishop, P. (2007) Long-term landscape evolution: linking tectonics and surface processes. *Earth Surface Processes and Landforms*, 32, 329-365. http://dx.doi.org/10.1002/esp.1493

Bliss, L.C. (1963) *Alpine Zone of The Presidential Range*. Illinois, Urbana.

Bogucki, D.J. (1977) Debris slide hazards in the Adirondack Province of New York state. *Environmental Geology*, 1(6), 317-328. http://dx.doi.org/10.1007/BF02380500

Boucher, D., Filion, L. et Hétu, B. (2003) Reconstitution dendrochronologique et fréquence des grosses avalanches de neige dans un couloir subalpin du mont Hog's Back, Gaspésie centrale (Québec). *Géographie physique et Quaternaire*, 57(2-3), 159-168.

Bradbury, J.A., Dingman, L.S. et Keim, B.D. (2002*a*) New England Drought and Relation of New England hydroclimate to large-scale atmospheric circulation patterns. *Journal of the American Water Resources Association*, 38, 1287-1299. http://dx.doi.org/10.1111/j.1752-1688.2002.tb04348.x

Bradbury, J.A., Keim, B.D. et Wake, C.P. (2002*b*) U.S. East Coast trough indices at 500hPa and New England winter climate variability. *Journal of Climate*, 15(23), 3509-3517. http://dx.doi.org/10.1175/1520-0442(2002)015<3509:USECTI>2.0.CO;2

Bradbury, J.A., Keim, B.D. et Wake, C.P. (2003) The influence of regional storm tracking and teleconnections on winter precipitation in the Northeastern United States. *Annals of the American Association of Geographers,* 93(3), 544-556. http://dx.doi.org/10.1111/1467-8306.9303002

Bradley, D.C. (1981) Late Wisconsinan mountain glaciation in the northern Presidential Range, New Hampshire. *Arctic and Alpine Research*, 13(3), 319-327. http://dx.doi.org/10.2307/1551038

Briffa, K.R., Schweingrubber, F.H., Jones, P.D., Osborn, T.J. et Shiyatov, S.G. (1998) Reduced sensitivity of recent tree-growth to temperature at high northern latitudes. *Nature* 391, 678-682. http://dx.doi.org/10.1038/35596

Breiman, L., Friedman, J.H., Olshen, R.A. et Stone, C.J. (1984) *Classification and Regression Trees*. New York: Chapman and Hall.

Burakowski, E.A., Wake, C.P., Braswell, B. et Brown, D.P. (2008) Trends in wintertime climate in the northeastern United States: 1965-2005. *Journal of Geophysical Research*, 113(D20). http://dx.doi.org/10.1029/2008JD009870

Burrows, C.J. et Burrows, V.L. (1976) Procedures for the Study of Snow Avalanche Chronology Using Growth Layers of Woody Plants. *Arctic Alpine Research Occasional Paper*, 23.

Bussières, B., Payette, S. et Filion, L. (1996) Déboisement et entourbement des hauts sommets de Charlevoix à l'Holocène supérieur: origine des étages alpin et subalpin. *Géographie physique et Quaternaire*, 50(3), 257-269. http://dx.doi.org/10.7202/033099ar

Butler, D.R. (1979) Dendrogeomorphological analysis of flooding and mass movement, Ram Plateau, Mackenzie Mountains, Northwest Territories. *The Canadian Geographer*, 23, 62–65. http://dx.doi.org/10.1111/j.1541-0064.1979.tb00638.x

Butler, D.R. et Malanson, G.P. (1985) A history of high-magnitude snow avalanches, southern Glacier National Park, Montana, U.S.A. *Mountain Research and Development*, 5(2), 175-182.

Butler, D.R. et Sawyer, C.F. (2008) Dendrogeomorphology and high-magnitude snow avalanches: a review and case study. *Natural Hazards and Earth System Sciences*, 8, 303-309. http://dx.doi.org/10.5194/nhess-8-303-2008

Butler, D.R., Sawyer, C.F. et Maas, J.A. (2010) Tree-ring dating of snow avalanches in Glacier National Park, Montana, USA. [Chapitre de livre]. Dans Stoffel, M., Bollschweiler, M., Butler, D.R. et Luckman, B.H. (dir.), *Tree-Rings and Natural Hazards : A State-of-the-Art* (p.35-46). Dordrecht : Springer.

Caine, N. (1980) The rainfall intensity: Duration control of shallow landslides and debris flows. *Geografiska Annaler : Series A, Physical Geography*, 62(1-2), 23-27. http://dx.doi.org/10.2307/520449

Camill, P. et Clark, J.S. (2000) Long-Term Perspectives on Lagged Ecosystem Responses to Climate Change: Permafrost in Boreal Peatlands and the Grassland/Woodland Boundary. *Ecosystems*, 3(6), 534-544. http://dx.doi.org/10.1007/s100210000047

Capers, R.S., Kimball, K.D., McFarland, K.P., Jones, M.T., Lloyd, A.H., Munroe, J.S., Fortin, G., Mattrick, C., Goren, J., Sperduto, D.D. et Paradis, R. (2013) Establishing alpine research priorities in Northeastern North America. *Northeastern Naturalist*, 20(4), 559-577. http://dx.doi.org/10.1656/045.020.0406

Capers, R.S. et Stone, A.D. (2011) After 33 years, trees more frequent and shrubs more abundant in Northeast U.S. alpine community. *Arctic, Antarctic and Alpine Research*, 43(4), 495-502. http://dx.doi.org/10.1657/1938-4246-43.4.495

Carlson, B.Z., Munroe, J.S. et Hegman, B. (2011) Distribution of Alpine Tundra in the Adirondack Mountains of New York, U.S.A. *Arctic, Antarctic and Alpine Research*, 43(3), 331-342. http://dx.doi.org/10.1657/1938-4246-43.3.331

Carrara, P.E. (1979) The determination of snow avalanche frequency through tree-ring analysis and historical records at Ophir, Colorado. *Geological Society of America Bulletin*, 90, 773-780. http://dx.doi.org/10.1130/0016-7606(1979)90<773:TDOSAF>2.0.CO;2

Casanueva, A., Rodriguez-Puebla, C., Frías, M.D. et Gonzales-Reviriego, N (2014) Variability of extreme precipitation over Europe and its relationships with teleconnection patterns. *Hydrology and Earth System Sciences*, 18, 709-725. http://dx.doi.org/10.5194/hess-18-709-2014

Castebrunet, H., Eckert, N. et Giraud, G. (2012) Snow and weather climatic control on snow avalanche occurrence fluctuations over 50 yr in the French Alps. *Climate of the Past*, 8, 855-875. http://dx.doi.org/10.5194/cp-8-855-2012

Casteller, A., Stöckli, V., Villalba, R. et Mayer, A.C. (2007) An Evaluation of dendroecological indicators of snow avalanche in the Swiss Alps. *Arctic, Antarctic and Alpine Research*, 39, 218-228. http://dx.doi.org/10.1657/1523-0430(2007)39[218:AEODIO]2.0.CO;2

Casteller, A., Christen, M., Villalba, R., Martinez, H., Stöckli, V., Leiva, J.C. et Barteit, P. (2008) Validating numerical simulations of snow avalanches using

dendrochronology: The Cerro Ventana event in Northern Patagonia, Argentina. *Natural Hazards and Earth Systems Sciences*, 8, 433-443. http://dx.doi.org/10.5194/nhess-8-433-2008

Casteller, A., Villalba, R., Araneo, D. et Stöckli, V. (2011) Reconstructing temporal patterns of snow avalanches at Lago des Desierto, southern Patagonian Andes. *Cold Region Science and Technology*, 67(1-2), 68-78. http://dx.doi.org/10.1016/j.coldregions.2011.02.001

Chiroiu, P., Stoffel, M., Onaca, A. et Urdea, P. (2015) Testing dendrogeomorphic approaches and thresholds to reconstruct snow avalanche activity in the Făgăraş Mountains (Romanian Carpathians). *Quaternary Geochronology*, 27, 1-10. http://dx.doi.org/10.1016/j.quageo.2014.11.001

Clark, G.M. et Schmidlin, T.W. (1992) Alpine periglacial landforms of eastern North America: A review. *Permafrost and Periglacial Processes*, 3(3), 225-230. http://dx.doi.org/10.1002/ppp.3430030309

Cogbill, C.V. (1985) Dynamics of boreal forest of the Laurentian Highlands, Canada. *Canadian Journal of Forest Research*, 15, 252-261. http://dx.doi.org/10.1139/x85-043

Cogbill, C.V. et White, P.S. (1991) The Latitude-Elevation Relationship for Spruce-Fir Forest and Treeline alond the Appalachian Mountain Chain. *Vegetatio*, 94(2), 153-175. http://dx.doi.org/10.1007/BF00032629

Colbeck, S.C. (1991) The layered character of snow covers. *Review of Geophysics*, 29, 81-96. http://dx.doi.org/10.1029/90RG02351

Coleman, J.S.M. et Rogers, J.C. (2003) Ohio River Valley winter moisture conditions associated with the Pacific-North American Teleconnection Pattern. *Bulletin of the American Meteorological Society* 16(6), 969-981. http://dx.doi.org/10.1175/1520-0442(2003)016<0969:ORVWMC>2.0.CO;2

Collins, M., The CMIP Modelling Groups (BMRC (Australia), CCC (Canada), CCSR/NIES (Japan), CERFACS (France), CSIRO (Austraila), MPI (Germany), GFDL (USA), GISS (USA), IAP (China), INM (Russia), LMD (France), MRI (Japan), NCAR (USA), NRL (USA), Hadley Centre (UK) and YNU (South Korea)). (2005) El Niño- or La Niña-like climate change? *Climate dynamics*, 24(1), 89-104. http://dx.doi.org/10.1007/s00382-004-0478-x

Collins, M.J. (2009). Evidence for changing flood risk in New England since the late 20th century. *JAWRA: Journal of the American Water Resources Association*, 45, 279–290. http://dx.doi.or/10.1111/j.1752-1688.2008.00277.x

Collins, M.J., Kirk, J.P., Pettit, J., DeGaetano, A.T., McCown, M.S., Peterson, T.C., Means, T.N. et Zhang, X. (2014) Annual floods in New England (USA) and Atlantic Canada: synoptic climatology and generating mechanisms. *Physical Geography*, 35(3), 195-219. http://dx.doi.org/10.1080/02723646.2014.888510

Colorado Avalanche Information Center (CAIC). (2015). *Statistics and Reporting.* Récupéré de http://avalanche.state.co.us/accidents/statistics-and-reporting/

Committee on Ground Failure Hazards Mitigation Research (CGFHMR). (1990) *Snow Avalanche Hazards and Mitigation in the United States.* Washington, National Academy Press.

Conlan, M.J.W., Tracz, D.R. et Jamieson, B. (2014) Measurements and weather observations at persistent deep slab avalanches. *Cold Regions Science and Technology*, 97, 104-112. http://dx.doi.org/10.1016/j.coldregions.2013.06.011

Corona, C., Rovéra, G., Lopez Saez, J., Stoffel, M. et Perfettini, P. (2010) Spatio-temporal reconstruction of snow avalanche activity using tree rings: Jean Jeanne avalanche talus, Massif de l'Oisans, France. *Catena*, 83, 107–118. http://dx.doi.org/10.1016/j.catena.2012.08.004

Corona, C., Lopez Saez, J., Stoffel, M., Bonnefoy, M., Richard, D., Astrade, L. et Berger, F. (2012) How much of the real avalanche activity can be captured with tree rings? An evaluation of classic dendrogeomorphic approaches and comparison with historical archives. *Cold Regions Science and Technology,* 74-75, 31-42. http://dx.doi.org/10.1016/j.coldregions.2012.01.003

Corona, C., Lopez Saez, J., Stoffel, M., Rovéra, G., Édouard, J.L. et Berger, F. (2013) Seven centuries of avalanche activity at Echalp (Queyras massif, southern French Alps) as inferred from tree rings. *The Holocene*, 23(2), 292-304. http://dx.doi.org/10.1177/0959683612460784

Coulibaly, P., Anctil, F., Rasmussen, P. et Bobée, B. (2000) A recurrent neural networks approach using indices of low-frequency climatic variability to forecast regional annual runoff. *Hydrological Processes*, 14 (15), 2755-2777. http://dx.doi.org/10.1002/1099-1085(20001030)14:15<2755::AID-HYP90>3.0.CO;2-9

Cwynar, L.C. et Spear, R.W. (2001) Lateglacial climate change in the White Mountains of New Hampshire. *Quaternary Science Reviews*, 20, 1265-1274. http://dx.doi.org/10.1016/S0277-3791(00)00151-7

Davis, M.B. (1969) Climatic changes in southern Connecticut recorded by pollen deposition at Rogers Lake. *Ecology*, 50(3), 409-422. http://dx.doi.org/10.2307/1933891

Davis, R.E., Elder, K., Howlett, D. et Bouzaglou, E. (1999) Relating storm and weather factors to dry slab avalanche activity at Alta, Utah, and Mammoth Mountain, California, using classification and regression trees. *Cold Regions Science and Technology*, 30(1–3), 79– 89. http://dx.doi.org/10.1016/S0165-232X(99)0032-4

Decaulne, A., Eggertsson, Ó. Et Sæmundsson, Þ. (2012) First dendrogeomorphologic approach of snow avalanche magnitude–frequency in Northern Iceland. *Geomorphology*, 167-168, 35-44. http://dx.doi.org/10.1016/jgeomorph.2011.11.017

Decaulne, A., Eggertsson, O., Laute, K. et Beylich, A.A. (2014) A 100-year extreme snow-avalanche record based on tree-ring research in upper Bødalen, inner Nordfjord, western Norway. *Geomorphology*, 218(1), 3-15. http://dx.doi.org/10.1016/j.geomorph.2013.12.036

Dixon, R.W., Butler, D.R., DeChano, L.M. et Henry, J.A. (1999) Avalanche hazard in Glacier National Park: an El Niño connection? *Physical Geography*, 20(6), 461-467. http://dx.doi.org/10.1080/02723646.1999.10642690

Dozier, J. et Painter, T.H. (2004) Multispectral and hyperspectral remote sensing of alpine snow properties. *Earth and Planetary Sciences*, 32, 465-494. http://dx.doi.org/10.1146/annurev.earth.32.101802.120404

Dubé, S., Filion, L. et Hétu, B. (2004) Tree-ring reconstruction of high-magnitude snow avalanches in the Northern Gaspé Peninsula, Québec, Canada. *Arctic, Antarctic and Alpine Research*, 36(4), 555-564. http://dx.doi.org/10.1657/1523-0430(2004)036[0555:TROHSA]2.0.CO;2

Dullinger, S., Gattringer, A., Thuiller, W., Moser, D., Zimmermann, N.E., Guisan, A., Willner, W., Plutzar, C., Leitner, M., Mang, T., Caccianiga, M., Dirnböck, T., Ertl, S., Fischer, A., Lenoir, J., Svenning, J.C., Psomas, A., Schmartz, D.R., Silc, U., Vittoz, P. et Hübler, K. (2012) Extinction debt of high-mountain plants under twenty-first century climate change. *Nature Climate Change*, 2, 619-622. http://dx.doi.org/10.1038/nclimate1514

Dumais, C., Ropars, P., Denis, M.P., Dufour-Tremblay, G. et Boudreau, S. (2014) Are low altitude alpine tundra ecosystems under threat ? A case study from the Parc National de la Gaspésie, Québec. *Environmental Research Letters*, 9, 1-10. http://dx.doi.org/10.1088/1748-9326/9/9/094001

Dyke, A.S., Andrews, J.T., Clark, P.U., England, J.H., Miller, G.H., Shaw, J. et Veillette, J.J. (2002) The Laurentide and Innuitian ice sheets during the Last Glacial Maximum. *Quaternary Science Reviews*, 21, 9-31. http://dx.doi.org/10.1016/S0277-3791(01)00095-6

Dyke, A.S. (2004) An outline of North American Deglaciation with an emphasis on central and northern Canada. [Chapitre de libre] Dans Ehlers, J. et Gibbard, P.L. (dir.), *Quaternary Glaciations – Extent and Chronology, Part II: North America* (p.323-344) *Developments in Quaternary Science*, 2b. Amsterdam : Elservier.

Eckert, N., Baya, H. et Deschatres, M. (2010) Assessing the Response of Snow Avalanche Runout Altitudes to Climate Fluctuations Using Hierarchical Modeling: Application to 61 Winters of Data in France. *Journal of Climate*, 23, 3157-3180. http://dx.doi.org/10.1175/2010JCLI3312.1

Eckert, N., Keylock, C.J., Castebrunet, H., Lavigne, A. et Naaim, M. (2013) Temporal trends in avalanche activity in the French Alps and subregions: from occurrences and runout altitudes to unsteady return periods. *Journal of Glaciology*, 59(213), 93-114. http://dx.doi.org/10.3198/2031JoG12J091

Engler, R., Randin, C.F., Thuiller, W., Dullinger, S., Zimmermann, N., Araujo, M.B., Pearman, P.B., Le Lay, G., Piedallu, C., Albert, C.H., Choler, P., Coldea, G., De Lamo, X., Dirnböck, T., Gégout, J.C., Gomez-Garcia, D., Grytnes, J.A., Heegard, E., Høistad, F., Nogués-Bravo, D., Normand, S., Puşcaş, M., Sebastià, M.T., Stanisci, A., Theurillat, J.P., Trivedi, M.R., Vittoz, P. et Guisan, A. (2011) 21st century climate change threatens mountain flora unequally across Europe. *Global Change Biology*, 17(7), 2330-2341. http://dx.doi.org/10.1111/j.1365-2486.2010.02393.x

Enos, P.C. (1969) Cloridorme Formation, middle Ordovician Flysch, Northern Gaspé Peninsula, Québec. *Geological Society of America Special Paper*, 117. http://dx.doi.org/10.1130/SPE117-p1

Esteban, P., Jones, P.D., Martin-Vide, J. et Mases, M. (2005) Atmospheric circulation patterns related to heavy snowfall days in Andorra, Pyrenees. *International Journal of Climatology*, 25, 319-329. http://dx.doi.org/10.1002/joc.1103

Fernald, M.L. (1907) The soil preferences of certain alpine and subalpine plants. *Rhodora Journal of the New England Botanical Club*, 9(105), 149-193.

Fernald, M.L. (1925) Persistence of plants in unglaciated areas of Boreal America. *Memoirs of the American Academy of Arts and Sciences*, 15, 558-572. http://dx.doi.org/10.2307/25058128

Ferguson, S.A., Moore, M.D., Marriott, R.T. et Speers-Hayes, P. (1990) Avalanche weather forecasting at the Northwest Avalanche Center, Seattle, Washington, U.S.A. *Journal of Glaciology*, 36, 57-66.

Filion, L. (1987) Holocene Development of Parabolic Dunes in the Central St. Lawrence Lowland, Québec. *Quaternary Research*, 28, 196-209. http://dx.doi.org/10.1016/0033-5894(87)90059-7

Filion, L., Payette, S., Gauthier, L. et Boutin, Y. (1986) Light rings in subarctic conifers as a dendrochronological tool. *Quaternary Research*, 26(2), 272-279. http://dx.doi.org/10.1016/0033-5894(86)90111-0

Fitzharris, B.B. (1987) A climatology of major avalanche winters in western Canada. *Atmosphere-Ocean*, 25(2), 115-136. http://dx.doi.org/10.1080/07055900.1987.9649267

Fitzharris, B.B. et Bakkehøi, S. (1986) A synoptic climatology of major avalanche winters in Norway. *Journal of Climatology*, 6, 431-446. http://dx.doi.org/10.1002/joc.3370060408

Fitzharris, B.B. et Schaerer, P.A. (1980) Frequency of major avalanche winters. *Journal of Glaciology*, 26(94), 43-52.

Flynn, R.H. (2008) *Flood of April in New Hampshire* (#2008-5120). United States Geological Survey.

Fontaine, R.A., 1987. *Flood of April 1987 in Maine, Massachusetts and New Hampshire* (#87-460). United States Geological Survey.

Fortin, G. et Hétu, B. (2009) Les extremes météorologiques hivernaux et leurs influences sur la couverture neigeuse dans les monts Chic-Chocs, Gaspésie, Canada. *Géographia Technica*, numéro spécial, 181-186.

Fortin, G. et, Hétu, B. (2014) Estimating winter trends in climatic variables in the Chic-Chocs Mountains, Canada (1970-2009). *International Journal of Climatology*, 34, 3078-3088. http://dx.doi.org/10.1002/joc.3895

Fortin, G., Hétu, B. et Germain, D. (2011) Climat hivernal et regimes avalancheux dans les corridors routiers de la Gaspésie septentrionale (Québec, Canada). *Climatologie*, 9-25. http://dx.doi.org/10.4267/climatologie.202

Fründt, B., Müller, T.J., Schulz-Bull, D.E. et Waniek, J.J. (2013) Long-term changes in the thermocline of the subtropical Northeast Atlantic (33°N, 22°W). *Progress in Oceanography*, 116, 246-260. http://dx.doi.org/10.1016/j.pocean.2013.07.004

Gądek, B. (2012) Debris slopes ventilation in the periglacial zone of the Tatra Mountains (Poland and Slovakia): The indicators. *Cold Regions Science and Technology*, 74-75, 1-10. http://dx.doi.org/10.1016/j.coldregions.2012.01.007

Garavaglia, V. et Pelfini, M. (2011) The role of border areas for dendrochronological investigations on catastrophic snow avalanches: A case study from the Italian Alps. *Catena*, 87(2), 209-215. http://dx.doi.org/10.1016/j.catena.2011.06.006

Garcia, C., Marti, G., Oller, P., Moner, I., Gavalda, J., Martinez, P. et Peña, J.C. (2009) Major avalanches occurrence at the regional scale and related atmospheric circulation patterns in the Easterne Pyrenees. *Cold Regions Sciences and Technology*, 59(2-3), 106-118. http://dx.doi.org/10.1016/j.coldregions.2009.07.009

Gaume, J., Chambon, G., Eckert, N. et Naaim, M. (2013) Influence of weak-layer heterogeneity on snow slab avalanche release: application to the evaluation of avalanche release depth. *Journal of Glaciology* 59(215), 423-437. http://dx.doi.org/10.3189/2013JoG12J161

Gauthier, D. et Jamieson, B.J. (2006) Towards a field test for fractur propagation propensity in weak snowpack layers. *Journal of Glaciology* 52(176), 164-168. http://dx.doi.org/10.3189/17275650678182896

Germain, D. (2005) *Dynamique des avalanches de neige en Gaspésie, Québec, Canada.* (Thèse de doctorat). Québec, Université Laval.

Germain, D. (2016) Snow avalanche hazard assessment and risk management in northern Quebec, Canada. *Natural Hazards*, 80(2), 1303-1321. http://dx.doi.org/10.1007/s11069-015-2024-z

Germain, D. et Hétu, B. (*sous presse*) Hillslope processes and related sediment fluxes on a fine-grained scree slope of Eastern Canada. [Chapitre de livre]. Dans Beylich, A.A., Dixon, J.C. et Zwolinski, Z (dir.), *Source-to-sink fluxes in Undisturbed Cold Environments*. Cambridge : Cambridge University Press.

Germain, D., Filion, L.et Hétu, B. (2005) Snow avalanche activity after fire and logging disturbances, northern Gaspé Peninsula, Quebec, Canada. *Canadian Journal of Earth Sciences*, 42, 2103-2116. http://dx.doi.org/10.1139/e05-087

Germain, D., Filion, L. et Hétu, B. (2009) Snow avalanche regime and climatic conditions in the Chic-Choc Range, eastern Canada. *Climatic Change*, 92(1-2), 141-167. http://dx.doi.org/10.1007/s10584-008-9439-4

Germain, D., Hétu, B. et Filion, L. (2010) Tree-ring based reconstruction of past snow avalanche events and risk assessment in Northern Gaspé Peninsula (Québec, Canada). [Chapitre de livre]. Dans Stoffel, M., Bollschweiler, M., Butler, D.R. et Luckman, B.H. (dir.), *Tree-Rings and Natural Hazards : A State-of-the-Art* (p.51-73). Dordrecht : Springer.

Gershunov, A. et Barnett, T.P. (1998) Interdecadal modulation of ENSO teleconnections. *Bulletin of the American Meteorological Society*, 79(12), 2715-2725. http://dx.doi.org/10.1175/1520-0477(1998)079<2715:IMOET>2.0.CO;2

Goldthwait, R.P., Billings, M.P. et Creasy, J.W. (1987) Mount Washington - Crawford Notch area, New Hampshire. [Chapitre de Livre]. Dans Roy, D.C. (dir.), *Northeastern Section of the Geological Society of America, Centennial field guide—vol. 5* (p.257-262).

Gordon, G. (1989) The Worst Weather in the World. *Windswept*, 30, 66-69.

Gosse, J.C., Bell, T., Gray, J.T., Klein, J., Yang, G. et Finkel, R. 2006. Using cosmogenic isotopes to interpret the landscape record of glaciation : Nunataks on Newfoundland ? [Chapitre de livre]. Dans Knight, P.J. (dir.), *Glacier science and environmental change* (p.442-446). Oxford : Blackwell.

Grabherr, G., Gottfried, M. et Pauli, H. (2010) Climate change impacts in alpine environments. *Geogaraphy Compass*, 4(8), 1133-1153. http://dx.doi.org/10.1111/j.1749-8198.2010.00356.x

Grant, A.N., Pszenny, A.A.P. et Fischer, E.V. (2005) The 1935-2003 air temperature record from the summit of Mount Washington, New Hampshire. *Journal of Climate*, 18, 4445-4453. http://dx.doi.org/10.1175/JCLI3547.1

Graveline, M.-H. et Germain, D. (2016) Ice-block fall and snow avalanche hazards in northern Gaspésie (eastern Canada): Triggering weather scenarios and process interactions. *Cold Regions Science and Technology*, 123, 81-90. http://dx.doi.org/10.1016/j.coldregions.2015.11.012

Gray, J.T. et Brown, R.J.E. (1979) Permafrost presence and distribution in the Chic-Chocs Mountains, Gaspésie, Québec. *Géographie physique et Quaternaire*, 33(3-4), 299-316. http://dx.doi.org/10.7202/1000366ar

Gray, J.T., Godin, É., Masse, J. et Fortier, D. (2009) Trois décennies d'observation des fluctuations du régime thermique du pergélisol dans le parc national de la Gaspésie. *Le naturaliste canadien*, 133(3), 69-77.

Guzzetti, F., Reichenbach, P., Cardinalli, M., Galli, M. et Ardizzone, F. (2005) Probabilistic landslide hazard assessment at the basin scale. *Geomorphology*, 72(1-4), 272-299. http://dx.doi.org/10.1016/jgeomorph.2005.06.002

Hächler, P. (1987) Analysis of the weather situations leading to severe and extraordinary avalanche situations. *International Association of Hydrological Sciences Publications*, 162: 295-304.

Hadley, K.S. et Knapp, P.A. (2011) Detection of high-wind events using tree-ring data. *Canadian Journal of Forestry Research*, 41(5), 1121-1129. http://dx.doi.org/10.1139/x11-030

Haeberli, W., Noetzli, J., Arkenson, L., Delaloye, R., Gärtner-Roer, I., Gruber, S., Isaksen, K., Kneisel, C., Krautblatter, M. et Phillips, M. (2010) Mountain permafrost: development and challenges of a young research field. *Journal of Glaciology*, 56(200), 1043-1058. http://dx.doi.org/10.3189/002214311796406121

Haegeli, P. et McClung, D.M. (1999, décembre) Classification of avalanche forecasting models. *International Conference on Avalanches*. Actes du colloque, à Saint Vincent, Italie, du 13 au 14 décembre 1999.

Haegeli, P. et McClung, D.M. (2007) Expanding the snow-climate classification with avalanche-relevant information: initial description of avalanche winter regimes for Southwestern Canada. *Journal of Glaciology*, 52(181), 266-276. http://dx.doi.org/10.3189/172756507782202801

Hargraves, R.B. et Roy, D.W. (1974) Paleomagnetism of Anorthosite in and around the Charlevoix Cryptoexplosion Structure, Quebec. *Canadian Journal of Earth Sciences*, 11, 854-859. http://dx.doi.org/10.1139/e74-085

Harris, C., Arenson, L.U., Christiansen, H.H., Etzelmüller, B., Frauenfelder, R., Gruber, S., Haeberli, W., Hauck, C., Hözle, M., Humlum, O., Isaksen, K., Kääb, A., Kern-Lütschg, M.A., Lehning, M., Matsuoka, N., Murton, J.B., Nötzli, J., Phillips, M., Ross, N., Seppälä, M., Springman, S.M. et Mühll, D.V. (2009) Permafrost and climate in Europe: Monitoring and modelling thermal, geomorphological and

geotechnical responses. *Earth Science Reviews*, 92, 117-171. http://dx.doi.org10.1016/j.earscirev.2008.12.002

Harsch, M.A., Hulme, P.E., McGlone, M.S. et Duncan, R.P. (2009) Are treelines advancing ? A global meta-analysis of treeline response to climate warming. *Ecology Letters*, 12, 1040-1049. http://doi.dx.org/10.1111/j.1461-0248.2009.01355.x

Hartley, S. et Keables, M.J. (1998) Synoptic associations of winter climate and snowfall variability in New England, USA, 1950-1992. *International Journal of Climatology*, 18, 281-298. http://dx.doi.org/10.1002/(SICI)1097-0088(19980315)18:3

Heinrich, I., Gärtner, H. et Monbaron, M. (2007) Wood anatomy and dendrogeomorphology – reaction wood varieties caused by different experimental treatments. *TRACE – Tree Rings in Archaeology, Climatology and Ecology*, 5, 224–232.

Hendrikx, J., Owens, I., Carran, W. et Carran, A. (2005) Avalanche activity in an extreme maritime climate: The application of classification trees for forecasting. *Cold Regions Science and Technology*, 43(1-2), 104-116. http://dx.doi.org/10.1016/j.coldregions.2005.05.006

Hendrikx, J., Johnson, J. et Southworth, E. (2013, octobre) Understanding travel behaviour in avalanche terrain: A new approach. *Proceedings of the International Snow Science Workshop.* Actes du colloque, à Chamonix, France, du 7 au 11 octobre 2013.

Hendrikx, J., Murphy, M. et Onslow, T. (2014) Classification trees as a tool for operational avalanche forecasting on the Seward Highway, Alaska. *Cold Regions Science and Technology*, 97, 113-120. http://dx.doi.org10.1016/j.coldregions.2013.08.009

Hétu, B. (2007) Les conditions météorologiques propices au déclenchement des avalanches de neige dans les corridors routiers du nord de la Gaspésie, Québec, Canada. *Géographie Physique et Quaternaire*, 61(2-3), 165-180. http://dx.doi.org/10.7202/038990ar

Hétu, B. et Bail, P. (1996) Évolution postglaciaire du regime hydrosédimentaire et vitesse de l'ablation dans un petit basin-versant des Appalaches près de Rimouski (Bas-Saint-Laurent, Québec). *Géographie physique et Quaternaire*, 50(3), 351-363.

Hétu, B. et Gray, J.T. (2000) Effects of environmental change on scree slope development throughout the postglacial period in the Chic-Choc Mountains in the northern Gaspe Peninsula, Quebec. *Geomorphology*, 32, 335-355. http://dx.doi.org/10.1016/S0169-555X(99)00103-8

Hétu, B., Gray, J.T., Gangloff, P. et Archambault, B. (2003) Postglacial talus-derived rock glaciers in the Gaspé Peninsula, Quebec (Canada). *Proceedings of the 8th International Conference on Permafrost.* Actes du colloque, 389-394.

Hétu, B., Brown, K. et Germain, D. (2011) Les victimes d'avalanche au Québec entre 1825 et 2009. *Le Géographe Canadien*, 55, 273-287.

Hétu, B., Fortin, G. et Brown, K. (2015) Climat hivernal, aménagement du territoire et dynamique des avalanches au Québec méridional : une analyse à partir des accidents connus depuis 1825. *Journal Canadien des Sciences de la Terre*, 52, 307-321. http://dx.doi.org/10.1139/cjes-2014-0205

Hétu, B., Van Steijn, H. et Vandelac, P. (1994) Les coulées de pierres glacées: un nouveau type de coulées de pierraille sur les talus d'éboulis. *Géographie physique et Quaternaire*, 48:3-22. http://dx.doi.org/10.7202/032969ar

Hirsch, M.E., DeGaetano, A.T. et Colucci, S.J. (2001) An East Coast winter storm climatology. *Bulletin of the American Meteorological Society*, 14(5), 882-899. http://dx.doi.org/10.1175/1520-0442(2001)014<0882:AECWSC>2.0.CO;2

Hiscott, R.N. et James, N.P. (1985) Carbonate debris flows, Cow Head Groupe, western Newfoundland. *Journal of Sedimentary Research*, 55(5), 735-745.

Housset, J.M., Girardin, M.P., Baconnet, M., Carcaillet, C., Bergeron, Y., 2015. Unexpected warming-induced growth decline in *Thuja occidentalis* at its northern limits in North America. *Journal of Biogeography*, 42(7), 1233-1245. http://dx.doi.org/10.1111/jbi.12508

Humlum, O. (1998) The climatic significance of rock glaciers. *Permafrost and Periglacial Processes*, 9(4), 375-395. http://dx.doi.org/10.1002/(SICI)1099-1530

Huntington, T.G., Hodgkins, G.A., Keim, B.D. et Dudley, R.W. (2004) Changes in the Proportion of Precipitation Occurring as Snow in New England (1949-2000). *Journal of Climate*, 17, 2626-2636. http://dx.doi.org10.1175/1520-0442(2004)017<2626;CITPOP>2.0.CO;2

Hurrell, J. et NCAR Staff (2014) The Climate Data Guide: Hurrell North Atlantic Oscillation (NAO) Index (station-based). Récupéré le 17 juillet 2015 de

https://climatedataguide.ucar.edu/climate-data/hurrell-north-atlantic-oscillation-nao-index-station-based

Ibe, R.A. (1985) Postglacial Montane Vegetational History Around Balsam Lake, Catskill Mountains, New York. Bulletin of the Torrey Botanical Club, 112(2), 176-186. http://dx.doi.org/10.2307/2996414

IPCC (International Panel on Climate Change) (2013). Climate Change 2013: The Physical Science Basis. Contribution to the Fifth Assessment Report of the IPCC. Cambridge: Cambridge University Press.

Jackson, S.T. et Whitehead, D.R. (1991) Holocene vegetation patterns in the Adirondack Mountains. *Ecology*, 72(2): 641-653. http://dx.doi.org/10.2307/2937204

Jamieson, B.J. et Stethem, C. (2002) Snow avalanche hazards and management in Canada : Challenges and progress. *Natural Hazards*, 26, 35-53. http://dx.doi.org/10.1023/A:1015212626232

Johansson, M., Callaghan, T.V., Rosiö, J. et Akerman, H.J. (2013) Rapid responses of permafrost and vegetation to experimentally increased snow cover in sub-arctic Sweden. *Environmental Research Letter*, 8(3), 035025. http://dx.doi.org/10.1088/1748-9326/8/3/035025

Johnson, C.J., Ehlers, L.P.W. et Seip, D.R. (2015) Witnessing extinction – Cumulative impacts across landscapes and the future loss of an evolutionarily significant unit of woodland caribou in Canada. *Biological Conservation*, 186, 176-186. http://dx.doi.org/10.1016/j.biocon.2015.03.012

Jomelli, V., Delval, C., Grancher, D., Escande, S., Brunstein, D., Hetu, B., Filion, L., et Pech, P. (2007) Probabilistic analysis of recent snow avalanche activity and weather in the French Alps. *Cold Regions Science and Technology*, 47(1-2), 180-192. http://dx.doi.org/10.1016/j.coldregions.2006.08.003

Jomelli, V., Khodri, M., Favier, V., Brunstein, D., Ledru, M.P., Wagnon, P., Blard, P.H., Sicart, J.E., Braucher, R., Grancher, D., Bourlès, D.L., Braconnot, P. er Vuille, M. (2011) Irregular tropical glacier retreat over the Holocene epoch driven by progressive warming. *Nature*, 474, 196-199. http://dx.doi.org/10.1038/nature10150

Jones, A.S.T. et Jamieson, B. (2004) Statistical avalanche-runout estimation for short slopes in Canada. *Annals of Glaciology*, 38(1), 363-372. http://dx.doi.org/10.3189/172756404781814960

Jones, G.V. et Davis, R.E. (1995) Climatology of Nor'easters and the 30 kPa Jet. *Journal of Coastal Research*, 11(4), 1210–1220.

Jones, M.T. et Willey, L.L. (2012) *The Eastern Alpine Guide*. New Salem : Beyond Ktaadn et Boghaunter Books.

Joosen, C. (2008, septembre) The importance of micro-scale avalanche forecasting in Mount Wsahington's Tuckerman and Huntington Ravines. *Proceedings of the International Snow Science Workshop.* Actes du colloque, à Whistler, Canada, du 21 au 27 septembre 2008.

Jutras, P. et Schroeder, J. (1999) Geomorphology of an exhumed Carboniferous paleosurface in the southern Gaspé Peninsula, Québec; paleoenvironmental and tectonic implications. *Géographie physique et Quaternaire*, 53(2), 249-263. http://dx.doi.org/10.7202/005690ar

Kalnay, E., Kanamitsu, M., Kistler, R., Collins, W., Deaven, D., Gandin, L., Iredell, M., Saha, S., White, G., Woollen, J., Zhu, Y., Leetmaa, A., Reynolds, R., Chelliah, M., Ebisuzaki, W., Higgins, W., Janowiak, J., Mo, K.C., Ropelewski, C., Wang, J., Roy, J. et Joseph, D. (1996) The NCEP/NCAR 40-year reanalysis project. *Bulletin of the American Meteorological Society*, 77, 437-471. http://dx.doi.org/10.1175/1520-0477(1996)077<0437:TNYRP>2.0.CO;2

Keylock, C.J. (2003) The North Atlantic Oscillation and snow avalanching in Iceland. *Geophysical Research Letters*, 30(5), 1254. http://dx.doi.org/10.1029/2002GL016272

Kogelnig-Mayer, B., Stoffel, M., Sneuly-Bollschweiler, M., Hüble, J. et Rudolf-Miklau, F. (2011) Possibilities and limitations of dendrogeomorphic time-series reconstructions on sites influenced by debris flows and frequent snow avalanche activity. *Arctic, Antarctic, and Alpine Research*, 43, 649-658. http://dx.doi.org/10.1657/1938-4246-43.4.649

Körner, C. (1998) A re-assessment of high elevation treeline positions and their explanation. *Oecologia*, 115, 445-459. http://dx.doi.org/10.1007/s004420050540

Kronholm, K. et Birkeland, K.W. (2005) Integrating spatial patterns into a snow avalanche cellular automata model. *Geophysical Research Letters*, 32, 19, L19504. http://dx.doi.org/10.1029/2005GL024373

Kull, C.A. et Magilligan, F.J. (1994) Controls over landslide distribution in the White Mountains, New Hampshire. *Physical Geography*, 15(4), 325-341. http://dx.doi.org/10.1080/02723646.1994.10642520

Labelle, C. et Richard, P.J.H. (1984) Histoire Postglaciaire de la Végétation dans la Région de Mont-Saint-Pierre, Gaspésie, Québec. *Géographie physique et Quaternaire*, 38(3), 257-274. http://dx.doi.org/10.7202/032567ar

LaChapelle, E. (1980) The fundamental processes in conventional avalanche forecasting. *Journal of Glaciology*, 26(94), 75-85.

Lafon, C.W. et Speer, J.H. (2002) Using dendrochronology to identify major ice storm events in oak forests of southwestern Virginia. *Climate Research*, 20(1), 41-54. http://dx.doi.org/10.3354/er020041

Lafortune, M., Filion, L. et Hétu, B. 1997. Dynamique d'un front forestier sur un talus d'éboulis actif en climat tempéré froid (Gaspésie, Québec). *Géographie physique et Quaternaire*, 51(1), 1-15. http://dx.doi.org/10.7202/004840ar

Lagadec, A., Boucher, E. et Germain, D. (2015) Spatiotemporal dynamics and hydro-climatic thresholds triggering river ice jams on the Mistassini River, Quebec. *Hydrological Processes*, 29(23), 4880-4890. http://dx.doi.org/10.1002/hyp.10537

Larocque, S.J., Hétu, B. et Filion, L. (2001) Geomorphic and dendroecological impacts of slushflows in central Gaspé Peninsula (Québec, Canada). *Geografiska Annaler : Series A, Physical Geography*, 83(4), 191-201. http://dx.doi.org/10.1111/j.0435-3676.2001.00154.x

Laternser, M. et Schneebli, M. (2002) Temporal trend and spatial distribution of avalanche activity during the last 50 years in Switzerland. *Natural Hazards*, 27, 201-230. http://dx.doi.org/10.1023/A:1020327312719

Lavoie, M. et Richard, P.J.H. (2000) Paléoécologie de la tourbière du Lac Malbaie, dans le Massif des Laurentides (Québec): Évaluation du rôle du climat sur l'accumulation de la tourbe. *Géographie physique et Quaternaire*, 54(2): 169-185. http://dx.doi.org/10.7202/004843ar

Laxton, S.C. et Smith, D.J. (2009) Dendrochronological reconstruction of a snow avalanche activity in the Lahul Himalaya, Northern India. *Natural Hazards*, 49(3), 459-467. http://dx.doi.org/10.1007/s11069-008-9288-5

Lebuis, J. et David, P.P. (1977) La stratigraphie et les évènements du Quaternaire de la partie occidentale de la Gaspésie, Québec. *Géographie physique et Quaternaire*, 31(3-4), 275-296. http://dx.doi.org/10.7202/1000278ar

Leonelli, G., Pelfini, M., D'Arrigo, R., Haeberli, W. et Cherubini, P. (2011) Non-stationary responses of tree-ring chronologies and glacier mass balance to climate in

the European Alps. *Arctic, Antarctic and Alpine Research*, 43(1), 56-65. http://dx.doi.org/10.1657/1938-4246-43.1.56

Lerner-Lam, A. (2007) Assessing global exposure to natural hazards: Progress and future trends. *Environmental Hazards*, 7, 10-17. http://dx.doi.org10.1016/j.envhaz.2007.04.007

Li, J., Gou, X., Cook, E.R. et Chen, F. (2006) Tree-ring based drought reconstruction for central Tien Shan area in northwest China. *Geophysical Research Letters*, 33, L07715. http://dx.doi.org/10.1029/2006GL025803

Lied, K. et Bakkehøi, S. (1980) Empirical calculations of snow avalanche run-out distance based on topometric parameters. *Journal of Glaciology* 26(94), 165-177.

Liverman, D., Batterson, M., Taylor, D. et Ryan, J. (2001) Geological hazards and disasters in Newfoundland and Labrador. *Canadian Geotechnical Journal*, 28, 936-956. http://dx.doi.org/10.1139/t01-022

Lloyd, A.H., Rupp, T.C., Fastie, C.L., Starfield, A.M. (2002) Patterns and dynamics of treeline advance on the Seward Peninsula, Alaska. *Journal of Geophysical Research*, 107, ALT 2-1-ALT 2-15. http://dx.doi.org/10.1029/2001JD000852.

Loehle, C. (2009) A mathematical analysis of the divergence problem in dendroclimatology. *Climatic Change*, 94, 233-245. http://dx.doi.org/10.1007/s10584-008-9488-8

Logan, S. et Witmer, F. (2012, septembre) Spatial, temporal, and space-time analysis of fatal avalanche accidents in Colorado and the United States, 1991 to 2011. *Proceedings of the International Snow Science Workshop.* Actes du colloque, à Anchorage, États-Unis, du 16 au 21 septembre 2012.

Lopez-Moreno, J.I., Vicente-Serrano, S.M., Morán-Tejeda, E., Lorenzo-Lacruz, J., Kenawy, A. et Beniston, M. (2011) Effects of the North Atlantic Oscillation (NAO) on combined temperature and precipitation winter modes in the Mediterranean mountains: observed relationships and projections for the 21st century. *Global Planetary Change*, 77(1-2), 62-76. http://dx.doi.org/10.1016/j.glopacha.2011.03.003

Lopez Saez, J., Corona, C., Stoffel, M., Schoenich, P. et Berger, F. (2012) Probability maps of landslide reactivation derived from tree-ring records: Pra Bellon landslide, southern French Alps. *Geomorphology*, 138, 189-202. http://dx.doi.org/10.1016/j.geomorph.2011.08.034

Lotter, A.F. (2003) Multi-proxy climatic reconstructions. [Chapitre de livre]. Dans Mackay, A., Battarbee, R., Birks, J. et Oldfield, F. (dir.), *Global change in the Holocene* (p.373-383). Londres : Arnold.

Löve, D. (1970) Subarctic and Subalpine: Where and What? *Arctic and Alpine Research*, 2(1), 63-73. http://dx.doi.org/10.2307/1550141

Luckman, B.H. (1977) The geomorphic activity of snow avalanche. *Geografiska Annaler. Series A, Physical Geography*, 59(1-2), 31–48.

Luckman, B.H. (2010) Dendrogeomorphology and Snow Avalanche Research. [Chapitre de livre]. Dans Stoffel, M., Bollschweiler, M., Butler, D.R. et Luckmand, B.H. (dir.), *Tree-Rings and Natural Hazards : A State-of-the-Art* (p.27-34). Dordrecht : Springer.

Luckman, B.H. et Fraser, G.W. (2001, septembre) Dendrogeomorphic investigations of snow avalanche tracks in the Canadian Rockies. In: *International conference on the future of dendrochronology*. Actes du colloque, à Davos, Suisse, du 22 au 26 septembre 2001.

Martin, J.P. et Germain, D. (*Sous presse*). Dendrogeomorphic reconstruction of snow avalanche regime and triggering weather conditions: A classification tree model approach. *Progress in Physical Geography*. http://dx.doi.org10.1177/0309133315625863

Matthews, J.A. et Wilson, P. (2015) Improved Schmidt-hammer exposure ages for active and relict pronival ramparts in southern Norway, and their palaeoenvironmental implications. *Geomorphology*, 246, 7-21. http://dx.doi.org/10.1016/j.geomorph.2015.06.002

Mazouz, R., Assani, A.A. et Rodríguez, M.A. (2013) Application of redundancy analysis to hydroclimatology : A case study of spring heavy floods in southern Quebec (Canada). *Journal of Hydrology*, 496, 187-194. http://dx.doi.org/10.1016/j.jhydrol.2013.035

McCammon, I. (2002) Evidence of heuristic traps in recreational avalanche accidents. *Proceedings of the International Snow Science Workshop.* Actes du colloque, à Pentincton, États-Unis, du 29 septembre au 4 octobre 2002.

McClung, D.M. (2001) Extreme avalanche runout: a comparison of empirical models. *Canadian Geotechnical Journal*, 38, 1254-1265. http://dx.doi.org/cgj-38-6-1254

McClung, D.M. (2002) The elements of applied avalanche forecasting part II: The physical issues and the rules of applied avalanche forecasting. *Natural Hazards*, 26, 131-146. http://dx.doi.org/10.1023/A:1015604600361

McClung, D.M. (2013) The effects of El Niño and La Niña on snow avalanche patterns in British Columbia, Canada, and central Chile. *Journal of Glaciology*, 59(216), 783-792. http://dx.doi.org/10.3189/2013JoG12J192

McClung, D.M. (2015) Mode II fracture parameters of dry snow slab avalanche weak layers calculated from the cohesive crack model. *International Journal of Fracture*, 193(2), 153-169. http://dx.doi.org/10.1007/s10704-015-0026-1

McClung, D.M. et Schaerer, P. (2006) *The Avalanche Handbook* (3e éd.). Seattle : Mountaineers Books.

Mears, A.I. (1975) Dynamics of dense snow avalanches interpreted from broken trees. *Geology*, 3, 521–523. http://dx.doi.org/10.1130/0091-7613(1975)3

Meister, R. (2002) Avalanches : Warning, rescue and prevention. *Avalanche News*, 62, 37-44.

Mercier, D. (2008) Paraglacial and paraperiglacial landsystems : concepts, temporal scales and spatial distribution. *Géomorphologie : Relief, Processus, Environnement*, 4, 223-234. http://dx.doi.org/10.4000/geomorphologie.7396

Messerli, B. et Ives, J.D. (1997) *Mountains of the world: A global priority*. Parthenon Publishing Group.

Miller, N.G. et Spear, R.W. (1999) Late-Quaternary history of the alpine flora of the New Hampshire White Mountains. *Géographie physique et Quaternaire*, 53(1): 137-157. http://dx.doi.org/10.7202/004854ar

Mock, C.J. et Birkeland, K.W. (2000) Snow avalanche climatology of the Western United States mountain ranges. *Bulletein of the American Meteorological Society*, 81(10), 2367-2392. http://dx.doi.org/10.1175/1520-0477(2000)081<2367;SACOTW>2.3.CO;2

Moran, P.A.P. (1950) Notes on continuous stochastic phenomena. *Biometrika*, 37, 17–23.

Morard, S., Delaloye, R. et Lambiel, C. (2010) Pluriannual thermal behaviour of low elevation cold talus slopes (western Switzerland). *Geographica Helvetica*, 65(2), 124-134. http://dx.doi.org/10.5194/gh-65-124-2010

Morin, J., Block, P., Rajagopalan, B. et Clark, M. (2008). Identification of large scale climatic patterns affecting snow variability in the eastern United States. *International Journal of Climatology* 28 (3), 315-328. http://dx.doi.org/10.1002/joc1534

Motta, R. et Haudemand, J.-C. (2000) Protective forests and silvicultural stability. *Mountain Research and Development*, 20(2), 180-187. http://dx.doi.org/10.1659/0276-4741(2000)020%5B0180%3APFASS%5D2.0.CO%3B2

Muntan, E., Andreu, L., Oller, P., Gutierrez, E. et Martinez, P. (2004) Dendrochronological study of the avalanche path Canal des Roc Roig. First results of the ALUDEX project in the Pyrenees. *Annals of Glaciology*, 38, 173-179. http://dx.doi.org/10.3189/172756404781815077

Muntan, E., Garcia, C., Oller, P., Marti, G., Garcia, A. et Gutierrez, E. (2009) Reconstructing snow avalanches in the southeastern Pyrenees. *Natural Hazards and Earth System Sciences*, 9, 1599-1612. http://dx.doi.org/10.5194/nhess-9-1599-2009

Nadim, F., Kjekstad, O., Domaas, U., Rafat, R. et Peduzzi, P. (2006) [Chapitre de livre]. Dans Arnold, M., Chen, R.S., Deichmann, U., Dilley, M., Lerner-Lam, A.L., Pullen, R.E. et Trohanis, Z.(dir.), *Natural Disasters Hotspots : Case Studies* (p.21-77). Washington : The World Bank Management Hazard Unit.

Nagelkerke, N.J.D. (1991) A note on a general definition of the coefficient of determination. *Biometrika*, 78, 691-692. http://dx.doi.org/10.1093/biomet/78.3.691

Ning, L. et Bradley, R.S. (2015) NAO and PNA influences on winter temperature and precipitation over the eastern United States in CMIP5 GCMs. *Climate Dynamics*, 1-20. http://dx.doi.org/10.1007/s00382-015-2643-9

Olejczyk, P. et Gray, J.T. (2007) The relative influence of Laurentide and local ice sheets during the last glacial maximum in the eastern Chic-Chocs Range, northern Gaspé Peninsula, Quebec. *Canadian Journal of Earth Sciences*, 44, 1603-1625. http://dx.doi.org/10.1139/e07-039

Ouellet, M.A. et Germain, D. (2014) Hyperconcentrated flows on a forested alluvial fan of eastern Canada: geomorphic characteristics, return period and triggering scenarios. *Earth Surface Processes and Landforms*, 39(14), 1876-1887. http://dx.doi.org/10.1002/esp.3581

Peitzch, E.H., Hendrikx, J., Fagre, D.B. et Reardon, B. (2012). Examining spring wet slab and glide avalanche occurrence along the Going-to-the-Sun Road corridor,

Glacier National Park, Montana, USA. *Cold Regions Science and Technology*, 78, 73-81. http://dx.doi.org/10.1016/j.coldregions.2012.01.012

Peng, C.Y.J., Lee, K.L. et Ingersoll, G.M. (2002) An introduction to Logistic Regresssion Analysis and Reporting. *The Journal of Educational Research*, 96(1), 3-14. http://dx.doi.org/10.1080/00220670209598786

Picklands, J. (1975) Statistical inference using extreme order statistics. *Annals of Statistics*, 3(1), 119-131.

Potter, N. (1969) Tree-ring dating of snow avalanche tracks and the geomorphic activity of avalanches, northern Absaroka Mountains, Wyoming. *Geological Society of America Special Paper*, 123, 141–165. http://dx.doi.org/10.1130/SPE123-p141

Price, M., Jansky, L. et Iatsenia, A.A. (2004) *Key issues for Mountain Areas*. Tokyo : United Nations University Press.

Putnam, A.E. et Putnam, D.E. (2009) Inactive and relict rock glaciers of Deboullie Lakes Ecological Reserve, northern Maine, USA. *Journal of Quaternary Science*, 24(7), 773-784. http://dx.doi.org/10.1002/jqs.1252

Rangachary, B. et Bandyopadhyay, B.K. (1987) An analysis of the synoptic weather pattern associated with extensive avalanching in the western Himalaya. *International Association of Hydrological Sciences Publication*, 162, 311-316.

Reardon, B.A., Pederson, G.T., Caruso, C.J. et Fagre, D.B. (2008) Spatial reconstructions and comparisons of historic snow avalanche frequency and extent using tree rings in Glacier National Park, Montana, U.S.A. *Arctic, Antarctic and Alpine Research*, 40(1), 148-160. http://dx.doi.org/10.1657/1523-0430(06-069)[REARDON]2.0.CO;2

Reimer, P.J., Baillie, M.G.L., Bard, E., Bayliss, A., Beck, J.W., Blackwell, P.G., Bronk Ramsey, C., Buck, C.E., Burr, G.S., Edwards, R.L., Friedrich, M., Grootes, P.M., Guilderson, T., Hajdas, I., Heaton, T., Hogg, A., Hughen, K., Kaiser, K., Kromer, B., McCormac, F., Manning, S., Reimer, R., Richards, D., Southon, J., Talamo, S., Turney, C., van der Plicht, J. et Weyhenmeye, C. (2009) INTCAL09 and MARINE09 Radiocarbon age calibration curves, 0-50,000 years cal BP. *Radiocarbon*, 51, 1111-1150.

Rémillard, A.M., Hétu, B., Bernatchez, P., Buylaert, J.P., Murray, A.S., St-Onge, G. et Geach, M. (2015) Chronology and palaeoenvironmental implications of the ice-wedge pseudomorphs and composite-wedge casts on the Magdalen Islands. *Boreas*, 44(4), 658-675. http://dx.doi.org/10.1111/bor.12125

Richard, P.J.H. (2009) *Chronologie de la déglaciation: de l'importance des années étalonnées (calibrées)*. Association Québécoise pour l'étude du Quaternaire. Récupéré de : http://www.er.uqam.ca/nobel/aqqua1/articles/ChronoDeglaciation.pdf

Richard, P.J.H. et Labelle, C. (1989) Histoire postglaciaire de la végétation au lac du Diable, mont Albert, Gaspésie, Québec. *Géographie physique et Quaternaire*, 43(3), 337-354. http://dx.doi.org/10.7202/032787ar

Richard, P.J.H., Veillette, J.J., Larouche, A.C., Hétu, B., Gray, J.T. et Gangloff, P. (1997) Chronologie de la déglaciation en Gaspésie: nouvelles données et implications. *Géographie physique et Quaternaire*, 51(2), 163-184. http://dx.doi.org/10.7202/033116ar

Robinson, S.C., Ketchledge, E.H., Fitzgerald, B.T., Raynald, D.J. et Kimmerer, R.W. (2010) A 23-year assessment of vegetation composition and change in the Adirondack alpine zone, New York State. *Rhodora*, 112: 355-377. http://dx.doi.org/10.3119/09-03.1

Rochefort, R.M., Little, R.L., Woodward, A. et Peterson, D.L. (1994) Changes in sub-alpine tree distribution in western North America: a review of climatic and other causal factors. *The Holocene*, 4(1), 89-100. http://dx.doi.org/10.1177/095968369400400112

Ruiz-Villanueva, V., Diez-Herrero, A., Stoffel, M., Bollschweiler, M., Bodoque, J.M. et Ballesteros, J.A. (2010) Dendrogeomorphic analysis of flash floods in a small ungauged mountain catchment (Central Spain). *Geomorphology*, 118, 383–392. http://dx.doi.org/10.1016/j.geomorph.2010.02.006

Sagoff, M. (2002) On the Value of natural Ecosystems: The Catskills Parable. *Politics and the Life Sciences*, 21(1), 19-25.

Salm, B. (1997) Principles of avalanche hazard mapping in Switzerland. [Chapitre de livre]. Dans Izumi, M., Nakamura, T. et Sack, R.L. (dir.), *Snow Engineering: Recent Advances* (p.531-538). Rotterdam: A.A. Balkema.

Schläppy, R., Jomelli, V., Grancher, D., Stoffel, M., Corona, C., Brunstein, D., Eckert, N. et Deschatres, M. (2013) A New Tree-Ring-Based, Semi-Quantitative Approach for the Determination of Snow Avalanche Events: use of Classification Trees for Validation. *Arctic, Antarctic and Alpine Research*, 45, 383-395. http://dx.doi.org/10.1657/1938-4246-45.3.383

Schläppy, R., Eckert, N., Jomelli, V., Stoffel, M., Grancher, D., Brunstein, D., Naaim, M. et Deschatres, M. (2014) Validation of extreme snow avalanches and related return periods derived from statistical-dynamical model using tree-ring techniques. *Cold Regions Science and Technology* 99, 12-26. http://dx.doi.org/10.1016/j.coldregions.2013.12.001

Schläppy, R., Jomelli, V., Eckert, N., Stoffel, M., Grancher, D., Brunstein, D., Corona, C. et Deschatres, M. (2015) Can we infer avalanche-climate relations using tree-ring data? Case studies in the French Alps. *Regional Environmental Change.* http://dx.doi.org/10.1007/s10113-015-0823-0

Schmid, L. Koch, F., Heilig, A., Prasch, M., Eisen, O., Mauser, W. et Schweizer, J. (2015) A novel sensor combination (upGPR-GPS) to continuously and nondestructively derive snow cover properties. *Geophysical Research Letters*, 42, 3397-3405. http://dx.doi.org/10.1002/2015GL063732

Schneebeli, M., Laternser, M. et Ammann, W. (1997) Destructive snow avalanche and climate change in the Swiss Alps. *Eclogae Geologica Helvetica*, 90, 457-461. http://dx.doi.org/10.5169/seals-168177

Schneuwly-Bollschweiler, M., Corona, C. et Stoffel, M. (2013) How to improve dating quality and reduce noise in tree-ring based debris-flow reconstructions. *Quaternary Geochronology*, 18, 110-118. http://dx.doi.org/10.1016/j.quageo.2013.05.001

Schweizer, J., Jamieson B.J. et Schneebeli, M. (2003) Snow avalanche formation. *Reviews of Geophysics*, 41(4), 1016. http://dx.doi.org/10.1029/2002RG000123

Schweizer, J., Kronholm, K., Jamieson, B.J. et Birkeland, K.W. (2008) Review of spatial variability of snowpack properties and its importance to avalanche formation. *Cold Regions Science and Technology*, 51, 253-272. http://dx.doi.org/10.1016.j.coldregions.2007.04.009

Seidel, T.M., Weihnrauch, D.M., Kimball, K.D., Pszenny, A.A.P., Soboleski, R., Crete, E. et Murray, G. (2009) Evidence of Climate Change Declines with Elevation Based on Temperature and Snow Records from 1930s to 2006 on Mount Washington, New Hampshire, U.S.A. *Arctic, Antarctic and Alpine Research*, 41(3), 362-372. http://dx.doi.org/10.1657/1938-4246-41.3.362

Shabbar, A., Higuchi, K., Skinner, W. et Knox, J.L. (1997) The association between the BWA index and winter surface temperature variability over eastern Canada and west Greenland. *International Journal of Climatology*, 17 (11), 1195-1210.

http://dx.doi.org/10.1002/(SICI)1097-0088(199709)17:11<1195::AID-JOC190>3.0.CO;2-U

Shroder, J.F.J. (1978) Dendrogeomorphological Analysis of Mass Movement on Table Cliffs Plateau, Utah. *Quaternary Research*, 9, 168-185. http://dx.doi.org/10.1016/0033-5894(78)90065-0

Shroder, J.F.J. (1980) Dendrogeomorphology : review and new techniques of tree-ring dating. *Progress in Physical Geography*, 4(2), 161-188. http://dx.doi.org/10.1177/030913338000400202

Shur, Y.L. et Jorgenson, M.T. (2007) Patterns of permafrost formation and degradation in relation to climate and ecosystems. *Permafrost and Periglacial Processes*, 17, 7-19. http://dx.doi.org/10.1002/ppp.582

Singh, A., Damir, B., Deep, K. et Ganju, A. (2015) Calibration of nearest neighbors for avalanche forecasting. *Cold Regions Science and Technology,* 109, 33-42. http://dx.doi.org/10.1016/j.coldregions.2014.09.009

Sirois, L. (1984) *Le plateau du mont Albert: étude phyto-écologique*. (Mémoire de maîtrise). Québec, Université Laval.

Smith, M.J. et McClung, D.M. (1997) Avalanche frequency and terrain characteristics at Rogers' Pass, British Colombia, Canada. *Journal of Glaciology*, 43(143), 165-171.

Solomina, O.N. (2002) Dendrogeomorphology: Research Requirements. *Dendrochronologia*, 20(1), 231-243. http://dx.doi.org/10.1078/1125-7865-00019

Spear, R.W. (1989) Late-Quaternary History of High-Elevation Vegetation in the White Mountains of New Hampshire. *Ecological Monographs*, 59(2), 125-151. http://dx.doi.org/10.2307/2937283

Spear, R.W., Davis, M.B. et Shane, L.C.K. (1994) Late Quaternary History of Low- and Mid-Elevation Vegetation in the White Mountains of New Hampshire. *Ecological Monographs*, 64(1), 85-109. http://dx.doi.org/10.2307/2937056

Speer, J.H. (2015) *Fundamentals of Tree-Ring Research.* Tucson: University of Arizona Press.

Sprugel, D.G. (1976) Dynamic structure of wave-regenerated Abies balsamea forests in the northeastern United States. *Journal of Ecology*, 64, 889-905. http://dx.doi.org/10.2307/2258815

Stethem, C., Jamieson, B.J., Schaerer, P., Liverman, D., Germain, D. et Walker, S. (2003) Snow avalanche hazards in Canada – a review. *Natural Hazards*, 28, 487-515. http://dx.doi.org/10.1023/A:1022998512227

Stoffel, M., Bollschweiler, M. et Hassler, G.R. (2006) Differentiating past events on a cone influenced by debris-flow and snow avalanche activity – a dendrogeomorphological approach. *Earth Surface Processes and Landforms*, 31(11), 1424-1437. http://dx.doi.org/10.1002/esp.1363

Stoffel, M. et Bollschweiler, M (2008) Tree-ring analysis in natural hazard research – an overview. *Natural Hazards Earth System Science*, 8, 187-202. http://dx.doi.org/10.5194/nhess-8-187-2008

Stoffel, M., Bollschweiler, M., Butler, D.R. et Luckman, B.H. (2010) Tree Rings and Natural Hazards : An introduction. [Chapitre de livre]. Dans Stoffel, M., Bollschweiler, M., Butler, D.R. et Luckman, B.H. (dir.), *Tree-Rings and Natural Hazards : A State-of-the-Art* (p.3-23). Dordrecht : Springer.

Stoffel, M., Butler, D.R. et Corona, C. (2013) Mass movements and tree rings: A guide to dendrogeomorphic field sampling and dating. *Geomorphology*, 200, 106-120. http://dx.doi.org/10.1016/j.geomorph.2012.12.017

Stoffel, M., Casteller, A., Luckman, B.H. et Villalba, R. (2012) Spatiotemporal analysis of channel wall erosion in ephemeral torrents using tree roots – An example from the Patagonian Andes. *Geology*, 40(3), 247-250. http://dx.doi.org/10.1130/G32751.1

Stoffel, M. et Corona, C. (2014) Dendroecological dating of geomorphic disturbance in trees. *Tree-Ring Research*, 70(1), 3-20. http://dx.doi.org/10.3959/1536-1098-70.1.3

Stoffel, M. et Hitz, O.M. (2008) Rockfall and snow avalanche impacts leave different anatomical signatures in the tree rings of juvenile Larix decidua. *Tree physiology*, 28(11), 1713-1720. http://dx.doi.org/10.1093/treephys/28.11.1713

Stokes, A. (2008) Ecotechnological solutions for slope stability: perspectives for future research. [Chapitre de livre]. Dans Norris J.E., Stokes, A., Mickovski, S.B., Cammeraat, E., van Beek, R., Nicoll B.C. et Achim, A. (dir.), *Slope Stability and Erosion Control: Ecotechnological Solutions* (p. 277-282). Dordrecht : Springer.

Szymczak, S., Bollschweiler, M., Stoffel, M. et Dikau, R. (2010) Debris-flow activity and snow avalanches in a steep watershed of the Valais Alps (Switzerland): Dendrogeomorphic event reconstruction and identification of triggers.

Geomorphology, 116(1-2), 107-114. http://dx.doi.org/10.1016/j.geomorph.2009.10.012

Teich, M. (2013) *Snow avalanches in forested terrain.* (Thèse de doctorat). Dresden, Technische Universität Dresden.

Thompson, W.B., Fowler, B.K. et Dorion, C.C. (1999) Deglaciation of the northwestern White Mountains, New Hampshire. *Géographie physique et Quaternaire*, 53(1), 59-77. http://dx.doi.org/10.7202/004882ar

Thompson, D.W.J. et Wallace, J.M. (2001) Regional Climate Impacts of the Northern Hemisphere Annular Mode. *Science*, 293, 85-89. http://dx.doi.org/10.1126/science.1058958

Thorson, R.M. et Schile, C.A. (1995) Deglacial eolian regimes in New England. *Geological Society of America Bulletin*, 107(7), 751-761. http://dx.doi.org/10.1130/0016-7606(1995)

Thumlert, S.J. (2014) *Stress Measurements of Localized Dynamic Loading in the Mountain Snow Cover.* (Thèse de doctorat). University of Calgary.

Thumlert S.J., Bellaire, S. et Jamieson, B.J. (2014, octobre) Relating avalanches to large-scale ocean – atmospheric oscillations. *Proceedings of the International Snow Science Workshop.* Actes du colloque, à Banff, Canada, du 28 septembre au 3 octobre 2014.

Titus, R. 2004. *The Catskills: A Geological Guide, 3rd Edition.* New York : Purple Mountain Press.

US National Weather Service (USNWS), Climate Prediction Center. 2015. *Cold and warm episodes by season: changes to the Oceanic Niño Index (ONI).* Récupéré le 31 août 2015 de http://www.cpc.ncep.noaa.gov/products/analysis_monitoring/ensostuff/ensoyears.shtml.

Vacchiano, G., Maggioni, M., Perseghin, G. et Motta, R. (2015) Effect of avalanche frequency on forest ecosystem services in a spruce–fir mountain forest. *Cold Regions Science and Technology*, 115, 9-21. http://dx.doi.org/10.1016/j.coldregions.2015.03.004

Vernay, M., Lafaysse, M., Mérindol, L., Girod, M. et Morin, S. (2015) Ensemble forecasting of snowpack conditions and avalanche hazard. *Cold Regions Science and Technology*, 120, 251-262. http://dx.doi.org/10.1016/j.coldregions.2015.04.010

Voiculescu, M. et Onaca, A. (2013) Snow avalanche assessment in the Sinaia ski area (Bucegi Mountains, Southern Carpathians) using the dendrogeomorphology method. *Area*, 45(1), 109-122. http://dx.doi.org/10.1111/area.12003

Voiculescu, M. et Onaca, A. (2014) Spatio-temporal reconstruction of snow avalanche activity using dendrogeomorphological approach in Bucegi Mountains Romanian Carpathians. *Cold Regions Science and Technology*, 104-105, 63-75. http://dx.doi.org/10.1016/j.coldregions.2014.04.005

Wachinger, G., Renn, O., Begg, C. et Kuhlicke, C. (2013) The risk perception paradox – Implications for governance and communication of natural hazards. *Risk Analysis*, 33(6), 1049-1065. http://dx.doi.org/10.1111/j.1539-6924.2012.01942.x

Wahl, K., Spooner, I. et Colville, D. (2007) Thin-Skinned Debris Flows in Cape Breton Highlands National Park, Nova Scotia, Canada. *Atlantic Geology*, 43, 45-56. http://dx.doi.org/2048/10.4138/4213

Walegur, M.T. et Nelson, F.E. (2003) Permafrost distribution in the Appalachian Highlands, northeastern USA. [Chapitre de livre]. Dans Philips, Springman et Anderson (dir.) *Permafrost* (p. 1201-1206). Liss, Swets and Zeitlinger.

Whipple, K.X. (2009) The influence of climate on the tectonic evolution of mountain belts. *Nature geoscience*, 2, 97-104. http://dx.doi.org/10.1038/ngeo413

Winkworth, R.C., Wagstaff, S.J., Glenny, D. et Lockhart, P.J. (2005) Evolution of the New Zealand mountain flora: Origins, diversification and dispersal. *Organisms, Diversity & Evolution*, 5, 237-247. http://dx.doi.org/10.1016/j.ode.2004.12.001

Yagouti, A., Boulet, G. et Vescovi, L. (2006) *Projet-MNEV-7 : Homogénéisation des séries de températures et analyse de la variabilité spatio-temporelle de ces séries au Québec méridional. Rapport #4 – Homogénéisation des séries de températures du Québec méridional et analyse de l'évolution du climat à l'aide d'indicateurs.* Québec: Consortium Ouranos.

Yokley, L., Hendrikx, J., Birkeland, K.W., Williams, K. et Leonard, T. (2014, octobre). Role of synoptic atmospheric condition in the formation and distribution of surface hoar. *Proceedings of the International Snow Science Workshop.* Actes du colloque, à Banff, Canada, du 28 septembre au 3 octobre 2014.

Zielonka, T., Holeska, J., Fleischer, P. et Kapusta, P. (2010) A tree-ring reconstruction of wind disturbances in a forest of the Slovakian Tatra Mountains, Western Carpathians. *Journal of Vegetation Science*, 21(1), 31–42. http://dx.doi.org/10.1111/j.1654-1103.2009.01121.x

Zimmermann, C. et Lavoie, C. (2001) A paleoecological analysis of a southern permafrost peatland, Charlevoix, Quebec. *Canadian Journal of Earth Sciences*, 38, 909-919. http://dx.doi.org/10.1139/e00-110